

**Endothelial *microRNA-24* contributes to capillary
density in the infarcted heart**

**Dissertation zur Erlangung des
naturwissenschaftlichen Doktorgrades
der Julius-Maximilians-Universität Würzburg**

Vorgelegt von

Jan Fiedler

aus Husum

Würzburg, 2010

Eingereicht am:

Mitglieder der Promotionskommission:

Vorsitzender: Prof. Dr. Thomas Dandekar

Gutachter: Prof. Dr. Johann Bauersachs

Gutachter: Prof. Dr. Thomas Dandekar

Betreuer: Prof. Dr. Dr. Thomas Thum

Tag des Promotionskolloquiums:

Doktorurkunde ausgehändigt am:

Dedicated to my family

Contents

Summary	1
Zusammenfassung	2
1. Introduction	
1.1 Cardiac remodelling and heart failure	3
1.2 Angiogenesis and apoptotic signalling	7
1.2.1 General mechanisms of angiogenesis	8
1.2.2 Apoptosis signalling	9
1.2.3 Endothelial cell apoptosis in the cardiovascular system	10
1.3 MicroRNAs (miRNAs): regulatory RNAs	12
1.3.1 MiRNAs in the cardiovascular system	15
1.3.1.1 Cardiomyocyte miRNAs	
1.3.1.2 Fibroblast miRNAs	
1.3.1.3 Endothelial miRNAs (angiomiRs)	
1.3.2 MiRNA antagonists (“antagomirs“) for <i>in vivo</i> application	23
1.4 <i>MiR-24</i> genelocus and <i>miR-24</i> function	25
1.5 Scope and aim of this study	28
2. Material and Methods	
2.1 Material	30
2.1.1 Equipment	30
2.1.2 Consumable material and chemicals	32
2.1.3 Provided kit systems	35
2.1.4 Solutions and buffers.	36
2.1.4.1 Cell culture media, components and used cells	
2.1.4.2 Cardiomyocyte preparation and fractionation of cardiac cells	
2.1.4.3 DNA electrophoresis	
2.1.4.4 Chromatinimmunoprecipitation (ChIP)	
2.1.4.5 SDS-PAGE and Western Blot	
2.1.5 Plasmids	43
2.1.6 Oligonucleotides and probes	43

2.1.7 Antibodies, enzymes and standard markers	46
2.1.8 FACS solution	49
2.1.9 Components for bacterial culture and bacteria strains	49
2.1.10 Animals	50
2.2 Methods	51
2.2.1 Cell culture	51
2.2.1.1 Cultivation of endothelial cells (ECs)	
2.2.1.2 Isolation and cultivation of neonatal rat cardiomyocytes and cardiacfibroblasts	
2.2.1.3 Cultivation of other applied cell types	
2.2.1.4 Transfection assays	
2.2.1.5 Luciferase reporter assay	
2.2.1.6 <i>In vitro</i> tube formation assay for ECs	
2.2.1.7 Viral transduction	
2.2.2 Molecular biology	53
2.2.2.1 RNA isolation	
2.2.2.2 DNA isolation	
2.2.2.3 Determination of RNA and DNA concentration	
2.2.2.4 Agarose gel electrophoresis	
2.2.2.5 Luciferase pMIR-Report cloning	
2.2.2.6 Real-time PCR analysis	
2.2.2.7 ChIP	
2.2.2.8 Affymetrix gene chips	
2.2.3 Protein biochemistry	59
2.2.3.1 Protein isolation	
2.2.3.2 Determination of protein concentration	
2.2.3.3 SDS-PAGE	
2.2.3.4 Western Blot	
2.2.3.5 Apoptosis array	
2.2.3.6 phospho-Bad ELISA	
2.2.4 Fluorescence-activated cell sorting (FACS)	62
2.2.4.1 Apoptosis staining	
2.2.4.2 Cell cycle propidium iodide (PI) stain	
2.2.4.3 Reactive oxygen species (ROS) detection	
2.2.5 Immunocytochemistry and immunohistochemistry	63
2.2.5.1 Immunocytochemistry	
2.2.5.2 Immunohistochemistry	
2.2.6 <i>In vivo</i> methods	64
2.2.6.1 Fractionation of cardiac cells from heart tissue	
2.2.6.2 Antagomir injection	
2.2.6.3 Myocardial infarction	
2.2.6.4 Echocardiography	
2.2.6.5 Matrigel implantation and determination of vasuclarization	
2.2.7 MicroRNA target prediction	66
2.2.8 Statistical analysis	66

3. Results

3.1 <i>MiR-24</i> is induced post myocardial infarction (MI)	67
3.1.1 <i>MiR-24</i> profiling reveals an ubiquitous expression panel	68
3.1.2 <i>MiR-24</i> is induced in ECs post hypoxia and in cardiac ECs post MI	69
3.2 <i>MiR-24</i> modulation in different cell types	72
3.2.1 <i>MiR-24</i> overexpression induces apoptosis specifically in ECs	74
3.2.2 Apoptosis array post <i>miR-24</i> modulation reveals dysregulation of anti-apoptotic HMOX1 and Bad protein	76
3.2.3 Elevated reactive oxygen species (ROS) upon <i>miR-24</i> overexpression in ECs	80
3.2.4 Capillary tube formation is impaired in <i>miR-24</i> overexpressing ECs	81
3.3 <i>MiR-24</i> regulates endothelial GATA2, H2A.X, PAK4 and RASA1	81
3.3.1 Luciferase reporter gene assays confirm <i>miR-24</i> targets GATA2, H2A.X, PAK4 and RASA1	85
3.3.2 Transient knockdown of <i>miR-24</i> targets GATA2, H2A.X, PAK4 and RASA1 induces apoptosis in ECs	87
3.3.3 GATA2 is a key player for cell cycle progression in ECs	88
3.3.4 Impairment in tube formation ability when silencing GATA2 or PAK	89
3.3.5 PAK4 and RASA1 are downregulated under hypoxic conditions in ECs	90
3.4 Affymetrix and ChIP data indicate GATA2-regulated genes related to angiogenic processes	91
3.4.1 Overexpression of murine Gata2 in ECs	92
3.4.2 Transcriptome analysis upon GATA2 modulation by Affymetrix gene chip . .	93
3.4.3 ChIP analysis for GATA2	95
3.4.4 Pro-angiogenic HMOX1 and SIRT1 are regulated on protein level by the <i>miR-24</i> target GATA2	97
3.5 Bad phosphorylation status is regulated by the <i>miR-24</i> target PAK4	99
3.6 In vivo treatment of myocardial infarction by a specific <i>miR-24</i> antagonist (antagomir) – antagomir-24 study	101
3.6.1 Antagomir-24 efficiently lowers cardiac <i>miR-24</i> expression	103
3.6.2 Heart function tests after MI	103
3.6.3 Cardiac angiogenesis is improved upon antagomir-24 treatment	105
3.6.4 Implantation of matrigel plugs to characterize global neovascularization <i>in vitro</i>	107

4. Discussion	109
4.1 <i>MiR-24</i> deregulation in cardiac disease	110
4.2 Induction of endothelial cell apoptosis by <i>miR-24</i>	112
4.3 Target-specific regulation for <i>miR-24</i> in ECs	115
4.4 Antagonizing <i>miR-24</i> as a therapeutic option in treatment of cardiovascular disease	119
4.5 Concluding remarks	122
References	I
Abbreviations	II
Publications	III
Curriculum Vitae	IV
Acknowledgement	V
Affidavit	VI

Summary

Cardiovascular disease is the most common mortality risk in the industrialized world. Myocardial infarction (MI) results in the irreversible loss of cardiac muscle, triggering pathophysiological remodelling of the ventricle and development of heart failure. Insufficient myocardial capillary density within the surviving myocardium after MI has been identified as a critical event in this process, although the underlying molecular signalling pathways of cardiac angiogenesis are mechanistically not well understood. The discovery of microRNAs (miRNAs, miRs), small non-coding RNAs with 19-25 nucleotides in length, has introduced a new level of the regulation of cardiac signalling pathways. MiRNAs regulate gene expression post-transcriptionally by binding to their complementary target messenger RNAs (mRNAs) and represent promising therapeutic targets for gene therapy.

Here, it is shown that cardiac *miR-24* is primarily expressed in cardiac endothelial cells and upregulated following MI in mice and hypoxic conditions *in vitro*. Enhanced *miR-24* expression induces endothelial cell apoptosis and impairs endothelial capillary network formation. These effects on endothelial cell biology are at least in part mediated through targeting of transcription factor GATA2, histone deacetylase H2A.X, p21-activated kinase PAK4 and Ras p21 protein activator RASA1. Mechanistically, target repression abolishes respective and secondary downstream signalling cascades. Here it is shown that endothelial GATA2 is an important mediator of cell cycle, apoptosis and angiogenesis at least in part by regulation of cytoprotective heme oxygenase 1 (HMOX1). Moreover, additional control of endothelial apoptosis is achieved by the direct *miR-24* target PAK4. Its kinase function is essential for anti-apoptotic Bad phosphorylation in endothelial cells. In a mouse model of MI, blocking of endothelial *miR-24* by systemic administration of a specific antagonist (antagomir) enhances capillary density in the infarcted heart and preserves cardiac function.

The current findings indicate *miR-24* to act as a critical regulator of endothelial cell apoptosis and angiogenesis. Modulation of *miR-24* may be potentially a suitable strategy for therapeutic intervention in the setting of ischemic heart diseases.

Zusammenfassung

Kardiovaskuläre Erkrankungen sind die häufigste Todesursache in der industrialisierten Welt. Nach Myokardinfarkt (MI) kommt es zum Verlust kardialen Gewebes und zu pathologischen Umbauprozessen im Herzen, die oftmals in einer Herzinsuffizienz münden. Dabei spielt eine insuffiziente Gefäßversorgung im überlebenden Myokard eine wichtige Rolle. Zugrunde liegende molekulare Mechanismen oder gentherapeutische Strategien zur Verbesserung der Angiogenese nach MI sind jedoch nur unzureichend verstanden und etabliert. Die Entdeckung sogenannter microRNAs (miRNAs, miRs), kleiner nicht-kodierender RNAs mit einer Länge von 19-25 Nukleotiden, zeigt eine neue Ebene der Komplexität bei der Regulation kardiovaskulärer Signalwege auf. So regulieren miRNAs die Genexpression post-transkriptional durch inhibitorische Bindung an komplementäre messenger RNAs. Die Modulation von miRNAs und damit nachfolgenden Gen-Netzwerken könnte daher ein wichtiger Baustein bei der Entwicklung neuer Therapiestrategien in der kardiovaskulären Medizin werden. In dieser Arbeit wird gezeigt, dass kardiale *miR-24* überwiegend in kardialen Endothelzellen exprimiert ist und nach Myokardinfarkt im Mausmodell sowie nach Hypoxie *in vitro* hochreguliert wird. Die verstärkte *miR-24*-Expression induziert endotheliale Apoptose und vermindert die Kapillarbildungsfähigkeit endothelialer Zellen in einem Angiogeneseassay. Diese funktionalen Defekte werden über die Repression des Transkriptionsfaktors GATA2, der Histon-Deacetylase H2A.X, der p21-aktivierten Kinase PAK4 und dem p21 Protein-Aktivator RASA1 vermittelt. GATA2 wird in dieser Arbeit als wichtiger Faktor für die Zellzykluskontrolle, Apoptose und Angiogenese beschrieben, wobei die Regulation direkter Effektoren wie Hämoxygenase 1 (HMOX1) essentiell ist. Weiterhin wird über die *miR-24*-abhängige Modulation von PAK4 endotheliale Apoptose kontrolliert. PAK4 weist eine anti-apoptotische Funktion auf, indem es zu einer Phosphorylierung des Proteins Bad führt. Die spezifische Repression endogener *miR-24* durch einen Antagonisten (Antagomir) in einem murinen MI-Modell erhöht die Kapillardichte im infarzierten Gewebe und verbessert die kardiale Funktion. Zusammenfassend zeigen die Erkenntnisse dieser Arbeit eine wichtige Funktion für *miR-24* bei der Regulation endothelialer Apoptose und Angiogenese. Die Modulation von *miR-24* könnte ein interessantes neues therapeutisches Konzept zur Verbesserung der Angiogenese nach MI darstellen.

1. Introduction

1.1 Cardiac remodelling and heart failure

Myocardial infarction (MI) often leading to heart failure is a serious clinical disorder and represents a critical health burden worldwide. Cardiovascular disease causes 48% of deaths in Europe (European Heart Network, 2008) and 35.3% of deaths in the United States (American Heart Association, 2005). Therefore therapeutic interventions regarding prevention and/or acute therapy have to be improved. These approaches rely on the current understanding of heart failure induced by cardiovascular disease including myocardial infarction (MI), coronary artery disease (CAD) or hypertension.

The heart is a complex organ, multi-chambered, built up from different cell types bearing specific features. The cardiomyocyte is terminally differentiated and conducts tension by shortening. In contrast, the extracellular matrix made up by collagen type I and III synthesized from cardiac fibroblasts provides a viscoelastic scaffold preventing sarcomeric deformation (Erlebacher *et al.*, 1984). Furthermore it links cardiomyocytes to adjacent vasculature and microcapillaries supplying the organ with nutritive blood flow (Weber, 1997). Cell to cell interaction, conduction and communication is important in healthy and diseased myocardium. Moreover, complex mechanisms regulate the hearts shape and biology thus altering cardiac performance. Mechanistically, certain molecular signalling processes are responsible for cardiac remodelling transducing fundamental reactions.

Cardiac remodelling relies on diverse stimuli or conditions (figure 1.1). For example, adjacent consequences like atrophy or physiologic hypertrophy are less harmful since characterized by a reversible state. In contrast, pathologic hypertrophy forced by persistent cardiac stress is the precursor for heart failure. Moreover, heart failure can be seen as a progressive disease affecting at least the neurohumoral system, genetic factors and global cardiac structure (Francis *et al.*, 1984, Mann, 1999, McMurray and Pfeffer, 2002).

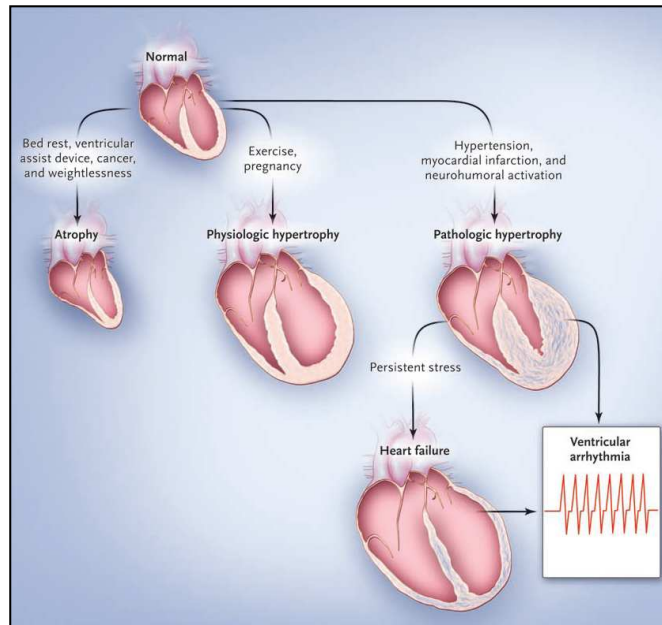


Figure 1.1: Conditions leading to atrophy and physiologic or pathologic hypertrophy. Pathologic hypertrophy is accompanied by several circumstances potentially leading to heart failure (Hill and Olson, 2008).

In general, heart failure is accompanied by myocardial hypertrophy. Initially, myocardial hypertrophy is characterized by the enlargement of resident cardiomyocytes thereby enhancing cardiac muscle power. Thus, this physiological growth reaction should directly support cardiac performance and outcome unless other risk factors are abandoned.

Leading factors for the development of maladaptive pathologic hypertrophy include MI and prolonged hypertension. Such factors accelerate cardiomyopathy and often disturb myocardial conduction. Persistent cardiac stress results in the irreversible loss of cardiac muscle, triggering remodelling of the cardiac muscle and the development of heart failure (reviewed in Jessup and Brozena, 2003, Hill and Olson, 2008). In addition, alterations in heart structure are accompanied by sustained interstitial fibrosis impairing and decreasing cardiac pump function.

Basically, cardiac remodelling post-MI is crucially dependent on the infarct size determining heart architecture alteration (McKay *et al.*, 1986). Immediately after this ischemic event, macrophages, monocytes and neutrophils infiltrate into the infarcted area contributing to local inflammatory response.

Infarct remodelling has been divided a long time ago into early phase (within 72 hours) and a late phase beginning thereafter. Since the infarct and myocyte death expand in early phase, ventricular rupture or aneurysm formation is possible (Erlebacher *et al.*, 1984). In contrast, late phase remodelling has to be seen as a more global alteration of ventricular shape resulting in dilatation, distortion and hypertrophy (Sutton and Sharpe, 2000 and figure 1.2). The underlying mechanisms following infarct expansion are diverse.

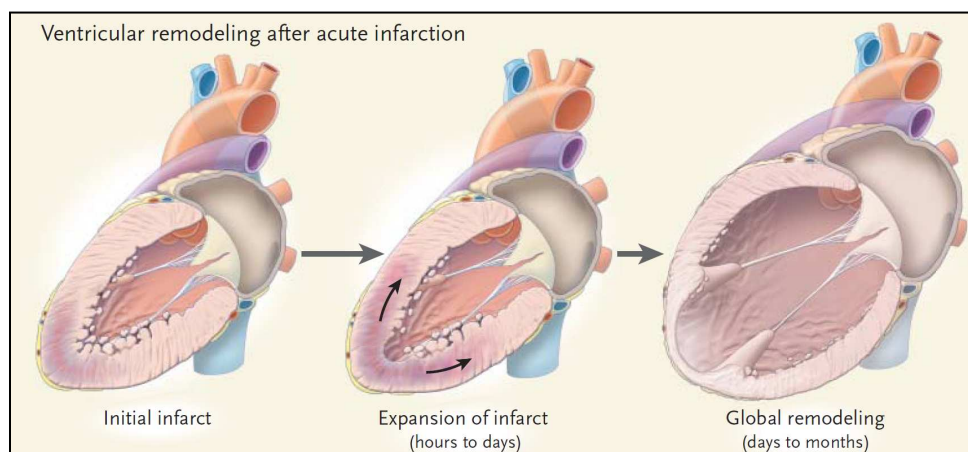


Figure 1.2: Time response for ventricular remodelling after myocardial infarction. Ischemic area expands within hours to days and finally results in global cardiac remodelling impeding systolic function (Jessup and Brozena, 2003).

Immediate infarct expansion is supported by the activation of matrix metalloproteinases (MMPs) released from neutrophils degrading extracellular matrix (Cleutjens *et al.*, 1995). Therefore infarct area progression is fast and results in wall thinning and ventricular dilatation establishing diastolic and systolic wall stress (Warren *et al.*, 1988). Then, wall stress defines a stimulus for cardiac hypertrophy which is transduced to intracellular signalling by angiotensin II (Ang II) release (Sadoshima *et al.*, 1992). This, in turn, increases the contractile force by enhancing protein synthesis of contractile assembly units in the myocyte. In contrast, cardiac fibroblasts are also stimulated for protein synthesis and proliferation supporting fibrosis and scar formation. Moreover, Ang II reprogrammes cardiac cells to a fetal transcriptome (fetal gene reprogramming) by induction of several transcription factors like c-fos, c-jun or c-myc further contributing to heart failure (Sadoshima *et al.*, 1993).

The noninfarcted zone (remote myocardium) is simultaneously affected by infarct expansion responding to preserve stroke volume and to antagonize infarct injury (Lew *et al.*, 1985). Additionally, alteration of circulatory hemodynamics triggers further neurohumoral response by activation of the renin-angiotension-aldosterone (RAAS) system and increases production of atrial and brain natriuretic peptides (ANP and BNP) counteracting Ang II signalling as an adaptive response (reviewed in Sutton and Shape, 2000).

The early remodelling phase is dominated by local inflammatory signalling that is transduced by mechanical forces throughout the whole ventricle leading over to late remodelling. Here myocardial repair is more in focus relying on collagen scar formation that distributes elevated wall stresses more evenly (Sutton and Shape, 2000). Deposition of collagen matrix begins at day 2 to 4 depending on collagen type and previous signalling (Cleutjens *et al.*, 1995). Briefly, the myocyte-released cytokine TGF- β 1 modifies fibroblast and macrophage chemotaxis and proliferation. Additionally, the phenotypic transition from interstitial fibroblasts to myofibroblasts is forced defining expression of receptors to Ang II and TGF- β 1. Furthermore myofibroblasts encode the ligands for these receptors, thus enabling the autoregulation of collagen turnover by MMPs (Desmouliere *et al.*, 1993). Nevertheless, the formation of a fibrin-fibronectin matrix is a prerequisite for adherence of myofibroblast building up the crescent scar (Knowlton *et al.*, 1992). Ongoing myofibroblast activation potentiates scar signalling leading to myocyte substitution within 28 days (Cleutjens *et al.*, 1995). Afterwards, myofibroblasts become apoptotic leaving behind a greatly increased extracellular scaffold.

The different remodelling phases offer various potential therapeutic approaches. Nevertheless treatment of heart failure is difficult and novel treatment strategies are warranted. Several pathophysiological mechanisms are stimulated upon cardiac dysregulation offering different therapeutic approaches. Since primary therapy is based on mechanical or pharmacological intervention some of the main counteracting opportunities should be highlighted here. It is well known that aldosterone production in the adrenal gland is increasing in heart failure leading to ventricular hypertrophy and dysfunction. Aldosterone antagonists are therefore powerful compounds to counteract these negative effects.

Besides pharmacological intervention, cell transplantation has been investigated in several clinical studies such as REPAIR-AMI (acute myocardial infarction) study (Schachinger *et al.*, 2006; Dill *et al.*, 2009). Here, the researchers questioned whether bone marrow derived progenitor cell transplantation inhibits processing of adverse remodelling events after myocardial infarction. In summary, cardiac outcome one year after intracoronary cell transfusion has been validated beneficial for patients, but the net effect on cardiac improvement was rather small and novel therapeutic strategies are needed.

1.2 Angiogenesis and apoptotic signalling

The generation of blood vessels in the developing embryo or in the adult is determined by two distinct processes: vasculogenesis and angiogenesis. While vasculogenesis comprises the *de novo* formation of blood vessels, angiogenesis involves growth of existing blood vessels. Additional *de novo* postnatal vasculogenesis might occur by progenitor cell differentiation to the endothelial lineage (Asahara *et al.*, 1999).

Suppressed oxygen supply results in myocyte necrosis and infarct expansion. Insufficient myocardial capillary density within the surviving myocardium after MI has been identified as a critical event in pathological remodelling. Myocardial capillaries are formed by endothelial cells (ECs) placing a scaffold building up the vasculature. Generally, ECs play fundamental roles in vascular development and disease. Formation of new blood vessels by stimulating pre-existing ECs (angiogenesis) is crucial for improvement in blood perfusion. Angiogenic stimuli activate ECs to migrate and proliferate thereby enhancing generation of primary capillaries. Afterwards, these structures undergo remodelling accompanied by sprouting, branching or intussusception. Furthermore smooth muscle cells may be recruited to sites of newly formed blood vessels lining the internal bloodstream layer. Angiogenesis can be beneficial in terms of ischemic disease, but on the other hand aberrant angiogenesis may be responsible for cancer progression (Hanahan *et al.*, 1996). Major angiogenic factors include vascular endothelial growth factor (VEGF) and basic fibroblast growth factor (bFGF). Moreover, VEGF is responsible for progenitor cell mobilization from the bone marrow (Asahara *et al.*, 1999). In contrast, anti-angiogenic factors like naturally occurring

thrombospondin-1 counteract VEGF and bFGF signalling thus balancing angiogenesis (Jimenez *et al.*, 2000).

1.2.1 General mechanisms of angiogenesis

Angiogenesis is a dynamic process based on extracellular signalling transduced by receptor-tyrosine kinases (RTKs) to the intracellular compartment thus activating gene transcription. VEGF and bFGF are important angiogenic modulators stimulating survival, proliferation, migration and differentiation of primary and stable ECs. Essentially, bFGF and VEGF have to be activated and sequestered in the extracellular matrix by plasminogen system proteinases of different families. Of note, urokinase-type plasminogen activator (u-PA) is essential for revascularization upon MI (Heymans *et al.*, 1999). In addition, hypoxia triggers VEGF expression by upregulation and stabilization of the transcription factor HIF-1 α (Forsythe *et al.*, 1996). Mechanistically, both bFGF and VEGF bind their RTK cell surface receptors. Ligand binding induces immediate receptor dimerization with subsequent intracellular autophosphorylation. This provides a basis for further signalling cascades transduced by Ras via mitogen-activated protein kinase (MAPK) to the cell nucleus (Cross and Claesson-Welsh, 2001). Interestingly, capillaries induced either by bFGF or VEGF show morphological differences implicating different roles for both angiogenic factors (Cao *et al.*, 2004). More importantly, the FGF system seems to control VEGF signalling during angiogenesis by control of VEGF expression (Seghezzi *et al.*, 1998; Presta *et al.*, 2005).

Endothelial cell survival or anti-apoptotic signalling activated by VEGF maintains and stabilizes newly formed blood vessels. The underlying mechanisms in human umbilical vein endothelial cells (HUVECs) comprise activation of the anti-apoptotic kinase, Akt/PKB, via a PI3K-dependent pathway (Gerber *et al.*, 1998). Sustained activation of cellular survival is reached by the upregulation of anti-apoptotic proteins like Bcl-2 thus inhibiting downstream caspase cascades (Gerber *et al.*, 1998). Furthermore, Akt activation stimulates the phosphorylation of the pro-apoptotic protein Bad thereby inhibiting apoptosis signalling (Khwaja, 1999). Additionally, sustained Akt activation enhances NO synthase expression thereby increasing second messenger NO (Dimmeler *et al.*, 1999; Fulton *et al.*, 1999).

Supporting the essential role of VEGF for EC survival, VEGF loss in mice is embryonal lethal due to enhanced EC apoptosis and hemorrhage (Carmeliet *et al.*, 1996, Ferrara *et al.*, 1996). In addition to the aforementioned angiogenic signalling angiogenesis can be routed by tiny non-coding RNAs (microRNAs) called “angiomiRs” which have been reviewed recently (Wang and Olson, 2009). Thereby, angiogenic factors are post-transcriptionally regulated and modulated.

Taken together, angiogenic signalling directly involves pro- or anti-apoptotic cascades. Underlying pathways and regulatory mechanisms are tightly embedded in fundamental cellular signal transduction networks.

1.2.2 Apoptosis signalling

The balance of cellular proliferation and apoptosis (programmed cell death) is an essential process during embryogenesis, organ development and in the adult regulating tissue homeostasis. In contrast to necrosis, apoptosis is characterized by an intact membrane structure. Additionally, apoptotic cells condense chromatin and shrink in size (Kerr *et al.*, 1972). The discovery of apoptotic pathways has led to a well-defined understanding of involved signalling cascades. Noteworthy, two pathways sharing common factors of the Bcl-2 protein family have been identified: An extrinsic guided by cell surface death receptors and an intrinsic pathway transduced by various Bcl-2 proteins directly affecting mitochondrial remodelling. Overall, both pathways aim towards the activation of cysteinyl aspartate proteases (caspases). Once activated, apoptosis cascades develop suicidal character thereby conducting substrate proteolysis and cellular destruction.

Briefly, the extrinsic pathway is triggered by the binding of death ligands like Fas or TNF α to their receptors therefore known as death receptors. Instantly, ligand binding induces conformational changes leading to the formation of an intracellular multiprotein complex (death induced signalling complex, DISC) recruiting and activating caspase-8 (Ashkenazi and Dixit, 1999). This initiator caspase then transduces death signals towards downstream executioner caspase-3 (Scaffidi *et al.*, 1998).

Additionally, caspase-8 might cleave Bid protein thus interacting and contributing to the intrinsic apoptosis pathway by altering mitochondrial architecture (Yin *et al.*, 1999). The mitochondria are the key cellular organelles for the intrinsic pathway (Newmeyer and Ferguson-Miller, 2003). Inducing signals comprise DNA damage, oxidative stress and growth factor deprivation. Underlying signal transduction is tightly regulated by gatekeeper Bcl-2 proteins that have opposing functions. Remarkable, pro-survival members like Bcl-2 or Bcl-xL are inhibited by direct interaction with Bad and Puma pro-apoptotic proteins characterized by a BH3 domain (Chen *et al.*, 2005). The direct inhibitory Bad Bcl-xL heterodimerization is reverted by kinase-dependent phosphorylation of Bad leading to a cytosolic sequestration with 14-3-3 proteins (Zha *et al.*, 1996). On the other hand, Bcl-2 and Bcl-xL counteract Bax and Bak function. These Bcl-2 proteins can oligomerize and structurally integrate into the mitochondrial outer membrane thus promoting pore formation and efflux of pro-apoptotic cytochrome c and Smac/Diablo (Mikhailov *et al.*, 2003). Moreover, mitochondria begin to fragment linking apoptosis to mitochondrial division machinery (Martinou and Youle, 2006). Cytosolic cytochrome c is bound by Apaf-1 thus scaffolding the apoptosome. Afterwards, this multimeric protein complex binds and activates caspase-9 (Hakem *et al.*, 1998; Shi, 2006). Additionally, Smac/Diablo can bind to caspase inhibitors thereby activating caspases independently from apoptosome mechanism (Du *et al.*, 2000). In cardiomyocytes, low levels of Apaf-1 require Smac/Diablo release from mitochondria for caspase activation. This mechanism delays apoptosis progress especially for post-mitotic cells offering an extra protection towards random death (Potts *et al.*, 2005). Interestingly, deregulated apoptotic events contribute to origin and progression of cardiovascular disease triggered by myocardial infarction for example. Meanwhile, global heart architecture suffers from the loss of cardiomyocytes and the decrease of surrounding vessels.

1.2.3 Endothelial cell apoptosis in the cardiovascular system

Generally, endothelial cells assembled in new vessels become stabilized may survive a long time. Therefore, endothelial survival necessarily serves as a potent mediator for the vasculature in the cardiovascular system. Nevertheless, programmed cell death (apoptosis) coordinates tissue homeostasis in development and adult tissue.

During embryonal development, VEGF depletion causes enhanced endothelial cell apoptosis (Carmeliet *et al.*, 1996, Ferrara *et al.*, 1996). Thereby, vascular abnormalities like hemorrhage appear which perturbate the generation of a proper vascular system. In the adult, pathological conditions such as congestive heart failure misbalance regulatory mechanisms in the cardiovascular system by inducing apoptosis in ECs thus leading to vessel remodelling (Rossig *et al.*, 2000).

Inductors of EC apoptosis include the inflammatory cytokine TNF α , reactive oxygen species (ROS), oxidized LDL or others (Robaye *et al.*, 1991; Dimmeler *et al.* 1997, 1999; Hermann *et al.*, 1997). Mechanistically, oxidized LDL and TNF α induce Akt dephosphorylation thus disabling the PI3K/Akt pathway (Hermann *et al.*, 2000). Furthermore, a lack of hemodynamic force results in EC apoptosis and vessel regression. Exposure of human ECs to laminar flow inhibits the activation of apoptotic caspase-3 via shear stress-stimulated release of NO. The second messenger NO then deactivates caspase-3 active site by S-nitrosylation (Hermann *et al.*, 1997). Pro-survival pathways for the endothelium are mostly mediated by the aforementioned pro-angiogenic cytokines VEGF and bFGF. By way of example, direct VEGF addition to cultured glucose-stressed ECs reverts the apoptotic phenotype (Yang *et al.*, 2008). Mechanistically, VEGF leads to suppression of Bax/Bcl-2 ratio, cleavage of caspase-3, reduction in excess ROS and prevention of calcium overload induced by high glucose concentration. Additionally, angiopoietin I (Ang I) may bind to Tie2 thus abrogating EC apoptosis via activation of PI3K/Akt pathway (Kim *et al.*, 1999, 2000).

In summary, endothelial cell apoptosis is dependent on different stimuli that also guide pro- or anti-angiogenic pathways (figure 1.3). Overall, intact capillary structure to provide nutrition and oxygen supply is a prerequisite for proper cardiac performance and function. The identification of potential genetic regulators is crucial for the development of appropriate therapeutics aiming at the modulation of angiogenesis. Besides the classical dogma of gene regulation by transcription factors, new gene regulatory pathways have risen offering great therapeutic opportunities.

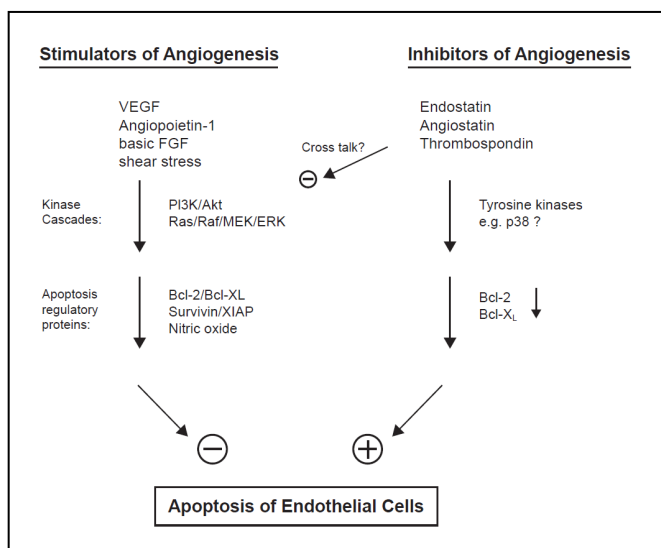


Figure 1.3: Regulatory stimuli influencing endothelial cell apoptosis. Diverse pro- or anti- angiogenic factors have an impact on the cellular apoptosis network (Dimmeler *et al.*, 2000).

1.3 MicroRNAs (miRNAs): regulatory RNAs

The discovery of small, 19-25 nucleotide long non-coding RNAs regulating gene expression post-transcriptionally in *C.elegans* in 1993 has established a broad field of research (Lee *et al.*, 1993; Wightman *et al.*, 1993). This new class of RNAs has been termed microRNAs (miRNAs) later on. Recently some issues about miRNA biology in mammals have been dissected while others are still unclear. More interestingly, miRNAs seem to be key players for many biological functions and processes including apoptosis (Brennecke *et al.*, 2003). Briefly, miRNAs are endogenous gene regulators, comprising more than 600 heavily conserved members still growing in number (data from miRBase at <http://microrna.sanger.ac.uk>). Thus, miRNAs are capable to regulate more than 30% of all protein-coding genes (Lewis *et al.*, 2005; Krutzfeldt and Stoffel, 2006; Griffiths-Jones *et al.*, 2008). MiRNAs repress target mRNAs through an antisense mechanism binding in the 3'-untranslated region (UTR) of mRNAs thereby inhibiting protein synthesis. In contrast to small inhibitory RNA (siRNA) mediated gene-silencing mammalian miRNAs often show partial complementary to respective mRNAs only. In cellular context a single miRNA might also be differently expressed.

More importantly, one miRNA has usually about at least 200 target mRNAs. Thus, miRNA-guided regulation of gene networks is quite usual because miRNAs *per se* affect more than one level of regulation. Investigations regarding miRNAs have been employed for various cell types and in diverse disease settings. Of note, miRNAs have been reported being dysregulated in human pathological disease like cancer or heart failure thereby offering interventional therapeutic approaches (Esquela-Kerscher and Slack, 2006; van Rooij and Olson, 2007; Thum *et al.*, 2007).

MiRNA biogenesis involves stepwise processes beginning with the transcription of miRNA genes, further processing towards functionally active miRNAs finally repressing translation (figure 1.4). Initially, miRNA genes characterized are transcribed by RNA polymerase II to primary miRNAs (pri-miRNAs) approximately 2 kb in length. Additionally, pri-miRNAs are 5' 7-methyl-guanosine (m7G)-capped and polyadenylated (Lee *et al.*, 2004).

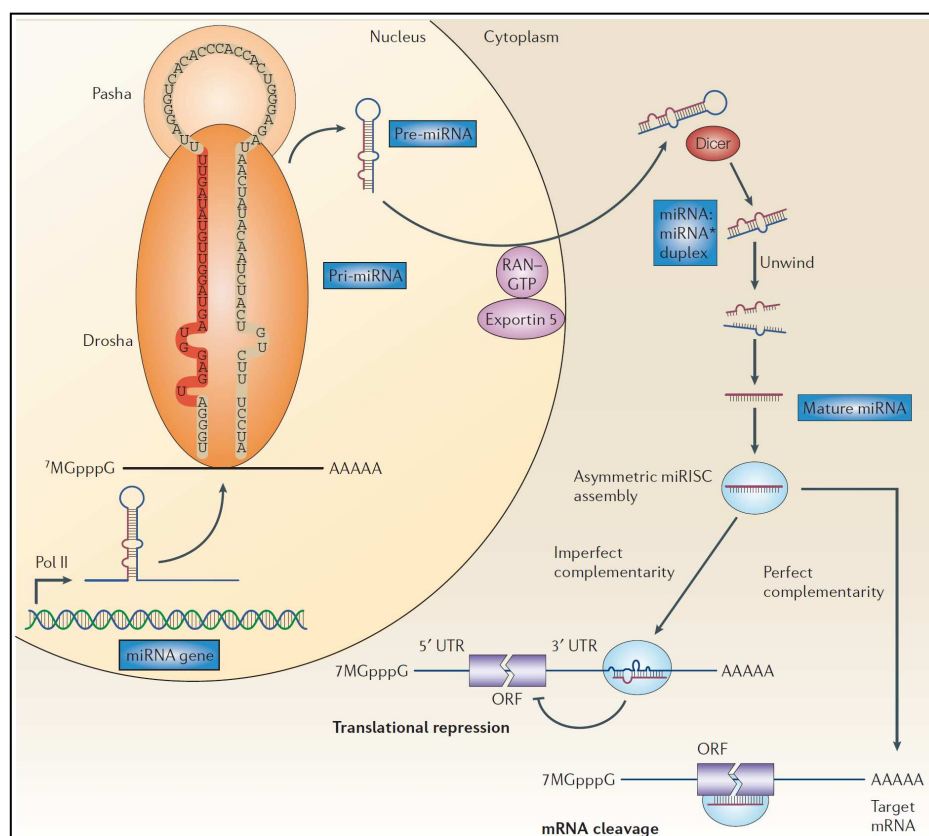


Figure 1.4: Overview on miRNA biogenesis and function. In the nucleus, miRNA genes are transcribed to pri-miRNA structures, processed and translocated by a nucleus export machinery to the cytoplasm. Here, miRNA and 3'-UTR target sequence form a heteroduplex leading to translational inhibition (Esquela-Kerscher and Slack, 2006).

Of note, miRNA genes are spread out the whole genome. Precisely, miRNA genes can occur within genes (intronic) or just between genes (intergenic). Intronic miRNAs or “miRtrons” are thus spliced and generated from primary gene transcripts of their host genes thereby offering an alternative mechanism to classical processing of pri-miRNAs (Ruby *et al.*, 2007). Moreover, miRNA genes are often clustered and transcribed in polycistronic manner cooperatively (Altuvia *et al.*, 2005). Nonetheless, the regulation of miRNA expression is mostly unclear. Some miRNA genes possess unique promoter or enhancer regions. By way of example, this scenario has been suggested for transcriptional activation by serum response factor (Niu *et al.*, 2007). In contrast, other miRNA gene loci are regulated by regulatory elements that are responsible for host gene transcription thus located far away.

In the nucleus, pri-miRNAs are further processed to stem-loop pre-miRNAs. A 500-600 kDa microprocessor complex consisting of the nuclear RNaseIII endonuclease Drosha and cofactor DiGeorge-syndrome critical region protein 8 (DGCR8, Pasha) is necessary to generate 60-70 nucleotide pre-miRNA. Interestingly, pre-miRNAs characterize a 3' overhang of 2 nucleotides being a signal for further recognition (Gregory *et al.*, 2004). Being the key of miRNA biogenesis, nuclear exportin-5 mediates translocation of pre-miRNAs to the cytoplasm (Lund *et al.*, 2004). In the cytosol, pre-miRNAs are cleaved by a RNaseIII enzyme Dicer containing complex along with the transactivating response RNA-binding protein (TRBP) (Hutvagner *et al.*, 2001). This step generates the mature hairpin duplex designated as miRNA-miRNA*. The inhibition of translation initiation is finally mediated by the RNA-induced silencing complex (RISC). Thus, one strand of the miRNA duplex is preferentially incorporated into RISC while the miRNA* strand is degraded (Gregory *et al.*, 2005). Nevertheless, a gene suppressive function for the miRNA* strand has been reported since it can associate with RISC proteins (Okamura *et al.*, 2008). The RISC scaffold is built up by proteins like aforementioned Dicer-TRBP complex and argonaute (AGO) proteins comprising a class of four members (Kim *et al.*, 2009). Essentially, TRBP guides Dicer and miRNA to AGO2 assembling RISC (Chendrimada *et al.*, 2005). Noteworthy, AGO2 characterizes endonucleolytic activity as well as inhibitory effects on binding of translation initiatory factor eIF4E to m7G capped sites. Thus AGO2 can be defined as the catalytic engine of RISC (Liu *et al.*, 2004; Kiriakidou *et al.*, 2007). Finally, RISC is guided to the 3'-UTR of potential target mRNAs.

Here, base pairing between the 5' seed region of the miRNA (bases two to eight) and target mRNA is predominantly crucial for tight binding. Additionally, seed region surrounding bases can support target mRNA recognition (Lewis *et al.*, 2005). Subsequently, further translation is stopped whereby underlying mechanisms may vary. Besides the aforementioned inhibition of translation initiation other mechanistical options include mRNA sequestration in cytoplasmic foci called P(processing) bodies or transcript degradation (Pillai *et al.*, 2007; Liu, 2008).

Interestingly, RNAs can be edited in their nucleotide sequence by adenosine deaminases (ADARs) (Bass, 2002). Thus, binding to the stem-loop structure of pre-miRNAs results in adenosine to inosine nucleotide change. In turn, inosine mimicks guanosine base thereby affecting miRNA target recognition as it has been reported for *miR-22* (Luciano *et al.*, 2004). Furthermore, RNA editing at position 1 or 2 of the predicted mature miRNA strand in the stem-loop of pre-*miR-22* influences strand choice for assembling RISC by altering thermodynamic parameter (Khvorova *et al.*, 2003; Schwarz *et al.*, 2003).

In summary, the field of miRNA biology opens a new level of cellular regulation, especially in regard to certain organ or cell-type specific mechanisms in disease. The biology of miRNAs bears a great potential to target and balance whole gene networks. As a result, understanding these effects is more complicated since the pluripotency of target recognition and regulation has to be kept in mind.

1.3.1 MiRNAs in the cardiovascular system

MicroRNAs contribute to both physiological and pathophysiological reactions in the cardiovascular system. Initially work has focused on miRNA deregulation in different cardiac stress models. Van Rooij *et al.* applied transverse aortic constriction (TAC) and a transgenic calcineurin mouse model both resulting in maladaptive responses of the heart. Performing microarrays from miRNAs, these disease model systems revealed several deregulated miRNAs. Additionally, *in vitro* transfection of selected miRNAs to cultured cardiomyocytes resulted in hypertrophic growth further underlying the deep impact on cardiac structure.

Noteworthy, some of the stress-model enhanced miRNAs have also been upregulated in end-stage heart failure hearts (van Rooij *et al.*, 2006). These important observations emphasize a potential role of miRNAs in settings of human cardiovascular disease.

Stress-conditions like persistent cardiac hypertrophy leading to cardiac failure have been described to rely on fetal gene expression (Izumo *et al.*, 1988). Recently, investigators have linked this fetal gene reprogramming to the expression of miRNAs in the heart. By the use of microarray analysis researchers have shown that the miRNA expression profile in failing hearts was comparable to that of fetal hearts. In addition, down- and upregulated target mRNAs matched the profile for up- and downregulated miRNAs. Therefore, combination of miRNA expression pattern and target prediction could explain fetal gene reprogramming in heart failure as our group has shown before (Thum *et al.*, 2007).

Next to different cardiac stress models transgene research has highlighted the importance of miRNAs in the cardiovascular system. In addition to the initial finding that miRNAs are deregulated upon cardiac stress van Rooij *et al.* constructed a transgene with cardiomyocyte specific overexpression of *miR-195*. Mice suffered from cardiac hypertrophy and heart failure, highlighting that one single deregulated miRNA can induce cardiac failure (van Rooij *et al.*, 2006).

Moreover, the miRNA processing factor Dicer has been manipulated in animal model by da Costa Martins *et al.* Hence, inducible cardiac Dicer knockout animals were generated because Dicer null knockouts *per se* are embryonal lethal due to misbalanced cardiogenesis (Zhao *et al.*, 2007). Both young and old mice developed cardiac failure when shutting down Dicer expression. More importantly, young mice died shortly after Dicer knockdown whereas older mice survived for a longer time. Hence, cardiac failure in younger mice was not accompanied by strong alterations in the myocardium as it appeared in the elderly. Obviously, this finding might be explained by an essential and stronger miRNA impact on cardiac structure in younger mice (da Costa Martins *et al.*, 2008).

DGCR8, another important factor of the miRNA processing machinery upstream of Dicer has recently been investigated in a knockout model. Cardiac-specific deletion led to dilated cardiomyopathy characterized by enhanced fibrosis and survival in median 31 days post birth. In contrast to the aforementioned conditional Dicer knockout, no hypertrophy was detectable (Rao *et al.*, 2009).

These *in vivo* observations implicate a principal *modus operandi* of miRNAs in the cardiovascular system. Moreover, cardiac-specific impact of several miRNAs has been reported. Thus, dissecting cardiac cells into cardiomyocytes, cardiac fibroblasts and endothelial cells may help to understand miRNA-guided gene regulation in the heart.

1.3.1.1 Cardiomyocyte miRNAs

Cardiomyocytes have a central role for cardiac function. Several miRNAs have been identified to be important for cardiomyocyte biology. *MiR-1* possesses an outstanding role based on its relative abundance in cardiac tissue covering 40% of all present miRNAs (Rao *et al.*, 2009). Initially, Zhao *et al.* showed that *miR-1* comprising the microRNAs *miR-1-1* and *miR-1-2* is primarily localized in the heart and skeletal muscle. The microRNA expression is regulated by serum response factor (SRF) which can bind to enhancer elements in the promoter region of *miR-1-2* stimulating transcriptional activity. Functional overexpression of *miR-1* with the use of β -myosin heavy chain (MHC) promoter in the developing heart caused a decrease in cardiomyocyte proliferation. This, in turn, misbalanced and inhibited correct ventricular function. On the molecular level, this observation could be explained by the regulative effect of *miR-1* towards the cardiac transcription factor Hand2 which is important for functional cardiogenesis (Zhao *et al.*, 2005). The group of Zhao *et al.* also constructed a *miR-1-2* mouse knockout transgene to analyze loss of a specific miRNA. Indeed, cardiac morphogenesis and performance was altered strikingly. Histological analysis revealed ventricular septum defects as well as cardiac edema which led to 50% embryonal lethality.

The aforementioned transcription factor Hand2 was induced on protein level giving again a clue for fatal cardiogenesis because Hand2 dosage is crucial for functional cardiac development (McFadden *et al.*, 2005). Moreover, electrical conduction was disturbed. The correct transducing mechanism is a prerequisite for ventricular depolarization in healthy state. Mechanistically, investigators found the *miR-1-2* target *Irx5*, a regulator of cardiac potassium channeling, is deregulated in mutant mice suggesting a commitment to the phenotype.

MiR-1 knockout mice exhibited a prolonged phase of mitotic adult cardiomyocytes inducing cardiac hyperplasia. Loss of *miR-1-2* might loosen inhibitory cell cycle control in differentiated cardiomyocytes (Zhao *et al.*, 2007). These *in vivo* studies provides evidence for a superior role of *miR-1* in the regulation of cardiac performance and function.

Since *miR-1* is transcribed in a bicistronic gene cluster with *miR-133*, this miRNA has also been investigated intensively. Indeed, *miR-133* also regulates cardiomyocyte signalling (Care *et al.*, 2007). Likewise, *miR-133* is highly expressed specifically in skeletal muscle and cardiac myocytes. Carè *et al.* also observed decreased levels of *miR-1* and *miR-133* in different models of murine cardiac hypertrophy as well as in human samples of heart failure. Therefore, investigators proposed that microRNA expression pattern is inversely correlated to cardiac hypertrophy. In line, *in vitro* experiments further emphasized the regulative role of *miR-133* for cardiomyocyte hypertrophy. Cardiomyocytes overexpressing *miR-133* were capable to inhibit hypertrophic response to stimulative phenylephrine. Furthermore, this inhibitory reaction was observed in modulated neonatal and adult cardiomyocytes. Again, *miR-133* expression was found to be low in phenylephrine-induced hypertrophic cardiomyocytes further supporting the idea of an inverse correlation of *miR-133* expression level towards progression of cardiac hypertrophy. Indeed, *in vitro* antagonizing *miR-133* caused quick progression of a hypertrophic response (induction of fetal genes, increase in protein synthesis and cell size). To analyze a functional relationship between *miR-133* and *miR-1*, experiments for *miR-133* were substituted to *miR-1*. These experiments pointed to a tight cooperation of these two miRNAs for the regulation of cardiac hypertrophy. Mice receiving osmotic minipumps delivering an antagonist for *miR-133* displayed that *miR-133* downregulation resulted in the formation of hypertrophic hearts. In addition, hypertrophic marker genes were upregulated in this setting.

To further explain downstream *miR-133* signalling bioinformatic and *in vitro* reporter gene assays validated potential *miR-133* targets. Substantial target regulation was reported for RhoA, Cdc42 and Whsc2 which are proteins linked to hypertrophic biology. Taken together, the observations describe a crucial and regulative role of *miR-133* for *in vitro* and *in vivo* cardiac hypertrophy.

The aforementioned induction of fetal genes in hypertrophic hearts comprises the well-known switch of the α -MHC ATPase to the expression of β -MHC ATPase (Lowe *et al.*, 1997; Nakao *et al.*, 1997). This modulation results mainly in decreased cardiac contractility. The group of van Rooij *et al.* deciphered a *miR-208* based mechanism that controls the α/β -MHC switch (van Rooij *et al.*, 2006). Noteworthy, *miR-208* is encoded by the intron 27 of the α -MHC gene and is also highly expressed in cardiac tissue compared to other organs. Specific blockade of T3-hormone signalling in wild-type mice led to a decrease in α -MHC, a subsequent increase in β -MHC and finally to a more slower decrease in *miR-208* expression suggesting high stability of this miRNA. *In vivo*, a mouse *miR-208* knockout showed a stunning reaction towards cardiac stress applied by trans-aortic banding: The typical hypertrophic response in wild-type animals was abandoned in the transgene. In addition, the transgene could not upregulate β -MHC but other cardiac stress markers indicating that *miR-208* is essential for the hypertrophy response but not for the expression of further cardiac stress proteins. These implications were further emphasized by the finding that transgenic overexpression of *miR-208* could upregulate β -MHC. Again, pharmacogenetic inhibition of T3-hormone signalling was applied to test for phenotypic transgene analysis. *MiR-208* knockout animals failed to induce β -MHC whereas induction was prominent in wild-type animals suggesting that *miR-208* interferes with specific transcriptional repressors of β -MHC. Mechanistically, THRAP1, a transcriptional co-regulator of hormone receptor signalling involved in β -MHC regulation at the transcriptional level was validated to be a direct *miR-208* target. These findings claim a substantial role of *miR-208* for cardiomyocyte stress response. More recently, these observations were extended by the finding that *miR-208* is also required for correct cardiac transcription factor GATA4 expression being a direct target for *miR-208* (Callis *et al.*, 2009). Additionally, gain- and loss-of function experiments for *miR-208* pointed to a role in cardiac biology.

1.3.1.2 Fibroblast miRs

Fibrosis is a maladaptive tissue response reaction existing in different disease conditions. A hallmark of cardiac fibrosis is the accumulation of collagens and extracellular matrix proteins impairing cardiac contractility and ventricular function.

Mechanistically, TGF- β signal transduction possesses a key function for extracellular remodelling during cardiovascular injury triggering extracellular remodelling (Khan and Sheppard, 2006). Besides the role of miRNAs for cardiomyocyte biology, several miRNA-based mechanisms have been deciphered for fibrotic cardiovascular events. Primarily, cardiac disease deregulated miRNAs have been chosen for mechanistical investigations aiming at fibrotic modulation.

Among the highly upregulated miRNAs in heart failure, *miR-21* action in cardiac failure could be described recently by our group (Thum *et al.*, 2008). More interestingly, *in situ* hybridization showed a specific upregulation in cardiac fibroblasts. This indicates cell-type-dependent impact of *miR-21*. Unravelling fibroblast-specific mechanisms *in vitro*, miRNA modulation was capable to modulate apoptosis. Antagonizing *miR-21* led to reduced survival of cardiac fibroblasts. Reduced cell survival was explained by a derepression of direct *miR-21* target Sprouty-1 which is primarily localized to fibroblast-enriched areas of the heart. Moreover, derepressing Sprouty-1 increased inhibition of pro-survival ERK signalling. Transferring these observations into an *in vivo* cardiac stress model, transverse aortic constriction was applied. Both prevention and treatment therapy aimed at antagonizing *miR-21* by sequestering endogenous miRNA with a complementary cholesterol-modified oligonucleotide (antagomir). Cardiac performance improved markedly in treatment groups and most remarkably, cardiac fibrosis was diminished (prevention strategy) or reversed (treatment strategy). The effective therapy has proven a promising approach for the modulation of cardiac fibrosis upon cardiac stress.

While investigating miRNAs found to be dysregulated upon myocardial infarction, van Rooij *et al.* concentrated on the mechanistic role of *miR-29* (van Rooij *et al.*, 2008).

In the group of downregulated miRNAs post MI, *miR-29* was found to be a critical regulator for the *in vivo* fibrotic response during cardiac remodelling. *miR-29* is also enriched in the fibroblast cell population in the heart. Moreover, predicted targets comprise extracellular matrix proteins and collagens. Thus, theoretically, downregulation of *miR-29* should derepress these mediators leading to enhanced fibrotic activity. Indeed, several collagens and matrix proteins were validated as direct *miR-29* targets supporting this theory. Further evidence was taken from animal experiments using a *miR-29* mimic post myocardial infarction. In this situation, enhancing *miR-29* decreased the fibrotic response. Additionally, aforementioned direct *miR-29* targets were downregulated. On the whole, this therapeutic approach reveals a tool to modulate fibrosis via impairing its fundamental factors.

Another crucial regulator of extracellular remodelling is connective tissue growth factor (CTGF) (Duisters *et al.*, 2009). Duisters *et al.* showed an increased CTGF expression upon cardiac stress *in vivo* which correlated to decreased amounts of *miR-30* and *miR-133*. As mentioned before, *miR-133* is cardiomyocyte enriched, whereas researchers found *miR-30* in a higher expression level in fibroblasts. Bioinformatic analysis revealed that both miRNAs might target CTGF. The origin of CTGF is diverse: fibroblasts produce CTGF, but also stressed cardiomyocytes secrete CTGF stimulating extracellular protein synthesis. *In vitro* assays established the direct CTGF regulation by *miR-30* and *miR-133* either in cardiomyocytes or fibroblasts. Hence, cell-type specific miRNA expression and target availability determines the impact of modulation in cardiomyocytes or fibroblasts. Although a concrete therapeutic therapy is missing in this study, useful clues are given for the modulation of cardiac fibrosis balanced by CTGF.

1.3.1.3 Endothelial miRs (angiomiRs)

The blood vessel network in the heart is responsible to provide sufficient nutrition and oxygen supply. Disturbance of endothelial biology may result in severe disorders of the heart. The importance of miRNAs for blood vessel formation was primarily shown in Dicer transgenic mice. Here, alteration of miRNA-processing Dicer led to embryonal lethality due to impaired vasculature in the developing embryo (Yang *et al.*, 2005).

Moreover, endothelium-specific and conditional Dicer knockout mice resulted in decreased angiogenic response to VEGF-stimulation. This underscores an *in vivo* requirement for endothelial miRNAs in angiogenesis (Suarez *et al.*, 2008). In addition, silencing Dicer or Drosha in cultured endothelial cells impaired angiogenic properties (Kuehbacher *et al.*, 2007; Suarez *et al.*, 2007).

The first study describing a miRNA profile in endothelial cells was done by Poliseno *et al.* Here, investigators found a distinct miRNA signature of highly expressed miRNAs. In addition, bioinformatic analysis revealed that important angiogenic transmembrane receptors may be targeted by abundant miRNAs. To assess functional impact, *in vitro* overexpression of *miR-221* and *miR-222* mixture impaired tube formation and migratory capacity. Furthermore, the angiogenic receptor c-kit was downregulated in *miRNA*-modulated cells. These findings emphasize that *miRNA*-modulation of ECs specifically regulates angiogenic mechanisms (Poliseno *et al.*, 2006).

Until now only one miRNA was suggested to be exclusively expressed in ECs. This pivotal feature belongs to *miR-126*. In 2008, three independent groups analyzed and reported vascular defects in *miR-126* deficient zebrafish and mice (Fish *et al.*, 2008; Wang *et al.*, 2008; Kuhnert *et al.*, 2008). In zebrafish, antagonizing experiments induced hemorrhage in the developing organism. *miR-126* morphants displayed collapsed endothelial lumens highlighting the role of *miR-126* for establishing vascular structure in development. Mechanistically, Spred1 which is a negative regulator of cell survival was validated as a direct *miR-126* target being theoretically derepressed in *miR-126* deficient zebrafish. To analyze this hypothesis, Spred1 was overexpressed in the developing zebrafish. Indeed, Spred1 upregulation caused a similar vascular phenotype also seen in the *miR-126* morphant (Fish *et al.*, 2008). In mice *miR-126* knockouts, miRNA-deletion caused a phenotype also characterized by severe vascular defects with hemorrhage and edema (Wang *et al.*, 2008). Remarkable, 40% of knockout animals died in embryonal phase or perinatally. Functional analysis further showed a reduced angiogenic response in knockout animals when considering EC migration into implanted matrigel plugs. More interestingly, in a model of myocardial infarction, *miR-126* deficient mice were not able to survive a three week time span upon MI. This emphasizes the need of *miR-126* dependent regulation for neovascularization supporting cardiac healing.

Again, Spred1 was reported being the crucial *miR-126* target. Downregulation of Spred1 by *miR-126* is necessary to transduce pro-survival signalling in endothelial cells thus inducing angiogenic events. The complexity of the *miR-126* genelocus has further been of potential interest. Since *miR-126* is located within an intron of the *Egfl7* gene, questions arose whether the vascular abnormalities seen in *miR-126* mice are due to the loss of *miR-126* or *Egfl7*.

Egfl7 knockout mice also suffer from vascular abnormalities which were proposed to rely on impaired angiogenic signalling mediated by chemoattractant *Egfl7* (Schmidt *et al.*, 2007). To address the question if *miR-126* or *Egfl7* is the key player for proper conductive vasculature, Kuhnert *et al.* generated mice deficient for minimal *miR-126* sequence and compared the phenotype to whole *Egfl7* knockouts. Finally, the aforementioned vascular defects were only observable in mice deficient of *miR-126* highlighting the requirement of *miR-126* for the developing and postnatal vasculature (Kuhnert *et al.*, 2008).

Combinatorial action of clustered miRNAs is another option for miRNA-guided regulation of angiogenesis. The oncogenic *miR-17~92* cluster was first described for inductive tumor expansion. The augmentation in tumor growth was explained by the direct downregulation of cluster targets thrombospondin-1 (Tsp1) and CTGF. Both targets are well-known negative angiogenic regulators. Thus, targeting *miR-17~92* cluster may serve as a promising approach in cancer research (Dews *et al.*, 2006). Besides its role in cancer, cluster member *miR-92* was recently attributed to anti-angiogenic function in ischemic disease and therefore was suggested to be a relevant therapeutic target (Dimmeler *et al.*, 2009).

1.3.2 MiRNA antagonists (“antagomirs”) for *in vivo* application

The abundance of miRNAs and the deregulation of miRNAs in many diseases opened a field of research to eliminate cellular miRNAs thereby derepressing miRNA targets. In 2005, Krutzfeldt *et al.* investigated the application of a modified RNA oligo (figure 1.5) complementary to a specific miRNA in mice (Krutzfeldt *et al.*, 2005, 2006). The so-called “antagomir” was injected in the tail vein and could specifically eliminate miRNA of interest

in several tissues except the brain. Moreover, the antagomir itself was not degraded by the *in vivo* exonuclease machinery since its sugar backbone is modified by stable phosphothioate bonds at 5' and 3' prime ends. Antagomir target recognition is importantly dependent on precise nucleotide sequence bearing a perfect match to miRNA of interest. Finally, the target miRNA:antagomir duplex is degraded in a cytosolic compartment which does not overlap with P(processing)-bodies indicating that this process is different from the small-inhibitory RNA (siRNA) pathway (Kruzfeldt *et al.*, 2005, 2007).

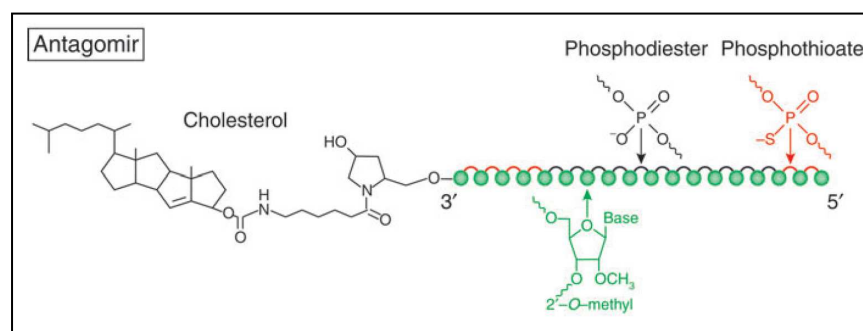


Figure 1.5: Chemical structure of an antagomir (Kruzfeldt *et al.*, 2006). The partially phosphothioate- and 2'-O-methyl-modified RNA oligo is linked to a cholesterol support.

Since this initial application several antagomirs have been tested for outcome on cardiac function. Essentially, deregulated miRNAs have been mostly chosen for further investigation. Antagonizing *miR-133* resulted in sustained cardiac hypertrophy, implicating a control mechanism for cardiac hypertrophy (Carè *et al.*, 2007). Antagomirs have also been used in therapeutic settings upon pathologic stress. Investigators have shown *miR-21* upregulation post MI. Consequently, mimicking pathologic stress, mice underwent trans-aortic constriction (TAC) and were treated with constant doses against *miR-21*. Treatment resulted in beneficial effects for cardiac performance measured by reduced fibrotic area and improved pump function compared to control antagomir treatment (Thum *et al.*, 2008). Although *miR-92a* has not been reported to be deregulated under pathological conditions in the heart, antagonizing this miRNA in a mouse model of hind limb ischemia and MI has showed an interesting finding. Angiogenesis improves in animals receiving antagomir-92a indicating a potential therapeutic value in ischemic diseases (Bonauer *et al.*, 2009).

Collectively, application of antagomirs *in vivo* can be a valuable tool to support healing or wounding processes. Nonetheless application has to be done carefully, since antagomirs can reach nearly every tissue which is connected to the blood stream. Side-effects in other organs might occur quite often. As a result, investigators try to modify antagomirs by cell type specific antibodies minimizing unwished off-target effects.

1.4 *MiR-24* genelocus and *miR-24* function

The human *miR-24* genelocus is encoded by two distinct chromosomal sites and is clustered with *miR-23a/b* and *miR-27a/b* (data from miRBase at <http://www.mirbase.org/> and figure 1.6). Mature sequences are identical but specified as *miR-24-1/2* since the genelocus for *miR-24-2* is intergenic, whereas *miR-24-1* is transcribed intronically from the host-gene encoding an aminopeptidase (data from Entrez Gene at <http://www.ncbi.nlm.nih.gov>). In addition, two minor mature miRNA sequences can be processed from the pre-miRNA stem loop structure designated as *miR-24-1/2**. The asteristik describes the complementary sequence to the mature miRNA sequence which is in 5'→3' direction.

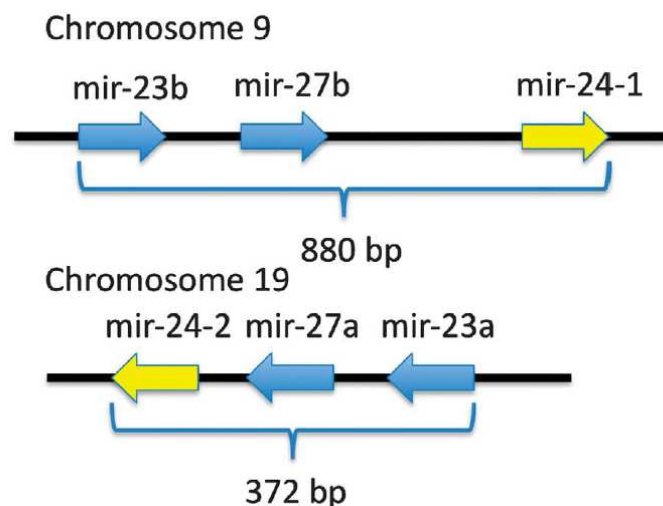


Figure 1.6: Overview on distribution of genomic *miR-24* loci. *miR-24* is transcribed with clustered miRs *miR-23a/b* and *miR-27a/b* from chromosome 9 and 11 (Chan *et al.*, 2010).

For the first time, detailed investigations regarding the clustered genelocus for *miR-23a-27a-24-2* revealed RNA Polymerase II-driven transcription of miRNA genes. Additionally, a promoter region has been defined comprising sequences with no obvious regulatory elements despite GC-boxes (Lee *et al.*, 2004). In addition, *miR-24-1* has been described to be potentially activated by hypoxic conditions probably through hypoxia-inducible factor-1 (HIF-1) in cancer cells, although the HIF-1 responding regulatory elements are located within 5 kb upstream. Therefore, *miR-24* has been classified as a hypoxia-regulated miRNA (HRM) besides others (Kulshreshtha *et al.*, 2007).

In contrast to the aforementioned *miR-24-2* genecluster, *miR-24-1* cluster is located intronically. Expression of the clustered *miR-23b-27b-24-1* miRNAs has been induced by BMP2 signalling in mice. Noteworthy, differential expression of clustered miRNAs has been observed indicating specific pri-miRNA processing (Sun F *et al.*, 2009). Moreover, and of interest, *miR-24* is upregulated by cardiac hypertrophy and in end-stage failing hearts (van Rooij, 2006). Additionally, *in vitro* overexpression in cardiomyocytes led to hypertrophic growth implicating a role in heart remodelling and interestingly, a cardiomyocyte-specific overexpressing *miR-24* transgene is embryonal lethal, suggesting a pivotal role for proper heart development.

MiR-24 expression has not been reported to be cell type specific (figure 1.7). Moreover this miRNA is expressed ubiquitously with highest expression level in heart and lung tissue assessed by Northern Blot and its expression was found to be repressed by SMADs (Sun Q *et al.*, 2008).

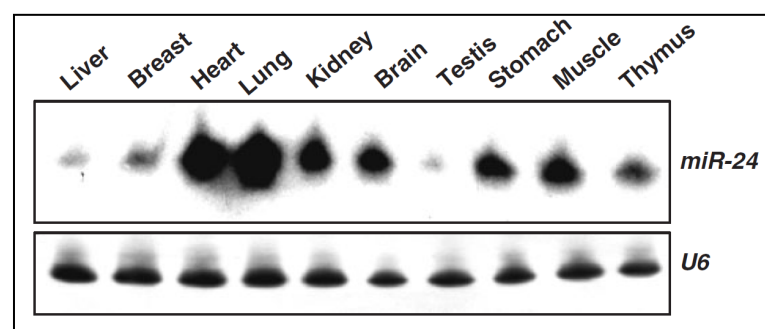


Figure 1.7: *miR-24* expression in different organs measured by Northern blot analysis (Sun Q *et al.*, 2008). *miR-24* expression is normalized to house keeping small nuclear RNA *U6* (*RNU6b*).

Downstream target analysis for *miR-24* has revealed some interesting issues about *miR-24* function. *MiR-24* has been investigated in the context of erythropoiesis in erythroleukemic K562 cells. Gain-of function experiments show the human activin type I receptor ALK4 (hALK4) to be a direct target. Consequently, SMAD2 signalling cascades are disturbed as well as downregulation of hemoglobin causing a delay in erythroid differentiation. Furthermore, *miR-24* expression level has also been observed to be inversely correlated with erythroid differentiation progress in CD34⁺ progenitor cell population (Wang *et al.*, 2008).

Another group has observed upregulation of *miR-24* when inducing blood cell differentiation with hemin. Here, the histone variant H2A.X involved in DNA repair is negatively regulated (Lal *et al.*, 2009). *In vitro*, H2A.X modulation causes higher susceptibility towards genotoxic insults, whereby overexpressing a *miR-24* insensitive H2A.X, variant could rescue the deficient phenotype. More importantly, the *miR-24* target H2A.X has recently been described to have a substantial role in neovascularization events (Economopoulou *et al.*, 2009). *In vitro*, hypoxic treatment of HUVECs led to the activation of H2A.X by phosphorylation. This activation was counteracted by the transient knockdown of H2A.X which decreased endothelial proliferation capacity under hypoxic conditions. Additionally, an *in vivo* model of hindlimb ischemia in endothelium specific H2A.X knockout animals validated and emphasized reduced neovascularization upon implantation of tumor cells. Thus, H2A.X seems to be a key player for hypoxia-driven neovascularization. Recent work also suggested that *miR-24* influences cell cycle progression thereby regulating cellular proliferation state (Lal *et al.*, 2009). Global transcriptome analysis in naturally *miR-24* low-expressing Hep2G cells revealed several cell cycle and DNA repair important factors being modulated when overexpressing *miR-24*. In line, cell cycle analysis showed an inhibitory effect for *miR-24* on cell cycle progression. Interestingly, downregulated targets like Myc contained a *miR-24* binding site (seed region), whereas others like E2F did not. Both transcription factors were validated by luciferase assay to be direct *miR-24* targets thus orchestrating gene networks. The downmodulation of Myc implicates that further microRNA responsive elements (MREs) are responsible for target recognition in the 3'-UTR of Myc which lack a seed region. Detailed investigation of myoblast development has revealed upregulation of *miR-24* which could be inhibited by TGF- β 1 forced SMAD3 signalling binding directly to proposed *miR-24* promoter region site (Sun Q *et al.*, 2008).

Moreover, TGF- β 1 repressed myogenesis can be modulated by overexpressing *miR-24* leading to enhanced myoblast differentiation. On the whole the authors suggest that this modulation is supported by simultaneous expression of *miR-24* clustered miRNAs. Nevertheless, *miR-24* has also been reported to have an impact on TGF- β signalling itself in fetal mouse liver development (Rogler *et al.*, 2009). Here, upregulation of the *miR-23b* cluster including *miR-23b*, *miR-27b* and *miR-24-1* targets SMAD proteins SMAD3, 4, 5 thereby diminishing TGF β signalling and influencing cell fate choice.

In fibroblast or carcinoma cells ectopic overexpression of *miR-24* regulates the tumor suppressor protein p16(INK4a) thereby affecting replicative senescence of these cells (Lal *et al.*, 2008). Additionally, antagonizing *miR-24* enhances p16(INK4a) protein level. *MiR-24* has been described to prevent retina apoptosis in developing *Xenopus laevis* (Walker and Harland, 2009). *In vivo*, antisense nucleotides (morpholinos) against *miR-24* induced retina cell apoptosis. In contrast, injecting *miR-24* in the developing *Xenopus* reverted malformation of the eye. Apoptosis modulation has also been observed while overexpressing the *miR-23a-27a-24-2* genecluster in human embryonic kidney cells (Chhabra *et al.*, 2009). Here, enhanced cluster expression induced apoptosis suggesting an impact on apoptosis signalling. Nevertheless, *miR-24* is not the only mediator but participates in coordinated pro-apoptotic regulation.

In summary, the current findings on *miR-24* indicate that this microRNA is an important regulator in diverse cellular types having an impact on development, differentiation and certain cellular signalling processes. In addition, *miR-24* clustered and genetically neighbouring miRNAs may support the impact on target regulation. Nevertheless, the role of *miR-24* in the cardiovascular system remains elusive.

1.5 Scope and aim of this study

Pathological cardiac remodelling post MI involves many signalling pathways being dysregulated. Genetic pathways in numerous cardiac cell types are subsequently altered with deleterious outcome. MiRNAs target several mRNAs thus regulating complex gene networks.

In diseased states, several cardiac miRNAs are deregulated and contribute to mRNA transcriptome alterations and cardiovascular disease (van Rooij *et al.*, 2006; Thum *et al.*, 2007). Underlying miRNA-guided molecular mechanisms in cardiac angiogenesis are less defined. Thus, in this study, the role of cardiac miRNAs in MI-induced cardiac remodelling is investigated. Moreover, potential regulatory mechanisms for cardiac angiogenesis are dissected. Specifically in this work, effects of MI-deregulated *miR-24* on endothelial function *in vitro* and *in vivo* are investigated. In context of MI *miR-24* function is unclear, especially in regard to neovascularization. Thus, *miR-24* guided mechanisms and characteristics in response to MI have to be investigated. In addition, endothelial *miR-24* targets have to be found and validated by *in vitro* assays. For *in vivo* translational research a disease setting of murine myocardial infarction is applied. Hence, *miR-24* is antagonized by a specific compound (antagomir) upon MI. Following a therapeutic periode basic heart parameters are determined and validated. Additionally, other aspects regarding *in vivo* heart remodelling are investigated, especially focusing on cardiac angiogenesis. Taken together, this work aims towards further functional clues, understanding and transparency of MI-deregulated *miR-24*.

2. Material and Methods

2.1 Material

2.1.1 Equipment

Table 2.1: Devices used for this work

Device	Type	Manufacturer
Autoclave	VARIOKLAV [®]	H+P Labortechnik, Oberschleissheim, Germany
Bioanalyzer	Agilent 2100 Bioanalyzer	Agilent, Böblingen, Germany
Bioanalyzer software	Agilent 2100 Expert	Agilent, Böblingen, Germany
Blotting apparatus	Mini Trans-Blot [®] Electrophoretic Transfer Cell	Bio-Rad, Munich, Germany
Bunsen burner	Campingaz Labogaz 206	Camping Gaz, Hungen- Inheiden, Germany
CellQuest software	CellQuest software	BD Biosciences, Franklin Lakes, USA
Centrifuge	Biofuge fresco	Thermo Fisher Scientific, Langenselbold, Germany
Centrifuge	Heraeus Megafuge 1.0R	Thermo Fisher Scientific, Langenselbold, Germany
ChemiImager	ChemiImager 5500	Alpha Innotech, San Leandro, USA
Chemi5500 software	Chemi5500	Alpha Innotech, San Leandro, USA
Cryotome	Leica CM1850	Leica Microsystems, Wetzlar, Germany
Echo device	Toshiba PowerVision 6000	Toshiba Medical Systems, Neuss, Germany
Electrophoresis chamber agarose gels	Mini Sub-Cell [®] GT	Bio-Rad, Munich, Germany
Electrophoresis chamber SDS-PAGE	Mini Protean [®] Tetra Cell	Bio-Rad, Munich, Germany
Electrophoresis chamber western blot	Mini Trans Blot Cell	Bio-Rad, Munich, Germany
ELISA reader	Multiplate reader 550	Bio-Rad, Munich, Germany

Device	Type	Manufacturer
FACS	FACS Calibur	BD Biosciences, Franklin Lakes, USA
Fluorescence microscope	Axiovert 135	Zeiss, Jena, Germany
Freezer (-20°C)	Liebherr comfort	Liebherr, Biberach an der Riss, Germany
Freezer (-80°C)	HERA freeze	Thermo Fisher Scientific, Langenselbold, Germany
Fridge (4°C)	BioCompact II 200	Gram-Bioline, Vojens, Denmark
Heating block	Thermomixer compact	Eppendorf, Hamburg, Germany
Incubator	HERA cell 150	Thermo Fisher Scientific, Langenselbold, Germany
Incubator	Function line	Thermo Fisher Scientific, Langenselbold, Germany
Incubator bacterial culture	INB400	Memmert, Schwabach, Germany
Laminar flow	Type UVF	BDK, Sonnenbühl-Genkingen, Germany
MACS cell sorter	MACS Multistand, OctoMACS Separation Unit	Miltenyi Biotech, Bergisch-Gladbach, Germany
Magnetic stirrer	RCT basic	IKA® Werke, Staufen, Germany
Microwave	MW7823	Severin, Sundern, Germany
Microscope	Wilovert 30	Hund, Wetzlar, Germany
Multi-plate reader	Synergy HT	BIO-TEK, Bad Friedrichshall, Germany
PCR cycler	T personal combi	Biometra, Göttingen, Germany
pH measurement device	Microprocessor pH Meter pH537	WTW, Weilheim, Germany
Photometer	Ultrospec3000	Pharmacia Biotech/Amersham, Piscataway, USA
Pipettes	0.1-2.5 µl /0.2-10 µl /10-100 µl /100-1000 µl	Eppendorf, Hamburg, Germany
Pipettor	Accu-jet® pro	BRAND, Wertheim, Germany
Power supply	Power Pac200	Bio-Rad, Munich, Germany
Real-time PCR device	iCycler®	Bio-Rad, Munich, Germany

Device	Type	Manufacturer
Real-time PCR software	iCycler® iQ™ software 3.1	Bio-Rad, Munich, Germany
Scale	Kern 440-45N	Kern, Balingen, Germany
Special accuracy weighing machine	TP214	Denver instrument, Göttingen, Germany
SigmaStat® software	SigmaStat software 2.03	SPSS, Chicago, USA
Rolling shaker	RM50	Via Hartenstein, Würzburg, Germany
ScanAlzye software	ScanAlzye 2.50	Eisen lab, Berkeley, USA
Scanner	Epson Perfection V500 photo	Epson, Meerbusch, Germany
ScionImage Software	Release Alpha 4.0.3.2	Scion, Frederick, USA
Shaker	Vibro-Shaker 50	Via Hartenstein, Würzburg, Germany
Shaker for bacterial culture	TH 30/SM-30	Edmund Bühler, Hechingen, Germany
Sonifier	Sonifier GM70, sonotrode MS72	Bandelin, Berlin, Germany
Table centrifuge	C1301, Labnet	Via neoLab, Heidelberg, Germany
Vacuum pump	N811KN.18, Neuberger	Via neoLab, Heidelberg, Germany
Vortexer	MS3 basic	IKA® Werke, Staufen, Germany
Water bath	WNB7	Memmert, Schwabach, Germany
X-ray film developer	Optimax	Protec, Oberstenfeld, Germany

2.1.2 Consumable material and chemicals

Table 2.2: Material applied

Material	Manufacturer
Blotting paper	GE Healthcare, Munich, Germany
Cell culture flasks	Greiner Bio-one, Frickenhausen, Germany
Cell culture plates	Thermo Fisher Scientific (Nunc), Langenselbold, Germany
Cryo tubes	Greiner Bio-one, Frickenhausen, Germany
FACS tubes	BD Biosciences, Franklin Lakes, USA
Falcon tubes	Greiner Bio-one, Frickenhausen, Germany

Material	Manufacturer
Gas cartouche	Camping Gaz, Hungen-Inheiden, Germany
Glas ware	Schott, Wertheim, Germany
Gloves	Semper care/Flexam
Pipette tips	Sarstedt, Nümbrecht, Germany
Plastic pipettes	Costar® Stripette via Materiallager Uniklink Würzburg
Primer	TIB MOLBIOL, Berlin, Germany
PVDF membrane	Bio-Rad, Munich, Germany
Sequencing reactions	MWG Biotech, Munich, Germany
Sterile filter	Schleicher & Schuell, Dassel, Germany
Tubes	Eppendorf, Hamburg, Germany or Sarstedt, Nümbrecht, Germany
X-ray film developer reagents	Agfa, Cologne, Germany
X-ray films	Fuji, Düsseldorf, Germany

All listed chemicals were purchased in pro analysi (p.a.) grade.

Table 2.3: Chemicals applied

Chemical/summ formular	Manufacturer
Acetic acid	Merck, Darmstadt, Germany
Acrylamide/Bisacrylamide 37.5:1	Roth, Karlsruhe, Germany
Agar	Roth, Karlsruhe, Germany
Agarose	Sigma-Aldrich, Taufkirchen, Germany
Ampicillin	Sigma-Aldrich, Taufkirchen, Germany
APS	Sigma-Aldrich, Taufkirchen, Germany
Braunol™	Braun, Melsungen, Germany
BSA	Sigma-Aldrich, Taufkirchen, Germany
Chloroform	Fluka, Steinheim, Germany
Chloroform/Isoamylalcohol	Roth, Karlsruhe, Germany
Cell lysis buffer	Cell Signaling, Danvers, USA
DAPI	Sigma-Aldrich, Taufkirchen, Germany
Dextrose	Merck, Darmstadt, Germany
Desferrioxamine	Sigma-Aldrich, Taufkirchen, Germany

Chemical/summ formular	Manufacturer
Dihydroethidium	Invitrogen, Karlsruhe, Germany
Dithiothreitol	Sigma-Aldrich, Taufkirchen, Germany
DMSO	Roth, Karlsruhe, Germany
Donkey serum	Invitrogen, Karlsruhe, Germany
Ethanol	Merck, Darmstadt, Germany
Ethylendiaminotetraacetat	Fluka, Steinheim, Germany
Formaldehyde	Merck, Darmstadt, Germany
Glycogen	Sigma-Aldrich, Taufkirchen, Germany
H ₂ O ₂ 30%	Sigma-Aldrich, Taufkirchen, Germany
Heparin	Fresenius, Bad Homburg, Germany
Hepes	Merck, Darmstadt, Germany
Salmon sperm DNA	Sigma-Aldrich, Taufkirchen, Germany
Hydrochloric acid	Merck, Darmstadt, Germany
Isopropanol	Fluka, Steinheim, Germany
KCl	Sigma-Aldrich, Taufkirchen, Germany
KH ₂ PO ₄	Sigma-Aldrich, Taufkirchen, Germany
LB powder	Roth, Karlsruhe, Germany
L-Glutamine	Sigma-Aldrich, Taufkirchen, Germany
Lipofectamine2000™	Invitrogen, Karlsruhe, Germany
Liquemin™	Roche, Penzberg, Germany
Loading buffer [3x]	Cell Signaling, Danvers, USA
Loading buffer [6x]	Fermentas, St. Leon-Rot, Germany
Luminol	Roth, Karlsruhe, Germany
Matrigel™	BD Biosciences, Franklin Lakes, USA
Matrigel™ high concentration	BD Biosciences, Franklin Lakes, USA
Methanol	Merck, Darmstadt, Germany
Methylbutan	Merck, Darmstadt, Germany
MgSO ₄	Sigma-Aldrich, Taufkirchen, Germany
NaCl	Sigma-Aldrich, Taufkirchen, Germany
NaHCO ₃	Sigma-Aldrich, Taufkirchen, Germany
NaH ₂ PO ₄	Merck, Darmstadt, Germany
NP40	Sigma-Aldrich, Taufkirchen, Germany

Chemical/summ formular	Manufacturer
PIPES	Sigma-Aldrich, Taufkirchen, Germany
Propidiumiodide	Sigma-Aldrich, Taufkirchen, Germany
Protein G sepharose	GE Healthcare, Munich, Germany
Sarkosyl	Sigma-Aldrich, Taufkirchen, Germany
Skim milk powder	Roth, Karlsruhe, Germany
Para-cumaric acid	Roth, Karlsruhe, Germany
Para-formaldehyde	Sigma-Aldrich, Taufkirchen, Germany
PBS	GIBCO/Invitrogen, Karlsruhe, Germany
Pefabloc™	Roche, Penzberg, Germany
Phenol/Chloroform/Isoamylalcohol	Roth, Karlsruhe, Germany
Protease blocker tablet 25x	Roche, Penzberg, Germany
RotiQuant™	Roth, Karlsruhe, Germany
SDS	Roth, Karlsruhe, Germany
Sodium hydroxide solution	Merck, Darmstadt, Germany
SYBR Safe™	Invitrogen, Karlsruhe, Germany
TEMED	Roth, Karlsruhe, Germany
TissueTek®	SAKURA via Hartenstein, Würzburg, Germany
TRIS, Trizma	Sigma-Aldrich, Taufkirchen, Germany
TritonX100	Merck, Darmstadt, Germany
Trizol™	Invitrogen, Karlsruhe, Germany
Trypsine	BD Biosciences, Franklin Lakes, USA
Tween20™	Roth, Karlsruhe, Germany
Vectashield™	Linaris, Bettingen, Germany
Vitamine B12	SERVA, Heidelberg, Germany

2.1.3 Provided kit systems

Table 2.4: Provided kit systems, ELISAs and arrays

Kit name	Catalogue number	Manufacturer
Agilent RNA 6000 nano reagents/RNA nano chips	#5067-1511	Agilent, Böblingen, Germany
Annexin-V-FLUOS staining kit	#11-858-777-001	Roche, Penzberg, Germany

Kit name	Catalogue number	Manufacturer
β -galactosidase assay kit	#E2000	Promega, Madison, USA
CD146 MicroBeads	#130-092-007	Miltenyi Biotec, Bergisch-Gladbach, Germany
DNeasy Blood & Tissue Kit	#69504	Qiagen, Hilden, Germany
GeneChip [®] Human 1.0 ST array	#901147	Affymetrix, High Wycombe, UK
HotStar <i>Taq</i> Mastermix kit	#203443	Qiagen, Hilden, Germany
iQ [™] Supermix	#170-8860	Bio-Rad, Munich, Germany
iScript select [™] cDNA synthesis kit	#170-8897	Bio-Rad, Munich, Germany
Luciferase assay kit	#E1500	Promega, Madison, USA
Mouse hemoglobin ELISA	#E-90HM	Immunology Consultants Laboratory Inc, Newberg USA
PathScan [®] Phospho-Bad (Ser112) Sandwich ELISA kit	#7182	Cell Signaling, Danvers, USA
PCR purification kit	#28104	Qiagen, Hilden, Germany
Plasmid purification kit	#12125, 12143	Qiagen, Hilden, Germany
pMIR-REPORT Kit	#AM5795	Ambion/Applied Biosystems, Carlsbad, USA
Proteome profiler apoptosis array	#ARY009	R&D Systems, Minnesota, USA
RNeasy mini kit	#74104	Qiagen, Hilden, Germany
Vector M.O.M basic kit	#BMK-2202	Vector Laboratories, Burlingame, USA

2.1.4 Solutions and buffers

2.1.4.1 Cell culture media, components and used cells

Table 2.5: Cell culture media and components

Medium/component name	Catalogue number	Manufacturer
Cryo-SFM	#C-29910	PromoCell, Heidelberg, Germany
DMEM	#C-71220	PromoCell, Heidelberg, Germany
EGM-2 plus supplements	#CC-4147	Cambrex Lonza, Basel, Switzerland

Medium/component name	Catalogue number	Manufacturer
FCS	#C-37360	Biochrome/Promocell
MEM Eagle (Joklik modification)	#M8028	Sigma-Aldrich, Taufkirchen, Germany
MEM	#1-33 V12-K	Amimed
OPTI-MEM [®]	#51985-026	GIBCO/Invitrogen, Karlsruhe, Germany
Pen/Strep	#C-42010	Promocell
Trypsine/EDTA	#L-2163	Biochrome, Berlin, Germany

Table 2.6: Cardiomyocyte medium MEM (Minimal Essential Medium)

Component	Stock	Amount/l MEM	Final concentration
MEM		10.5 g	
BrdU	20 mM	5 ml	0.1 mM
Vitamin B12	2 mg/ml	1 ml	2 µg/ml
L-Glutamine		292 mg	2 mM
NaHCO ₃		350 mg	4.2 mM
Ad 1000 ml dH ₂ O			
Sterile filtration			
Pen/Strep	1000x	1 ml	1x

Table 2.7: Cell types/cell lines used in this work

Cell type	Catalogue number	Manufacturer
HEK293 (Human Embryonic Kidney)		Kind gift from Anahia-Paula Arias-Loza (AG Pelzer, cardiology, University Hospital Würzburg)
HUVEC (Human Umbilical Vein Endothelial cells)	#CC-2519	Cambrex Lonza, Basel, Switzerland
H9C2 (Rat Cardiomyocyte Cell Line)	#CRL-1446	LGC Standards GmbH, Wesel, Germany
NRCM (Neonatal Rat Cardiomyocytes)		Own preparation
NRCF (Neonatal Rat Cardiac Fibroblasts)		Own preparation

2.1.4.2 Cardiomyocyte preparation and fractionation of cardiac cells

Table 2.8: Cardiomyocyte preparation medium CBFHH (Calcium- and Bicarbonate-Free Hanks' solution with HEPES)

Component	Stock	Amount/l CBFHH [ml]	Final concentration
NaCl	3.42 M	40 ml	137 mM
KCl	0.53 M	10 ml	5.36 mM
MgSO ₄ *7H ₂ O	81 mM	10 ml	0.81 mM
Dextrose	555 mM	10 ml	5.55 mM
KH ₂ PO ₄	44 mM	10 ml	0.44 mM
Na ₂ HPO ₄	34 mM	10 ml	0.34 mM
HEPES pH 7.4	0.206 M	100 ml	20.06 mM
Ad 1000 ml dH ₂ O			
Sterile filtration			
Pen/Strep	1000x	1	1x

Table 2.9: T&D (Trypsin and Dnase) solution

Component	Stock	Amount/100 ml CBFHH	Final concentration
DNase	2 mg/ml in 0.15 M NaCl	1 ml	0.02 mg/ml
Trypsine	1.5 mg/ml	100 ml	1.5 mg/ml

Table 2.10: Collagenase solution for fractionation of cardiac cell types

Component	Final concentration
Butanedione monoxime	10 mM
Calcium chloride	20 µM
Collagenase II	1 mg/ml
Ad Joklik medium	

2.1.4.3 DNA Electrophoresis

Table 2.11: 50x TAE (Tris-Acetate-EDTA) buffer for DNA electrophoresis

Component	Stock	Amount/l	Final concentration
Tris		242 g	2 M
Acetic acid (glacial)		57.1 ml	
EDTA	0.5 M pH 8.0	100 ml	0.05 M
Ad 1000 ml dH ₂ O			

2.1.4.4 Chromatin Immunoprecipitation (ChIP)

Table 2.12: Buffers for ChIP

Cell lysis buffer			
Component	Stock	Amount/100 ml	Final concentration
KCl	1 M	8.5 ml	85 mM
NP40	100% (w/v)	0.5 ml	0.5% (w/v)
PIPES pH 8.0	1 M	0.5 ml	5 mM
Ad 100 ml dH ₂ O			
IP dilution buffer			
Component	Stock	Amount/100 ml	Final concentration
EDTA	0.5 M	0.24 ml	1.2 mM
NaCl	5 M	3.34 ml	167 mM
Tris-HCl pH 8.1	1 M	1.67 ml	16.7 mM
TritonX100	100% (w/v)	1.1 ml	1.1% (w/v)
Ad 100 ml dH ₂ O			
Dialysis buffer			
Component	Stock	Amount/500 ml	Final concentration
EDTA	0.5 M	2 ml	2 mM
Sarkosyl	10% (w/v)	10 ml	0.2% (w/v)
Tris-HCl pH 8.0	1 M	25 ml	50 mM
Ad 500 ml dH ₂ O			

IP wash buffer			
Component	Stock	Amount/500 ml	Final concentration
DOC	10% (w/v)	50 ml	1% (w/v)
LiCl	2.5 M	100 ml	500 mM
NP40	100% (w/v)	5 ml	1% (w/v)
Tris-HCl pH 9.0	1 M	50 ml	100 mM

Ad 500 ml dH₂O

Elution buffer			
Component	Stock	Amount/10 ml	Final concentration
SDS	10% (w/v)	1 ml	1% (w/v)
NaHCO ₃	500 mM	2 ml	100 mM

Ad 10 ml dH₂O

Proteinase K buffer 5x			
Component	Stock	Amount/10 ml	Final concentration
EDTA pH 8.0	0.5 M	0.5 ml	25 mM
SDS	10% (w/v)	1.25 ml	1.25% (w/v)
Tris-HCl pH 7.5	1 M	0.5 ml	50 mM

Ad 10 ml dH₂O

TE buffer			
Component	Stock	Amount/100 ml	Final concentration
EDTA	0.5 M	0.2 ml	1 mM
Tris-HCl pH 7.5	1 M	1 ml	10 mM

Ad 100 ml dH₂O

2.1.4.5 SDS-PAGE and Western blot

Table 2.13: Gel recipe for separating gel (SDS-PAGE), 2 gels

Component	10%	12%	15%
dH ₂ O	10.42 ml	8.75 ml	6.25 ml
1.5 M Tris-HCl pH 8.8, 0.4% (w/v) SDS	6.25 ml	6.25 ml	6.25 ml
30% (w/v) Acrylamide/Bisacrylamide	8.33 ml	10 ml	12.5 ml
10% (w/v) APS	100 μ l	100 μ l	100 μ l
TEMED	10 μ l	10 μ l	10 μ l

Table 2.14: Gel recipe for 5% (v/v) stacking gel (SDS-PAGE), 2 gels

Component	Volume
dH ₂ O	3.81 ml
1 M Tris-HCl pH 6.8, 0.4% (w/v) SDS	1.6 ml
30% (w/v) Acrylamide/Bisacrylamide	820 μ l
10% (w/v) APS	50 μ l
TEMED	5 μ l

Table 2.15: 10x SDS-PAGE electrophoresis buffer

Component	Amount/l	Final concentration (10x)	Final concentration (1x)
Glycin	144 g	1.92 M	192 mM
SDS	10 g	1% (w/v)	0.1% (w/v)
Tris	30 g	250 mM	0.81 mM
Ad 1000 ml dH ₂ O			

Table 2.16: 10x Western blot transfer buffer

Component	Amount/l	Final concentration (10x)	Final concentration (1x)
Glycin	144 g	1.92 M	192 mM
Tris	30 g	250 mM	0.81 mM

Ad 1000 ml dH₂O**Table 2.17:** TBST western blot washing buffer

Component	Amount/l	Final concentration
NaCl	16 g	274 mM
Trizma 1 M pH 7.6	40 ml	40 mM
Tween20	2 ml (v/v)	0.2% (v/v)
Ad 2000 ml dH ₂ O		

Table 2.18: Luminol reagent for Western blot detection

Solution	Amount
25 mg Luminol in 50 ml 0.1 M Tris-HCl pH 8.6	2 ml
10 mg p-cumaric acid in 10 ml DMSO	0.8 ml
H ₂ O ₂ (30% v/v)	2.4 µl
dH ₂ O	3 ml

2.1.5. Plasmids

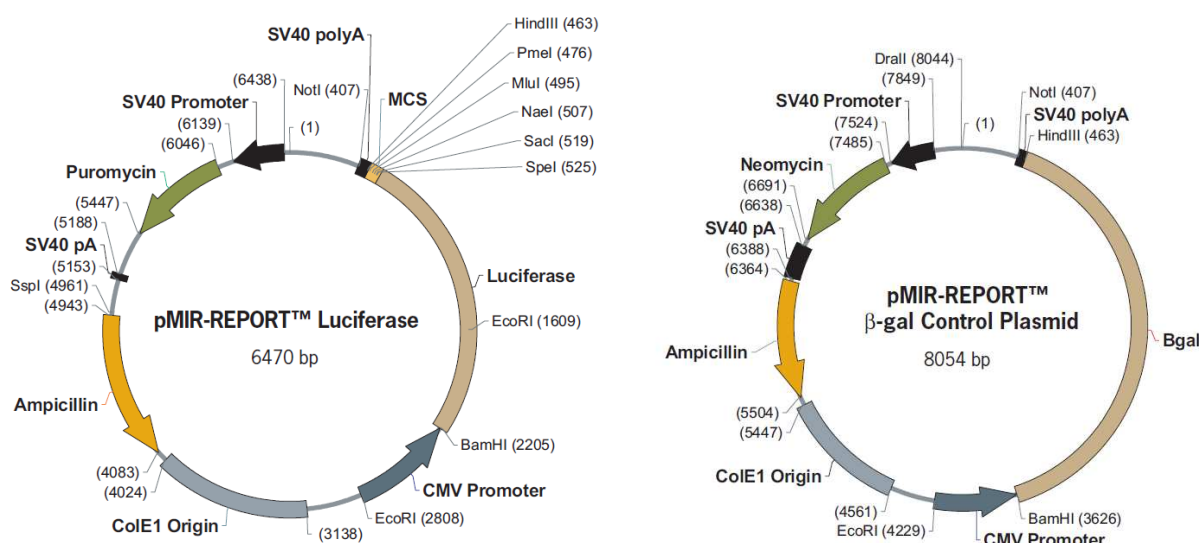


Figure 2.1: Plasmids supplied from Ambion in the Luciferase assay kit

The supplied pMIR-REPORT Luciferase plasmid from Ambion was further used for cloning vector constructs bearing human-*GATA2*-3'-UTR, mouse-*GATA2*-3'-UTR, human-*PAK4*-3'-UTR, human-*RASA1*-3'-UTR and human *H2AX*-3'-UTR.

2.1.6 Oligonucleotides and probes

Table 2.19: siRNAs applied in this work

siRNA	Catalogue number	Manufacturer
<i>GATA2</i> (human)	sc-37228	Santa Cruz Biotechnology, Santa Cruz, USA
<i>H2AX</i> (human)	sc-62464	Santa Cruz Biotechnology, Santa Cruz, USA
<i>PAK4</i> (human)	sc-39060	Santa Cruz Biotechnology, Santa Cruz, USA
<i>RASA1</i> (human)	sc-29467	Santa Cruz Biotechnology, Santa Cruz, USA
Scrambled siRNA control-A	sc-37007	Santa Cruz Biotechnology, Santa Cruz, USA

Table 2.20: miRNAs applied in this work

miRNA	Catalogue number	Manufacturer
<i>hsa-miR-24</i>	PM10737	Applied Biosystems, Foster City, USA
<i>hsa-anti-miR-24</i>	AM10737	Applied Biosystems, Foster City, USA
<i>hsa-miR-22</i>	PM11752	Applied Biosystems, Foster City, USA
<i>hsa-miR-210</i>	PM10516	Applied Biosystems, Foster City, USA
pre-miR miRNA precursor molecules-negative control #2	AM17111	Applied Biosystems, Foster City, USA
anti-miR miRNA precursor molecules-negative control #1	AM17010	Applied Biosystems, Foster City, USA
Cy3 pre-miR negative control #1	AM17120	Applied Biosystems, Foster City, USA

Table 2.21: TaqMan miRNA detection assays applied in this work

miRNA	Catalogue number	Manufacturer
<i>hsa-miR-24</i>	#4373072	Applied Biosystems, Foster City, USA
<i>RNU6B</i>	#4373381	Applied Biosystems, Foster City, USA

Table 2.22: Antagomirs applied in this work

Antagomir	Sequence	Manufacturer
Antagomir-24	5'-CTGTTCCCTGCTGAACTGAGCCA-chol-3'	Regulus Therapeutics, Carlsbad, USA
Scrambled antagomir	5'-ACAAACACCAUUGUCACACUCCA-chol-3'	Regulus Therapeutics, Carlsbad, USA

Table 2.23: Primer sequences used for pMIR-REPORT cloning with restriction sites underlined

3'-UTR	Primer (forward, reverse)	Product size [bp]
<i>GATA2</i> (human)	forward: 5'-AAA <u>ACTAGT</u> GGAACAGATGGACGTCGAG-3' reverse: 5'-AAA <u>AAGCTT</u> GCAGCTTCGGCCTCAAAG-3'	700
<i>GATA2</i> (mouse)	forward: 5'-AAA <u>ACTAGT</u> ACTTCCTCCTGCCAGCCTA-3' reverse: 5'-AAA <u>AAGCTT</u> CCGAGGGTTTAGCAGAAAAG-3'	700
<i>H2A.X</i> (human)	forward: 5'-AAA <u>ACTAGT</u> GCCCCATTTCCCTTCCAG-3' reverse: 5'-AAA <u>AAGCTT</u> GGTGTTAAGAGCCCTTGCAG-3'	1360
<i>PAK4</i> (human)	forward: 5'-AAA <u>ACTAGT</u> TTTGCTGGGGGTAGATGAGAC-3' reverse: 5'-AAA <u>AAGCTT</u> TGGTTCTTCAGGCAGTGGTTC-3'	620
<i>RASA1</i> (human)	forward: 5'-AAA <u>ACTAGT</u> TCCAAGATTCTGCTGGTGAA-3' reverse: 5'-AAA <u>AAGCTT</u> TGGCAGCTGATGAGGTTGTCT-3'	750

Table 2.24: Primer sequences used for ChIP-PCR

Promoter region	Primer (forward, reverse)	Product size [bp]
BMP and activin membrane-bound inhibitor (<i>BAMBI</i>)	forward: 5'-TCTCAGGTTTTGGAGGGAGA-3' reverse: 5'-GGCCGAGACTGACACTCAAT-3'	259
Endothelial cell specific molecule 1 (<i>ESM1</i>)	forward: 5'-CAAGTGATATGCCAGGGTCA-3' reverse: 5'-TGGTTGTTTTGCATGAGGAC-3'	136
Heme oxygenase 1 (<i>HO1</i>)	forward: 5'-CATCACCAGACCCAGACAGA-3' reverse: 5'-AAGGCCGACTTTAAGGGAAG-3'	133
Netrin 4 (<i>NTN4</i>)	forward:	180

	5'-GAGCCAGTTATTCAGCAAAGAAA-3' reverse: 5'-ATGCAGAGGCCATGCTAATC-3'	
Sirtuin 1 (<i>SIRT1</i>)	forward: 5'-GGAGTCACAGTGTGCCAGAA-3' reverse: 5'-CCTTCCTTTCTAGCGTGAGC-3'	201

2.1.7 Antibodies, enzymes and standard markers

Table 2.25: Primary antibodies applied in this work (Western blot and ChIP)

Antibody/Antigen	Catalogue number	Manufacturer
Akt	#9272	Cell Signaling Technology, Danvers, USA
Bad	Ab28840	Abcam, Cambridge, USA
GAPDH	ab8245	Abcam, Cambridge, USA
GATA2	arp31855	Aviva Systems Biology, San Diego, USA
GATA2	ab22849	Abcam, Cambridge, USA
GATA2 (ChIP)	sc-267x	Santa Cruz Biotechnology, Santa Cruz, USA
GFP	ab1218	Abcam, Cambridge, USA
H2.AX	ab11175	Abcam, Cambridge, USA
HIF1 α	sc-10790	Santa Cruz Biotechnology, Santa Cruz, USA
HMOX1 (HO1)	AF3776	R&D Systems, Minnesota, USA
Lamin A/C	sc-6215	Santa Cruz Biotechnology, Santa Cruz, USA
Mouse control-IgG (ChIP)	sc-2025	Santa Cruz Biotechnology, Santa Cruz, USA
PAK4	ab19007	Abcam, Cambridge, USA
p44/42 MAP Kinase	#9102	Cell Signaling Technology, Danvers, USA

Antibody/Antigen	Catalogue number	Manufacturer
phospho-Akt	#9271	Cell Signaling Technology, Danvers, USA
phospho-p44/42 MAP Kinase (Thr202/Tyr204)	#9101	Cell Signaling Technology, Danvers, USA
RASA1/GAP	ab2922	Abcam, Cambridge, USA

SIRT1	ab32441	Abcam, Cambridge, USA
TBP	ab818	Abcam, Cambridge, USA

Table 2.26: Secondary antibodies applied in this work (Western blot)

Antibody	Catalogue number	Manufacturer
Anti-rabbit-IgG-HRP	#7074	Cell Signaling Technology, Danvers, USA
Anti-mouse-IgG-HRP	#7076	Cell Signaling Technology, Danvers, USA
Anti-goat-IgG-HRP	sc-2020	Santa Cruz Biotechnology, Santa Cruz, USA
Precision Protein™ StrepTactin-HRP	#161-0380	Bio-Rad, Munich, Germany

Table 2.27: Primary antibodies applied in this work (Immunocyto-/histochemistry)

Antibody	Catalogue number	Manufacturer
CD31	ab28364	Abcam, Cambridge, USA
CD31	ab24590	Abcam, Cambridge, USA
CD31	MCA2388	Serotec
GATA2	arp31855	Aviva Systems Biology, San Diego, USA
PAK4	ab19007	Abcam, Cambridge, USA
RASA1/GAP	ab2922	Abcam, Cambridge, USA
Troponin I	sc-15368	Santa Cruz Biotechnology, Santa Cruz, USA

Table 2.28: Secondary Alexa Fluor® antibodies applied in this work (Immunocyto/histo-chemistry)

Alexa Fluor®	Catalogue number	Manufacturer
Donkey anti-rabbit 488	A21206	Invitrogen, Karlsruhe, Germany
Donkey anti-rat 488	A21208	Invitrogen, Karlsruhe, Germany
Donkey anti-mouse 488	A21202	Invitrogen, Karlsruhe, Germany
Donkey anti-rabbit 594	A21207	Invitrogen, Karlsruhe, Germany
Donkey anti-mouse 594	A21203	Invitrogen, Karlsruhe, Germany

Table 2.29: Enzymes applied in this work

Enzyme	Catalogue number	Manufacturer
Collagenase	C0130	Sigma-Aldrich, Taufkirchen, Germany
DNase	DN25	Sigma-Aldrich, Taufkirchen, Germany
<i>HindIII</i> (+buffer)	R0104S	New England Biolabs, Frankfurt, Germany
Proteinase K	P2308	Sigma-Aldrich, Taufkirchen, Germany
RNAse A	R6513	Sigma-Aldrich, Taufkirchen, Germany
<i>SpeI</i> (+ buffer)	R0133L	New England Biolabs, Frankfurt, Germany
T4 DNA Ligase (+ buffer)	M0202S + B0202S	New England Biolabs, Frankfurt, Germany

Table 2.30: Standard markers applied in this work

Standard marker	Catalogue number	Manufacturer
DNA electrophoresis standard	#SM0241	Fermentas, St. Leon-Rot, Germany
Precision Plus Protein standard	#161-0374	Bio-Rad, Munich, Germany

2.1.8 FACS solutions

Table 2.31: Annexin-V-FLUOS staining solution for apoptosis detection

Component	Amount/1 ml
Annexin-V-FLUOS solution	20 μ l
Incubation buffer	1 ml
Propidium iodide solution	20 μ l

Table 2.32: Propidium iodide (PI) solution for cell cycle analysis

Component	Final concentration
Propidium iodide	50 μ g/ml
RNase A	0.1 mg/ml
Triton X-100	0.05% (v/v)

2.1.9 Components for bacteria culture and bacteria strains

Table 2.33: LB and LB-agar media

LB-media	
Component	Amount/l LB
LB	25 g

Ad 1000 ml dH₂O, then autoclave

LB-agar	
Component	Amount/l LB
LB	25 g
Agar (separate bottle)	15 g

Ad 1000 ml dH₂O (split for LB and agar), then autoclave

The desired antibiotic ampicillin (final concentration 100 μ g/ml) was added after autoclaving and cooling down of solutions to 50-60 °C. Afterwards, LB-agar plates were spilled.

Table 2.34: Applied bacteria strain

Name	genotype	Catalogue number	Manufacturer
One Shot® TOP10 Chemically Competent <i>E. coli</i>	F- <i>mcrA</i> Δ (<i>mrr-hsdRMS-mcrBC</i>) ϕ 80 <i>lacZ</i> Δ M15 Δ <i>lacX74 recA1</i> <i>araD139</i> Δ (<i>araleu</i>) 7697 <i>galU galK rpsL</i> (StrR) <i>endA1</i> <i>nupG</i>	#C4040-10	Invitrogen, Karlsruhe, Germany

2.1.10 Animals

All animal experiments were approved by local authorities and conducted according to the German law of animal protection.

Mice were purchased from Harlan-Winkelmann (Borchen, Germany). Inbred C57BL/6 mice were male, 8-10 weeks old and approximately 20-25 g in weight.

2.2 Methods

2.2.1 Cell culture

2.2.1.1 Cultivation of endothelial cells (ECs)

Human umbilical vein endothelial cells (HUVECs) were cultured in EGM-2 media supplemented with 20% (v/v) fetal calf serum (FCS) and supplements. Cells were grown in a humidified atmosphere at 5% CO₂ and 37°C. Hypoxic conditions were simulated by incubating HUVECs with 1% O₂, 5% CO₂ for 24 h. Furthermore, cells were splitted up to passage 10.

2.2.1.2 Isolation and cultivation of neonatal rat cardiomyocytes and cardiac fibroblasts

Hearts were removed from newborn rats (day 0), put into calcium- and bicarbonate-free HEPES-buffered Hanks' medium, cut into pieces and digested with trypsin/DNase under constant stirring. The collected primary cells were passed through a cell strainer (40 µm) and then seeded in a pre-plating step onto uncoated plastic dishes and incubated for 60 min at 37°C. The supernatant (containing the cardiomyocytes) was collected and the adherent cells were washed several times and cultured in minimal essential medium (MEM) containing 5% (v/v) FCS. These cultures contained almost exclusively primary cardiac fibroblasts. The cells in the supernatant that was collected were plated in MEM containing vitamin B12, NaHCO₃ and 5% (v/v) FCS. This cell population was almost exclusively cardiomyocytes. After 1 d in culture medium was replaced to DMEM with 10% (v/v) FCS and antibiotics. Cardiac fibroblasts were cultured at 5% CO₂, cardiomyocytes at 1% CO₂.

The rat cardiomyocyte cell line H9C2 was cultured in DMEM media supplemented with 10% (v/v) FCS and antibiotics in a humidified atmosphere at 5% CO₂ and 37°C.

2.2.1.3 Cultivation of other applied cell types

The human embryonic kidney cell line HEK-293 was cultured in DMEM media with 10% (v/v) FCS and antibiotics in a humidified atmosphere at 5% CO₂ and 37°C.

2.2.1.4 Transfection assays

Transient liposomal transfection of small-inhibitory RNAs (siRNAs) or microRNAs was done according to manufacturers' instructions. Therefore cells were splitted into 6wells one day before transfection to reach 60-70% confluence on day of transfection. Specific siRNAs/miRNAs, control siRNA/miRNA and 4 μ l Lipofectamine2000 per 6well were mixed separately and incubated for 5 min with Opti-MEM I media. Complexes were added together and incubated for 20 min. Media was changed to antibiotic-free media before adding liposomal siRNA complexes (final concentration 150 nM for siRNA and 100 nM for miRNAs). Cells were incubated for 4 h before changing the media to fresh medium. Silencing of proteins or miRNA targets was monitored 48 h (siRNA) or 72 h (miRNAs) post transfection by western blot analysis. Specific details about the used siRNAs and miRNAs are given in tables 2.19/20.

2.2.1.5 Luciferase reporter assay

A luciferase reporter assay system was applied to validate potential miRNA targets. *luciferase* gene expression can be downregulated by binding of certain miRNAs in 3'-UTR of *luciferase* reporter gene. The cloned constructs were co-transfected with miRNAs of interest (table 2.20) and *beta-galactosidase* control plasmid (figure 2.1) into HEK293 reporter cells in 48wells by use of Lipofectamine2000. 0.2 μ g plasmid DNA each, 100 nM miRNA and 0.5 μ l of Lipofectamine2000 were applied. Cells were incubated for 24 h before measuring luciferase and β -galactosidase activity on a multi-plate reader according to manufacturers' instructions.

2.2.1.6 *In vitro* tube formation assay for ECs

A matrigel based assay was applied to test capillar formation of ECs *in vitro*. Therefore ECs were pre-treated by siRNA or miRNA modulation as mentioned before. Then cells were harvested and 15000 cells in 200 μ l EGM-2 media with supplements were seeded on Matrigel coated 8well chamber slides. After 6 and 24 h pictures were taken on a Zeiss Axiovert microscope. Experimental outcome was measured qualitatively.

2.2.1.7 Viral transduction

The generation of a murine N-terminal GFP tagged GATA2 adenovirus was done by the laboratory of Prof. Stefan Engelhardt (Pharmacology, Rudolf-Virchow Center, Würzburg, Germany). Following biosafety level 2 experiments were done in the laboratory of Prof. Stefan Engelhardt.

For viral transduction experiments cells were grown to subconfluence and infected with viral particles in a multiplicity of infection (m.o.i.) of 40 for 24-48 h. Additionally, a YFP control virus was also applied with same m.o.i..

2.2.2 Molecular biology

2.2.2.1 RNA isolation

RNA isolation of cell culture cell pellets or animal tissue was done either with Qiagen RNeasy mini kit or TRIzol reagent. For TRIzol RNA isolation samples were homogenized with 1 ml TRIzol for 5 min at RT. 200 μ l chloroform was added, samples were mixed and incubated for 2-3 min at RT. Samples were centrifuged at 11900 x g for 15 min at 4°C. Afterwards the upper phase was taken and mixed with 500 μ l isopropyl alcohol following 10 min incubation at RT. Then samples were centrifuged at 11900 x g for 10 min at 4°C. The resulting RNA pellet was washed with 70% (v/v) ethanol and centrifuged at 7370 x g for 5 min at 4°C. Afterwards RNA pellet was suspended in appropriate amounts of DEPC-treated water.

2.2.2.2 DNA isolation

Genomic DNA from cell pellets was isolated with the Qiagen DNeasy Blood & Tissue Kit.

2.2.2.3 Determination of RNA and DNA concentration

RNA and DNA concentrations were determined by measurement of absorption at 260 nm (A_{260}) and 280 nm (A_{280}) in a UV-spectrophotometer versus dH₂O as reference. The absorption of suspended DNA or RNA is proportional to concentration at A_{260} .

For DNA 1.0 A_{260} unit equals 50 $\mu\text{g/ml}$ DNA and for RNA 1.0 A_{260} unit equals 40 $\mu\text{g/ml}$ RNA. The A_{260}/A_{280} ratio was measured and only preparations with a ratio between 1.8 and 2.0 were considered to be pure.

2.2.2.4 Agarose gel electrophoresis

For qualitative analysis of DNA band pattern agarose gel electrophoresis was applied. Therefore, 1.8% (m/v) agarose gels were prepared by heating agarose in 0.5 TAE buffer. Samples were mixed with 6x loading dye solution and loaded onto the gel with an appropriate DNA ladder. Electrophoresis run was performed for 60 min at 90 V in 0.5 TAE buffer.

2.2.2.5 Luciferase pMIR-REPORT cloning

A putative 3'-UTR miRNA binding sequence was cloned into *SpeI* and *HindIII* cloning site of pMIR-REPORT vector (figure 2.1). In advance, 3'-UTR of mRNA containing the miRNA binding site was PCR amplified from whole genomic DNA (human or mouse) with appropriate primers (table 2.23). Primers were designed with Primer3 (http://frodo.wi.mit.edu/cgi-bin/primer3/primer3_www.cgi).

PCR setup

10 μl HotStar*Taq*-Mix

2.5 μl primerpair (forward/reverse) [4 μM]

2.5 μl genomic DNA (human/mouse) [100 $\text{ng}/\mu\text{l}$]

PCR protocol:

94°C 10 min, [94°C 1 min, 57°C 30 sec, 72°C 1 min] \times 40, 72°C 10 min, 4°C hold

PCR products were purified with Qiagen PCR purification kit and analyzed for correct band pattern on a 1.8% (m/v) agarose gel. The amplified 3'-UTR sequences and pMIR-REPORT vector were double-digested for 2 h at 37°C with appropriate restriction enzymes before purification with Qiagen PCR purification kit.

Restriction digestion setup

A) Insert (3'-UTR)	B) Vector
20 µl PCR product	1 µl vector pMIR-REPORT [3 µg/µl]
2 µl <i>SpeI</i> [10 U/µl]	6 µl <i>SpeI</i> [10 U/µl]
1 µl <i>HindIII</i> [20 U/µl]	3 µl <i>HindIII</i> [20 U/µl]
3 µl NEB buffer 2 [10x]	2 µl NEB buffer 2 [10x]
4 µl dH ₂ O	8 µl dH ₂ O

Afterwards insert and vector were ligated with T4 DNA ligase o/n at 16°C before T4 DNA ligase inhibition for 15 min at 65°C.

Ligation setup

20 µl 3'-UTR
0.5 µl vector 1:10 diluted
3 µl 10x T4 buffer
1.5 µl T4 DNA ligase
5 µl dH₂O

Finally, *E. coli* TOP10 cells were heat-transformed with the ligation sample. Therefore, 50 µl competent were thawed on ice and 10 µl ligation mix was added. After 20 minutes incubation on ice, cells were heat-shocked for 90 seconds at 42°C. Cells were then cooled on ice for 2 minutes. Afterwards 500 µl SOC media was added and cells mixed on a vortexing platform for 45 min at 37°C. Then 100-200 µl cell suspension were plated on LB-Amp plates and incubated o/n at 37°C. The next day transformants were picked and inoculated to LB-Amp-media o/n at 37°C. Plasmid preparation was done the next day with Qiagen mini plasmid kit. For verification of positive transformants double-digestion with *SpeI* and *HindIII* was performed for 1 h at 37°C.

Qualitative restriction digestion setup

5 μ l isolated plasmid DNA (pDNA)

0.5 μ l *Spe*I [10 U/ μ l]

0.5 μ l *Hind*III [20 U/ μ l]

2 μ l NEB buffer 2 [10x]

12 μ l dH₂O

Afterwards samples were analyzed for positive band pattern on a 1.8% (m/v) agarose gel. The constructs were further subjected to sequencing for final validation. For greater amounts of pDNA plasmid preparation was done with the Qiagen midi plasmid kit.

2.2.2.6 Real-time PCR analysis

For detection of miRNAs in samples different TaqMan MicroRNA assays were applied. Specific details about the used assays are given in table 2.21. In a first step, total RNA was reverse transcribed.

cDNA reaction setup for miRNA detection

2 μ l sample total RNA [100-1000 ng/ μ l]

3 μ l iScript reaction mix [5x]

1 μ l reverse transcriptase

3 μ l miRNA primer for reverse transcription

6 μ l dH₂O

Cycler protocol:

25°C 5 min, 42°C 30 min, 85°C 5 min, 4°C hold

Afterwards, Real-time PCR analysis was performed in an ICycler. Data analysis was supported by a standard curve created from a mixture of all analyzed samples and a subsequent 5-fold dilution series. Analysis was performed with ICycler Software 3.0.

Real-time PCR reaction setup for miRNA detection

1.33 μ l sample 1:2 diluted

10 μ l iQ Supermix [2x]

7.67 μ l dH₂O

Cycler protocol:

95°C 10 min, [95°C 15 sec, 60°C 1 min]x40, 15°C hold

2.2.2.7 ChIP

Chromatin immunoprecipitation (ChIP) is a technique to detect protein-DNA interactions. Here, transcription factor GATA2 controlled target DNA sequences were investigated. In advance, Protein G Sepharose beads were blocked o/n at 4°C with 100 μ g salmon sperm DNA and 100 μ g BSA per 100 μ l 50% (v/v) beads. HUVECs from confluent T75 flasks were first cross-linked by adding 1% (v/v) formaldehyde for 10 min at RT. Cross-linking was stopped by addition of 2.5 M Glycine to a final concentration of 125 mM for 5 min at RT. Cells were washed once with ice-cold PBS before scraped and harvested. The pellet was lysed in lysis buffer on ice for 10 min with interval vortexing. Next, the lysate was sonified to yield DNA fragments from 100-1000 bp in length. Therefore, 12 intervals for each 30 seconds were applied (Bandelin Sonifier GM70, sonotrode MS72, cycle 0.5, maximum amplitude strength). Samples were kept on ice for the whole procedure. Afterwards, samples were centrifuged at maximum speed (10 min, RT). From these cleared lysates 100 μ l aliquots were separately taken to measure sonification efficiency. Therefore samples were heated o/n at 65°C. Then, 100 μ l dH₂O and Proteinase K (0.5 mg/ml final) were added and samples are incubated for 3 h at 42°C. Finally, total DNA after sonification was purified with Qiagen PCR purification kit before agarose gel analysis. To reduce non-specific background cleared lysates were pre-cleared on 50 μ l 50% (v/v) blocked Protein G Sepharose beads twice for 2 h at RT. Afterwards, samples were divided into 500 μ l aliquots and filled up with 1 ml IP dilution buffer. Samples were subjected to either immunoprecipitation with 5 μ g GATA2 antibody or control mouse IgGs o/n at 4°C.

To block non-specific background 250 µg BSA and 24 µg salmon sperm DNA were added. One sample with cell lysis and IP dilution buffer was named “mock” control. The next day GATA2-DNA cross-links were collected by 15 min incubation with 50 µl 50% (v/v) Protein G beads at 4°C on a rotating wheel. Samples were centrifuged (3000 x g, 1 min, 4°C) and beads were washed twice with dialysis buffer and four times with IP wash buffer. Finally beads were washed twice with TE-buffer. Antibody-GATA2-DNA complexes were eluted from the beads by adding 150 µl IP elution buffer. Samples were heated at 65°C and kept on a vortexing platform for 10 min. The elution step was repeated and combined eluates were reverse crosslinked by addition of 5 M NaCl (0.3 M final concentration) for 4 hours at 65°C. Samples were cooled on ice and subjected to RNA degradation by adding 10 µg RNase A and incubation for 30 min at 37°C. Next samples were mixed with 2.5 volumes 100 % (v/v) ethanol and incubated o/n at -20°C. On the following day DNA was pelleted (maximum speed, 20 min, 4°C) and protein was digested from the samples by addition of 100 µl TE buffer, 25 µl 5x proteinase K buffer and 6.25 µl (20 µg/µl) proteinase K (2 h, 55°C). DNA was further extracted by phenol-chloroform-isoamylalcohol (PCI) extraction (1 volume sample on 1 volume PCI, maximum speed, 10 min, RT). The upper phase was mixed with 1 volume chloroform-isoamylalcohol and centrifuged (maximum speed, 10 min, RT). Again, the upper phase was taken and 1/10 volume 5 M NaCl and 5 µg glycogen were added. Samples were mixed with 2.5 V 100% (v/v) ethanol and incubated o/n at -20°C. The next day DNA was pelleted (maximum speed, 10 min, 4°C) and washed with 70% (v/v) ethanol. Pellets were air-dried and solved in 60 µl TE buffer before purification with Qiagen PCR purification kit.

For ChIP primer design 2000-2500 bp upstream promoter region of candidate target genes was identified by Ensembl Genome Browser (<http://www.ensembl.org/index.html>). Then the promoter region was screened for potential GATA2 binding sites by the use of ALLGEN-Promo (http://alggen.lsi.upc.es/cgi-bin/promo_v3/promo/promoinit.cgi?dirDB=TF_8.3). Afterwards, primers were designed to amplify potential GATA2 binding site. Finally, PCR analysis of chipped DNA fragments was done with appropriate primers (table 2.24).

PCR setup

2.5 µl chipped DNA

2.5 µl primerpair [4 µM]

10 µl HotStar*Taq* Mix

PCR protocol:

94°C 10 min, [94°C 1 min, 57°C 30 sec, 72°C 1 min]x33, 72°C 10 min, 4°C hold

2.2.2.8 Affymetrix gene chips

To assess RNA integrity number (RIN) for downstream array analysis total RNA was subjected to capillar chromatography in an Agilent bioanalyzer 2100 according to manufacturers' instructions. Therefore 1 µl of isolated total RNA was analyzed with Agilent RNA nano chips for 18 and 28 S RNA peaks in an electropherogramm.

Afterwards total RNA underwent microarray (Human Exon Gene ST array) analysis in the laboratory of Dr. Susanne Kneitz (IZKF Microarray Core Facility, University of Würzburg). Data acquisition was done with a R programmed software (Dr. Paolo Galuppo, Cardiology, University Hospital Würzburg) or Affymetrix expression console.

2.2.3 Protein biochemistry

2.2.3.1 Protein isolation

Total protein was isolated from samples by 10 min incubation with cell lysis buffer plus 4 mM protease-blocker Pefabloc on ice. Lysis was supported by interval vortexing. Samples were then centrifuged (8000 x g, 10 min, 4°C) to obtain soluble protein.

2.2.3.2 Determination of protein concentration

Protein concentration was measured by Bradford assay quantification (Bradford, 1970). Therefore 1 μ l sample was mixed with 800 μ l dH₂O and 200 μ l RotiQuant reaction mix. The mixture was incubated for 5 min at rt before measuring absorbance at 595 nm (A_{595}) in a UV-spectralphotometer versus reference. Protein concentration was obtained by comparing A_{595} to a protein standard curve of BSA [0.2-20 mg/ml].

2.2.3.3 SDS-PAGE

Samples were mixed with sample buffer and DTT and heat-denatured for 5 min at 95°C. Then denatured proteins were separated by discontinuous SDS-PAGE. Therefore, 10-15% acrylamide gels were prepared. Electrophoretic separation was performed in a mini gel apparatus for 90-120 min at 20-30 mA. Afterwards gels were blotted onto PVDF-membranes.

2.2.3.4 Western blot

Western blot was applied in a wet blot technique. Prior to electrophoretic transfer, PVDF membrane was activated in methanol for 1 min. Then it was washed in distilled water for 2 min before 5 min equilibration in transfer buffer. Western blot was performed o/n at constant 30 V.

The next day membranes were blocked with 5% (w/v) skim milk powder for 30 min. After three times washing with TBST membranes were incubated with appropriate antibodies diluted in 5% (w/v) skim milk powder in TBST for 3 h at RT or o/n at 4°C. Details about the used primary antibodies are in table 2.25. Following antibody incubation membranes were again washed three times with TBST before incubation with appropriate secondary antibodies linked to horseradish peroxidase (HRP) (see table 2.26) for 1 h at RT. The secondary antibodies were 1:10.000 diluted in 5% (w/v) skim milk powder in TBST. Afterwards membranes were washed three times with TBST. For antigen detection luminol reagent was added to the membranes. Finally membranes were covered with X-ray films. Time for developing X-ray films was depending on antigen. Bands on X-ray films were quantified by the use of Scion Image Alpha 4.0.3.2.

2.2.3.5 Apoptosis array

The apoptosis array system was supplied by R&D Systems (Proteome profiler array) and was performed by manufacturers' instructions. Briefly, cell pellets were lysed in lysis buffer and 200 µg total protein was incubated with the array membrane. For detection membranes were incubated with antibody cocktail/Streptavidin-HRP secondary antibody. Chemiluminescent reaction was performed and exposition to X-ray films was done for 30 sec to 10 min. Details about the spotted antigens are in table 2.35.

Table 2.35: Overview on the spot distribution of the apoptosis array (R&D, Minnesota, USA)

Coordinate	Target/Control	Coordinate	Target/Control
A1, A2	Positive Control	C13, C14	HO-2/HMOX2
A23, A24	Positive Control	C15, C16	HSP27
B1, B2	Bad	C17, C18	HSP60
B3, B4	Bax	C19, C20	HSP70
B5, B6	Bcl-2	C21, C22	HTRA2/Omi
B7, B8	Bcl-x	C23, C24	Livin
B9, B10	Pro-Caspase-3	D1, D2	PON2
B11, B12	Cleaved Caspase-3	D3, D4	p21/CIP1/CDNK1A
B13, B14	Catalase	D5, D6	p27/Kip1
B15, B16	clAP-1	D7, D8	Phospho-p53 (S15)
B17, B18	clAP-2	D9, D10	Phospho-p53 (S46)
B19, B20	Claspin	D11, D12	Phospho-p53 (S392)
B21, B22	Clusterin	D13, D14	Phospho-Rad17 (S635)
B23, B24	Cytochrome c	D15, D16	SMAC/Diablo
C1, C2	TRAIL R1/DR4	D17, D18	Survivin
C3, C4	TRAIL R2/DR5	D19, D20	TNF RI/TNFRSF1A
C5, C6	FADD	D21, D22	XIAP
C7, C8	Fas/TNFSF6	D23, D24	PBS (Negative Control)
C9, C10	HIF-1 α	E1, E2	Positive Control
C11, C12	HO-1/HMOX1/HSP32		

2.2.3.6 Phospho-Bad ELISA

For detection of intracellular phosphorylated Bad protein (Ser112) a phospho-Bad ELISA (R&D Systems) was applied according to manufacturers' instructions. Therefore, cells in 6wells were harvested and lysed with cell lysis buffer. Protein concentration was determined and samples were adjusted to 0.3 µg/µl protein. Then 100 µl sample were diluted with 100 µl sample buffer and incubated to antibody-coated wells for 2 h at 37°C. Afterwards plates were washed and incubated with 100 µl detection antibody for 1 h at 37°C. Again, plate was washed before incubation with 100 µl HRP-linked secondary antibody for 30 min at 37°C. Washing was repeated and finally wells were incubated with 100 µl substrate solution for 10 min at 37°C. Detection reaction was stopped by addition of 100 µl stop solution. Plates were immediately measured in an ELISA reader for A₄₅₀. Measurements were adjusted to total BAD protein determined by Western blot.

2.2.4 Fluorescence-activated cell sorting (FACS)

FACS measurements were performed on a FACS Calibur (BD Biosciences, Germany) flow cytometer. Data acquisition and analysis was performed with CellQuest software (BD Biosciences, USA).

2.2.4.1 Apoptosis staining

Apoptosis was measured with the Annexin-V-Fluos kit (Roche, Germany) according to manufacturers' instructions. Here necrotic cells can be separated from apoptotic cells by double staining of PI and Annexin-V-Fluorescein. Only Annexin-V-Fluorescein single positive cells can be named apoptotic. Briefly, cells were harvested and washed. Afterwards cell pellets were incubated with 100 µl staining solution for 15 min at RT. Then 500 µl incubation buffer was added and samples underwent FACS analysis.

2.2.4.2 Cell cycle propidium iodide (PI) stain

Cell cycle analysis was performed by propidium iodide staining. Therefore cells were harvested, suspended in 500 µl PI staining solution and incubated at 37°C for 40 min.

Afterwards cells were washed with PBS. Finally cell pellets were resuspended in 300-500 μ l PBS and subjected to FACS analysis.

2.2.4.3 Reactive oxygen species (ROS) detection

The redox-sensitive, cell-permeable fluorophore dihydroethidium (DHE) becomes oxidized in the presence of O_2^- to yield fluorescent ethidium. Thus, dye oxidation is an indirect measure of the presence of reactive oxygen intermediates. MiRNA-transfected HUVECs were incubated with DHE (2.5 μ M) for 30 min at rt. After washing, HUVECs were immediately analyzed with FACS.

2.2.5 Immunocytochemistry and immunohistochemistry

Immunofluorescent detection of samples was done with an Axiovert microscope (Zeiss, Germany). Pictures were taken with the support of Axiovision 4.5 software (Zeiss, Germany).

2.2.5.1 Immunocytochemistry

Cells were grown to confluence in 4 or 8well chamber slides for analysis. Confluent cells were fixed with 4% (w/v) p-formaldehyde in PBS for 15 min at RT. Then cells were permeabilized with 0.1% (v/v) Triton X-100 in PBS for 10 min at RT. After washing samples were blocked with 5% (v/v) donkey serum for 30 min at RT. Next, cells were washed and incubated with specific antibodies diluted in 5% (v/v) donkey serum (table 2.27). Again, samples were washed and then incubated with appropriate Alexa fluorophore secondary antibodies (table 2.28) for 30 min at RT. Finally cells were washed and stained with DAPI (1:1000 dilution) for 5 min at RT.

2.2.5.2 Immunohistochemistry

For immunohistochemistry frozen hearts were mounted in tissue tek and slowly frozen by the use of methylbutan. Then, frozen hearts were sliced into 10 μ m sections and air-dried for 30 min. Samples were fixed by acetone for 3 min at RT and dried for 10 min. After washing with PBS samples were blocked with 5% (v/v) donkey serum for 30 min at RT. Incubation with appropriate primary antibodies in 1% (v/v) donkey serum was performed o/n at 4°C.

Optionally, mouse on mouse (MOM) kit was applied to detect mouse antigens with mouse primary antibodies. The next day samples were washed and incubated with appropriate Alexa fluorophore secondary antibodies diluted in 1% (v/v) donkey serum for 30 min at RT. Finally slides were washed and stained with DAPI (1:1000 dilution) for 5 min at RT. Finally slides were mounted with Vectashield. Details about the used antibodies are in table 2.27/28.

2.2.6 *In vivo* methods

2.2.6.1 Fractionation of cardiac cells from heart tissue

The thorax of mice was opened and the aorta was cannulated. After washing with 37°C PBS, the heart together with the cannula was removed and perfused with a collagenase solution in Joklik medium for 5 min. Then the heart was placed in 37°C pre-warmed collagenase solution for further 25 min and was subsequently minced and filtered through a nylon mesh (200 µm pore size). Then, cardiomyocytes were separated by a sedimentation step in 15 ml falcon tubes. The noncardiomyocyte cell fraction retained in the supernatant was incubated with CD146-antibodies coupled to MicroBeads and subjected to magnetic affinity cell sorting according to the manufacturers' recommendations.

2.2.6.2 Antagomir injection

Antagomirs were designed and provided by Regulus Therapeutics (USA). Details on sequence information can be found in table 2.22. Antagomirs were diluted in nuclease-free water and 100 µl at concentrations of 5 mg/kg and 80 mg/kg were applied to mice via retroorbital injection.

2.2.6.3 Myocardial infarction

Male mice underwent coronary artery ligation for the production of MI. Briefly, mice were anesthetized, placed on a heating pad, intubated and ventilated with a mixture of oxygen and isoflurane. After left lateral thoracotomy and exposure of the heart by retractors, the left anterior descending coronary artery (LAD) was permanently ligated. For control reasons, mice were also subjected to surgery without application of MI (sham-operated animals).

Successful production of MI was checked by measurements of ST-elevation in electrocardiograms as well as impaired left ventricular wall motion by echocardiography. Animals that did not show ST-elevation and impaired left ventricular wall motion after myocardial infarction were excluded from further studies. Fourteen days after MI, additional echocardiography measurements were performed and finally hearts were excised and cut into transverse sections. From the middle ring, sections were cut and stained with appropriate antibodies (see above). Cardiac dimensions and function were analyzed by pulse-wave Doppler echocardiography essentially.

2.2.6.4 Echocardiography

Echocardiographic studies were performed under light anesthesia with spontaneous respiration using isoflurane. An ultrasonographer experienced in rodent imaging performed the echocardiography, operating a Toshiba PowerVision 6000 and a 15 MHz transducer. Short-axis two-dimensional echocardiographic images were obtained at the midpapillary and apical levels of the left ventricle and stored as digital loops. Frame acquisition rates using the loop mode reached 100 MHz, allowing excellent temporal resolution for two-dimensional analysis. At the same anatomic levels, short-axis M mode images were obtained with a sweep speed of 100 mm/s. Echocardiographic studies were performed after the surgical procedure at weeks four and eight. Endocardial borders were traced at end-systole and end-diastole utilizing a prototype off-line analysis system (NICE, Toshiba Medical Systems, The Netherlands). Using the end-systolic and -diastolic areas, fractional area changes were calculated at both levels as $[(\text{end-diastolic area} - \text{end-systolic area})/\text{end-diastolic area}]$ (Merkle *et al.*, 2007).

2.2.6.5 Matrigel implantation and determination of vascularization

300 μl Matrigel™ Basement Membrane Matrix High Concentration supplemented with 600 ng/ml bFGF, 300 ng/ml VEGF and 25 U/ml Heparin were injected subcutaneously into wildtype C57BL/6 mice and harvested two weeks later. Animals were treated post implantation with Antagomir-24 or a scrambled control antagomir (5 mg/kg at day 0 and day 2) by retroorbital injection. Half of the plug was lysed in cell lysis buffer and samples were measured for haemoglobin amount with a Mouse Hemoglobin ELISA.

Hemoglobin amount was normalized to total protein. Additionally, plugs were frozen in TissueTek, sliced, stained with CD31 antibodies and investigated by fluorescence microscopy.

2.2.7 MicroRNA target prediction

The miRNA databases and target prediction tools miRBase (<http://microrna.sanger.ac.uk/>, Griffiths-Jones *et al.*, 2004, 2006, 2008), PicTar (<http://pictar.mdc-berlin.de/>, Krek *et al.*, 2005) and TargetScan (<http://www.targetscan.org/index.html>, Lewis *et al.*, 2005; Grimson *et al.*, 2007; Friedman *et al.*, 2009) were used to screen and identify *in silico* potential miRNA targets.

2.2.8 Statistical analysis

Average data are presented as mean and s.e.m. unless stated different. Statistical analysis was carried out using SigmaStat (SPPS, Chicago, USA). For statistical comparison of two groups, unpaired, two-tailed Student's t-test or Mann-Whitney Rank Sum test was used. In case of comparison of more than two groups one-way ANOVA was applied.

Differences were considered significant when $p < 0.05$. Otherwise, p values were described as n.s. (not significant). In the figures, significant p values are indicated by asterisk (* = $p < 0.05$; ** = $p < 0.01$; *** = $p < 0.001$).

3. Results

3.1 *MiR-24* is induced post myocardial infarction (MI)

MiRNA-dependent regulation of target proteins has been described in different organs and cell types thus highlighting a potential therapeutic value for disease. More interestingly, several studies indicated that miRNAs are deregulated upon cardiac failure (Thum *et al.*, 2007; van Rooij *et al.*, 2008). The up- or downregulation of cardiac miRNAs was also suggested to be a critical regulatory step for cardiac wound healing (Care *et al.*, 2007; Thum *et al.*, 2008; Bonauer *et al.*, 2009). Thus, miRNA deregulation may impact on essential cardiac signalling cascades which result in reduced cardiac function. Previously, upregulation of *miR-24* in a murine hypertrophy model was reported (van Rooij *et al.*, 2006). Other data gained in our group also indicated *miR-24* upregulation to be induced by cardiac stress in a rat MI model.

To validate these data, *miR-24* expression level was profiled in the left ventricle (LV) of infarcted mice hearts and compared to control animals. Mice underwent permanent coronary ligation, whereas controls received sham-operation only. Successful performance of infarcts was validated by ECG analysis and measured by impaired wall motion using echocardiography. After 14 d of intervention, hearts were prepared, total LV RNA was isolated, reverse transcribed and analyzed by real-time quantitative PCR with specific primers to *miR-24* and the house-keeping miRNA *RNU6b*. RT-PCR revealed a significant increase of *miR-24/RNU6b* ratio in infarcted versus sham operated animals (2.34 ± 0.44 vs. 1 ± 0.16 , $p < 0.05$; figure 3.1). This indicates that *miR-24* is regulated in cardiac remodeling post MI.

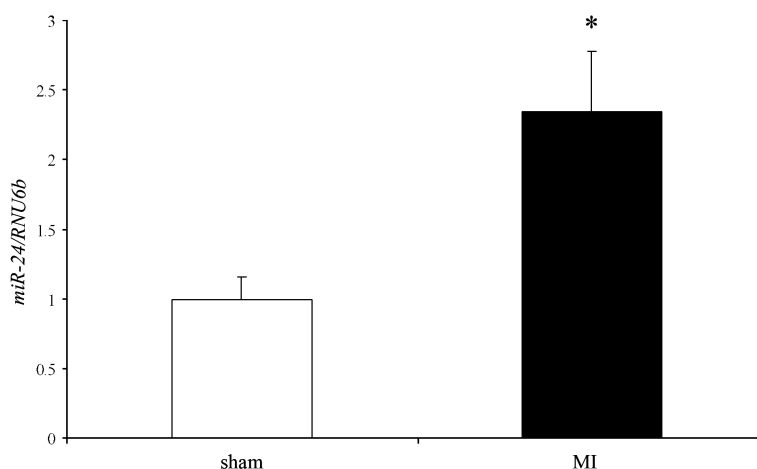


Figure 3.1: Ratio of *miR24/RNU6b* in sham versus infarcted (MI) mice hearts. Hearts were prepared 14 d after coronary ligation and LV underwent total RNA isolation and miRNA detection. N = 6 to 7 animals per group. * = $p < 0.05$

3.1.1 *MiR-24* profiling reveals an ubiquitous expression panel

MiRNA-dependent effects crucially depend on their cellular expression level. Cardiac injury changed *miR-24* expression in the infarcted heart. Since the heart comprises different cell types, the cellular source of *miR-24* upregulation is unclear. To test for possible differences in basal *miR-24* expression, an expression screen profiling endogenous *miR-24* was performed. This might give an initial clue to a possible cell type enriched expression, which has been reported for some miRNAs, e.g. *miR-126* for endothelial cells (ECs) (Fish *et al.*, 2008; Wang *et al.*, 2008; Kuhnert *et al.*, 2008). Therefore, real-time PCR detection of *miR-24* was performed in total RNA samples from different cell types and organs (figure 3.2). The resulting qualitative profile verified *miR-24* expression in endothelial cells as well as in cardiomyocytes which are key cellular components in the heart. Comparing the organ panel, higher *miR-24* signals were found in muscle, brain, spleen and heart. On the whole, *miR-24* screening revealed ubiquitous abundance of this microRNA. This indicates that *miR-24* is not a cell-type or organ specific miRNA based on human samples.

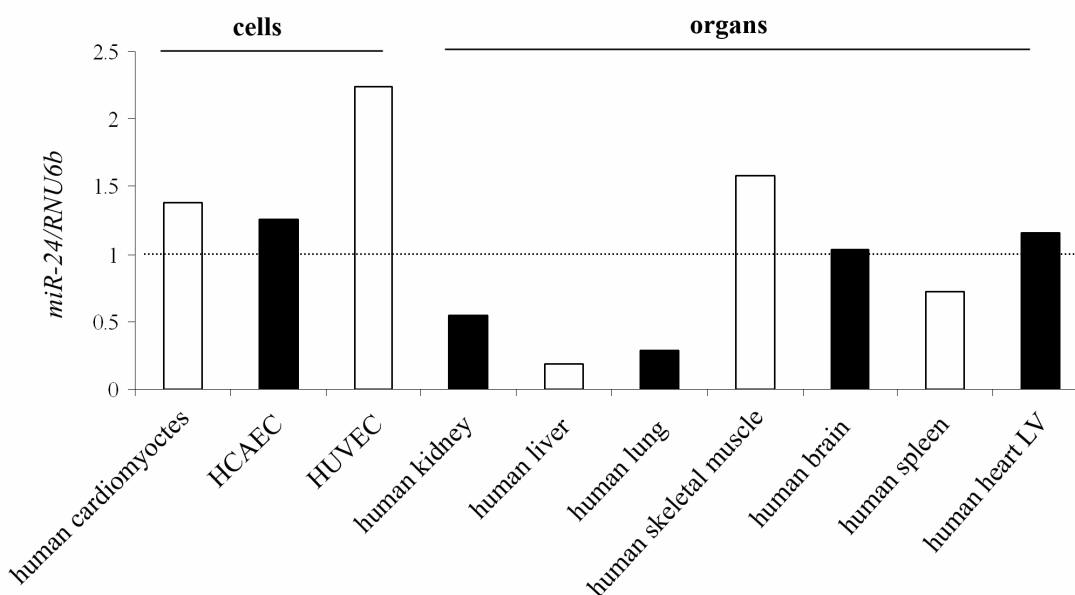


Figure 3.2: Ratio of *miR24/RNU6b* in various cell types and organs. Total RNA was prepared or provided from cell and organ samples and underwent miRNA detection with specific primers to *miR-24* and *RNU6b*.

3.1.2 *MiR-24* is induced in ECs post hypoxia and in cardiac ECs post MI

The regulation of miRNA expression depends on transcriptional activities occurring in the whole genome. Therefore, recruitment of transcription factors to its DNA binding sites is the trigger for induction or repression of transcription sites. Thus, identification of transcription factors regulating miRNA expression would be favorable to understand upstream miRNA signalling. Transcriptional regulation of the *miR-24-1* gene locus has been observed during hypoxic conditions by hypoxia-inducible factor α (HIF1 α) (Kulshreshtha *et al.*, 2007). A hypoxic environment is a major hallmark of myocardial infarction. Indeed, *miR-24* was found to be upregulated in the infarcted heart. To test the hypothesis if hypoxia induces *miR-24* in ECs or neonatal rat cardiomyocytes, cells were subjected to 1% (v/v) O₂ for 24 h and thereafter miRNA expression level was monitored. Interestingly, the expression level of *miR-24* was induced by hypoxic treatment in endothelial cells compared to normoxic environment (2.16 ± 0.12 vs. 1 ± 0.15 , $p < 0.01$; figure 3.3) but not in cardiomyocytes (data not shown).

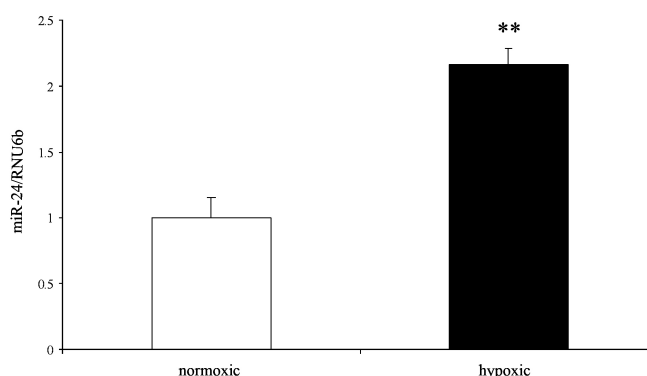


Figure 3.3: Relative *miR-24* expression during hypoxia *in vitro*. Endothelial cells were incubated in normoxic (21% v/v O₂) or hypoxic (1% O₂ v/v) conditions for 24 h before miRNAs were detected by TaqMan RT-PCR. *RNU6b* served as a house-keeping miRNA. N =3 experiments per group. ** = $p < 0.01$

A key player for hypoxic signalling is the aforementioned HIF1 α which mediates transcriptional control during hypoxic conditions (Kvietikova *et al.*, 1995; Huang *et al.*, 1996). *In vitro*, this transcription factor can be stabilized by a chemical agent, desferrioxamine (DFA), thus inhibiting its proteosomal degradation (Wang and Semenza, 1993). To test for potential HIF1 α -dependent transcriptional regulation of *miR-24* in ECs, HIF1 α was stabilized chemically by desferrioxamine (DFA) *in vitro*. In Western Blot experiments, HIF1 α upregulation was observable 6 h after DFA treatment in EC nuclear extract (figure 3.4).

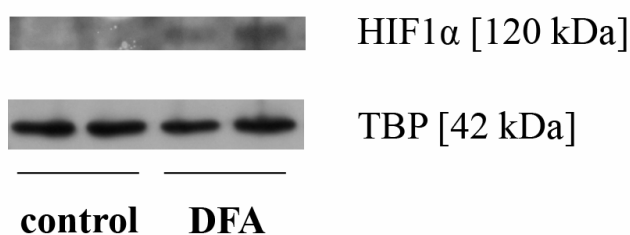


Figure 3.4: Representative Western Blot of HIF1 α in control or desferrioxamine (DFA, 150 μ M) treated HUVECs. Control and DFA-treated group were incubated for 6 h before protein isolation. Nuclear extracts were blotted onto PVDF membrane, followed by detection with appropriate antibodies. TATA-box binding protein (TBP) was used as a loading control.

Next, *miR-24* expression was investigated in DFA-treated, HIF1 α stabilized ECs. RT-PCR was applied to measure endogenous miRNA expression in isolated total RNA.

Nevertheless, the induction of HIF1 α protein measured by Western Blot before was not accompanied by a synergistic induction in *miR-24* expression compared to control level (0.85 ± 0.08 vs. 1 ± 0.05 , $p = \text{n.s.}$; figure 3.5).

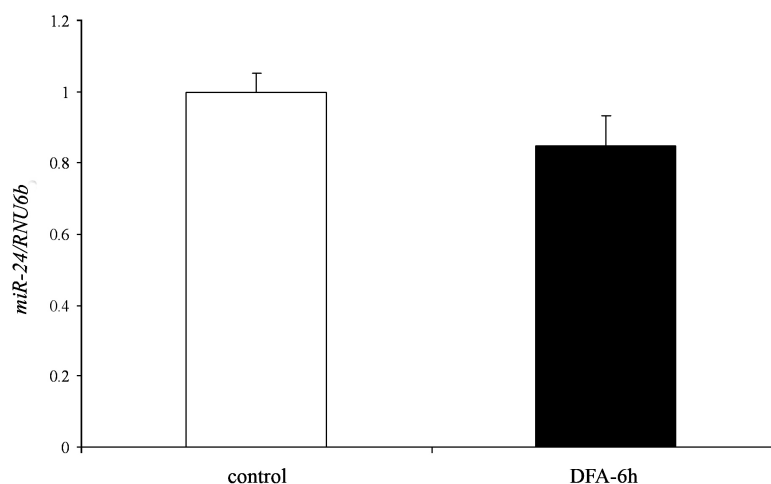


Figure 3.5: *miR-24* expression analysis in control and desferrioxamine (DFA) treated HUVECs. HUVECs were cultured for 6 h with or without the presence of 150 μM DFA. Afterwards, total RNA was isolated and RT-PCR analysis was performed. N = 4 per group.

Whether the *miR-24* expression pattern varies at different time points remains to be determined.

Myocardial infarction (MI) upregulated *miR-24* expression in total hearts 14 d after intervention (figure 3.1). The cellular source mostly contributing to enhanced expression is so far unclear. To address this issue, sham-operated and infarcted animals underwent cellular fractionation of heart tissue two days after intervention. In a first step, cardiomyocytes were separated from the non-cardiomyocyte fraction by sedimentation as described (Thum *et al.*, 2008). Afterwards, cardiac endothelial cells were isolated and enriched by incubation with magnetically-labeled CD146 beads. Finally, total RNA from cardiomyocytes and endothelial cells was subjected to miRNA-expression analysis. Endogenous *miR-24* expression was higher in cardiac ECs compared to cardiomyocytes (3.45 ± 0.40 vs. 1 ± 0.18 , $p < 0.001$; figure 3.6). Of great importance, *miR-24* expression level remained constant in cardiomyocytes either isolated from sham-operated or infarcted animals (1 ± 0.18 vs. 0.73 ± 0.22 , $p = \text{n.s.}$; figure 3.6).

In contrast, expression in cardiac endothelial cells increased post MI compared to sham control (7.17 ± 0.35 vs. 3.45 ± 0.40 , $p = <0.001$; figure 3.6).

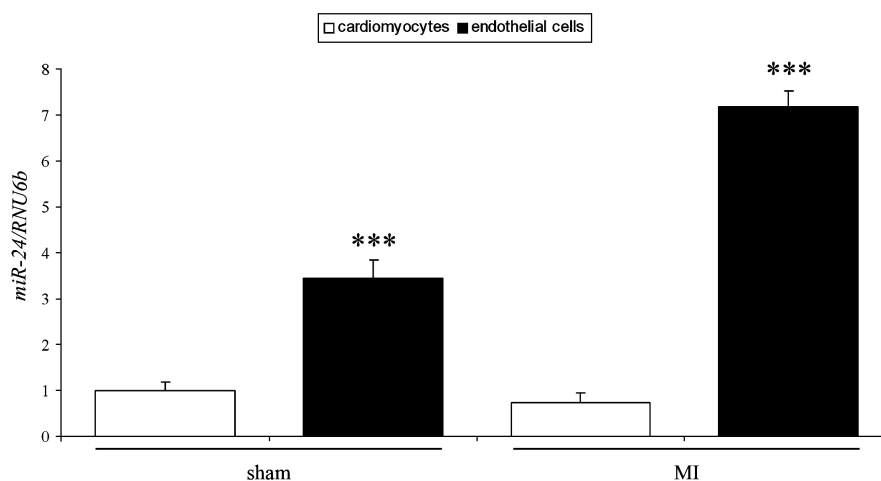


Figure 3.6: *MiR-24* expression analysis in murine cardiomyocytes or cardiac endothelial cells in sham-operated or animals post MI. Total hearts were isolated 2d after myocardial infarction or sham-operation. Then fractionation of cardiomyocytes and endothelial cells followed. *MiR-24* and relevant house-keeping *RNU6b* level was calculated by real-time PCR analysis. N =4 animals per group. *** = $p < 0.001$

Taken together, hypoxia or myocardial infarction induces expression of *miR-24* in cardiac endothelial cells. Its transcriptional regulation, however, remains unclear.

3.2 *MiR-24* modulation in different cell types

The availability of synthetic *miR-24* precursors or antagonists offers the possibility to perform *in vitro* gain- and loss-of function experiments. Therefore, we modulated *miR-24* expression in the most prominent cardiac cells, namely cardiomyocytes, fibroblasts and endothelial cells. Cardiomyocytes and fibroblasts were prepared and isolated from young-born rats whereas HUVECs served as an endothelial cell model. Synthetic scrambled (scr), precursor (pre) or antagonist (anti) miRNA oligonucleotides were transfected liposomally for 72 h. Afterwards, transfection efficiency was measured by miRNA-specific real-time PCR. In addition, Cy3-labeled miRNAs were transfected to monitor transfection efficiency.

As can be seen in figure 3.7, neonatal rat cardiomyocytes exhibited the strongest ability to incorporate exogenous Cy3-miRNA due to their large size in comparison to endothelial cells or fibroblasts.

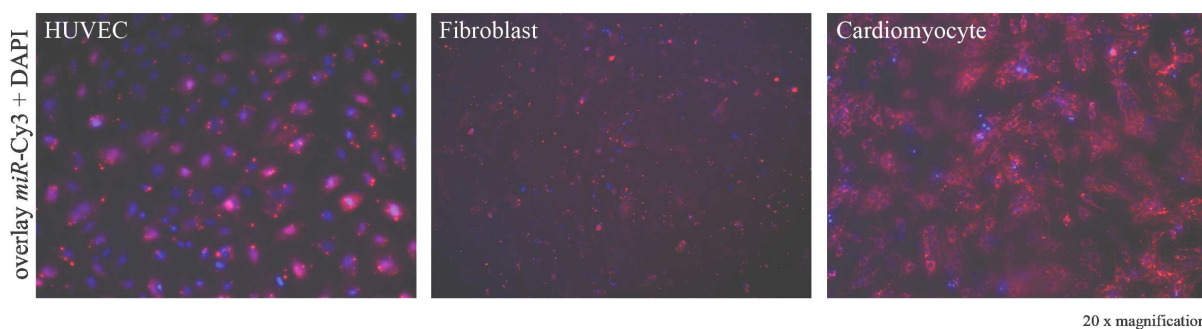


Figure 3.7: Liposomal transfection of Cy3-labeled miRNA precursor oligonucleotides in different cardiac cells. 100 nM of miR-Cy3 (red) was transfected for 72 h before fluorescent imaging was performed. Nuclei were stained with DAPI (blue).

Quantitative miRNA expression analysis further characterized the modulation of *miR-24* expression level (figure 3.8). While pre-*miR-24* transfection increased *miR-24* levels in endothelial cells (521.81 ± 147.96 vs. 10 ± 3.04 ; $p < 0.05$), fibroblasts (399.31 ± 69.08 vs. 10 ± 1.17 ; $p < 0.05$) and cardiomyocytes (3391.29 ± 570.43 vs. 10 ± 0.52 ; $p < 0.001$), transfection of anti-*miR-24* significantly repressed endogenous *miR-24* in endothelial cells (1.52 ± 0.81 vs. 10 ± 3.04 ; $p < 0.05$), fibroblasts (5.78 ± 1.24 vs. 10 ± 1.17 ; $p < 0.05$) and cardiomyocytes (0.14 ± 0.07 vs. 10 ± 0.52 ; $p < 0.001$). These experiments prove the general capability to modulate *miR-24* expression in different cardiac cell types *in vitro*.

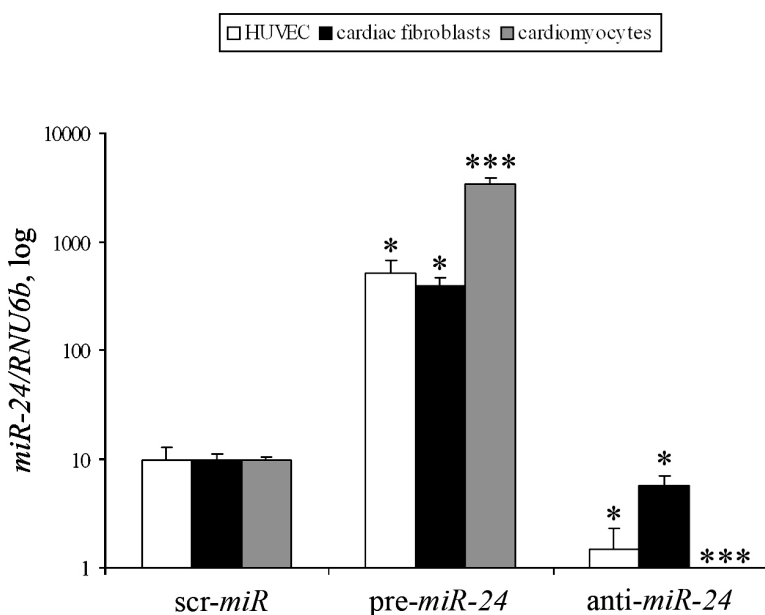


Figure 3.8: Transfection efficiency of *miR-24* precursor or antagonist in cardiomyocyte, fibroblast and endothelial cells. 100 nM of scrambled (scr) miRNA, pre-*miR-24* or anti-*miR-24* was transfected for 72 h before total RNA isolation and subsequent miRNA RT-PCR analysis. N = 4 per group. * = $p < 0.05$; *** = $p < 0.01$

3.2.1 *MiR-24* overexpression induces apoptosis specifically in ECs

The functional consequences of *miR-24* upregulation upon MI are unclear. It is well established that MI-dependent cardiac remodeling includes changes such as apoptosis, fibrosis and neoangiogenesis. Thus, modulating *miR-24* expression level might lead to severe functional changes in cardiac cells. To dissect the impact of *miR-24* modulation in the different cardiac cell types (cardiomyocytes, fibroblasts and endothelial cells) changes in apoptosis were tested by FACS. Annexin-V was used to mark early apoptotic cells since this protein binds with high affinity to phosphatidylserine (PS) which flips from the inner to the outer membrane side while apoptosis is initiated (Koopman *et al.*, 1994). In addition, cells were stained with propidium iodide (PI) to discriminate between necrotic and apoptotic cells because a prominent hallmark of apoptosis is the integrity of cellular membrane so only necrotic cells can incorporate PI.

While analyzing Annexin-V positive and PI-negative cells, only *miR-24* overexpressing ECs but not cardiomyocytes or cardiac fibroblasts showed a significant increase (2.78 ± 0.38 vs. 1 ± 0.016 ; $p < 0.05$) in apoptosis rate (figure 3.9). Moreover, even antagonizing endogenous *miR-24* in ECs reduced cell death (0.62 ± 0.04 vs. 1 ± 0.016 ; $p < 0.001$). Since cardiac fibroblasts and cardiomyocytes were unaffected in terms of apoptosis measurement, the proceeding experiments focused on *miR-24* function in ECs.

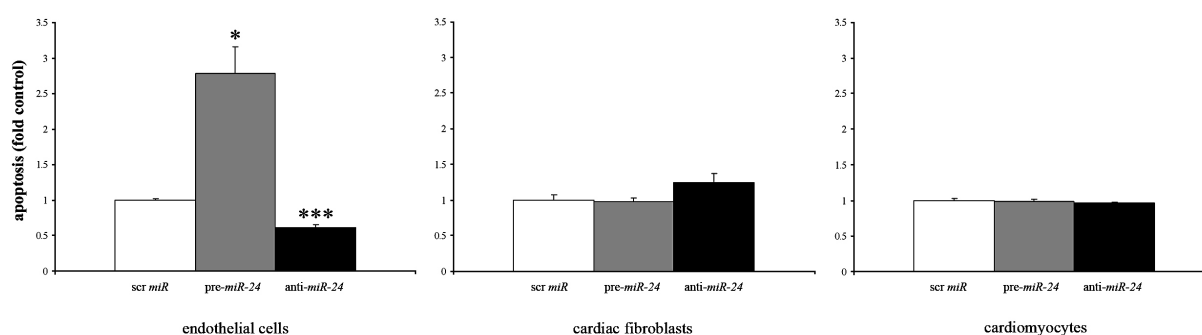


Figure 3.9: Apoptosis analysis in *miR-24* modulated ECs, cardiac fibroblasts and cardiomyocytes. Cells were miRNA-transfected for 72 h (100 nM each) and then underwent Annexin-V-FITC/PI staining. Samples were then analyzed on a FACS Calibur. Cells were gated on Annexin-V positive, PI-negative cells. N=4 per group. * = $p < 0.05$; *** = $p < 0.001$

Hypoxia-induced upregulation of *miR-24* in ECs raised the question, if antagonizing *miR-24* would reduce apoptosis rate induced by oxygen depletion. Therefore *miR-24* was either up- or downregulated in ECs for 72 h. Afterwards cells underwent hypoxic treatment (1% O₂) for 24 h. Finally apoptosis analysis was performed. Indeed, antagonizing *miR-24* in ECs reduced the apoptosis rate (1.54 ± 0.12 vs. 2.58 ± 0.12 ; $p < 0.001$) in hypoxic atmosphere (figure 3.10). Thus, *miR-24* downregulation is beneficial under stress conditions. For ECs, this observation implicates a shelter mechanism towards reduced oxygen concentration and cellular stress.

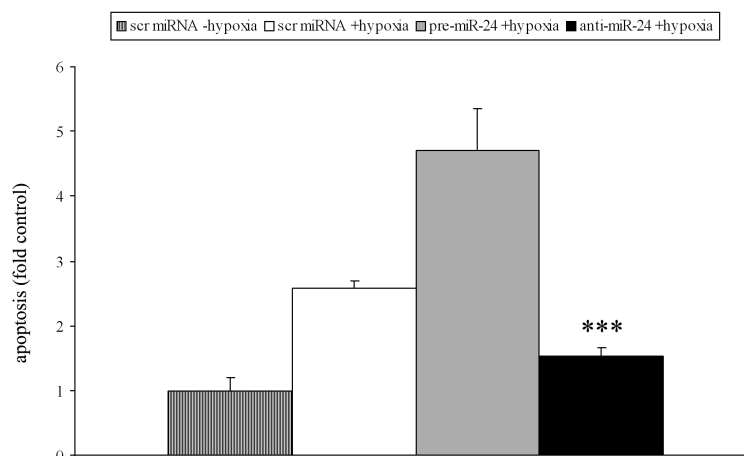


Figure 3.10: Apoptosis analysis in miRNA modulated ECs that were additionally exposed to hypoxic stress. ECs were miRNA transfected (100 nM each) for 72 h and then incubated in 1% O₂ for 24 h. Afterwards samples underwent Annexin-V-FITC/PI staining and were analyzed by FACS. N = 4 experiments per group. *** = $p < 0.001$

3.2.2 Apoptosis array post *miR-24* modulation reveals dysregulation of anti-apoptotic HMOX1 and pBAD protein

Cellular death induced by the extrinsic or intrinsic apoptosis pathway is mediated by diverse factors. Obviously, in ECs an apoptotic programme is initiated by upregulation of *miR-24* (figure 3.8). Nevertheless, underlying signal pathways remain elusive. To monitor the changes in the expression of key apoptotic players and to gain a better understanding for *miR-24* induced EC apoptosis, *miR-24* overexpressing HUVECs were analyzed using a specified apoptosis protein array (figure 3.11).

Here, the expression of 35 apoptosis-related factors was investigated simultaneously on a protein array. Control and *miR-24* modulated cell lysates were incubated to this array (figure 3.11). Finally, comparison of protein expression levels revealed deregulated protein levels induced by forced expression of *miR-24* (figure 3.12).

The strongest upregulation in protein levels was found for HIF-1 α (1.5-fold upregulation), FAS (+1.46-fold upregulation), SMAC/DIABLO (+1.42-fold upregulation), HSP27 (+1.38-fold upregulation) and HTRA2 (+1.32-fold upregulation) protein.

In contrast, a prominent reduction was observed for total Bad (0.54-fold downregulation) and HMOX1 protein (0.57-fold downregulation).

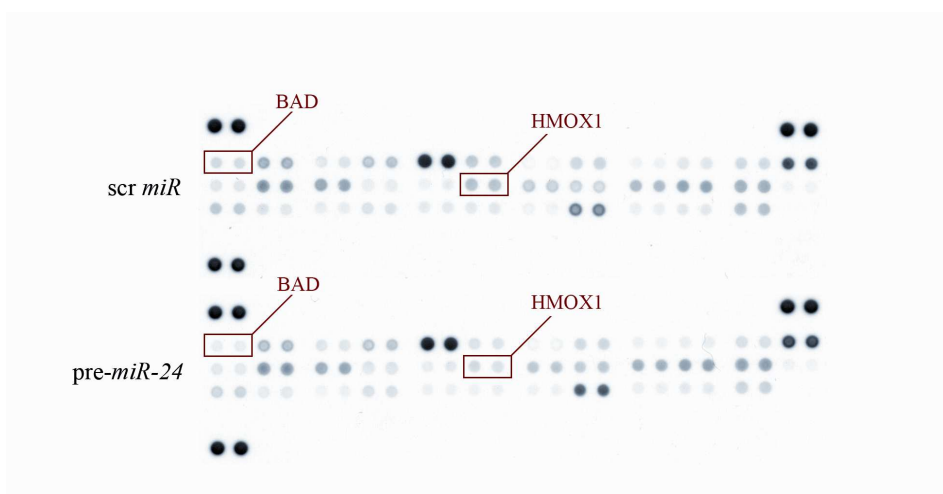


Figure 3.11: Apoptosis array membrane analyzed with control and *miR-24* modulated (100 nM each) cell lysates. 35 different antibodies to apoptosis markers were spotted and hybridized in duplicate to the membrane. 200 μg of total cell lysates were incubated with membranes and developed with a chemiluminescent method. Group lysates were a pool of three different experiments.

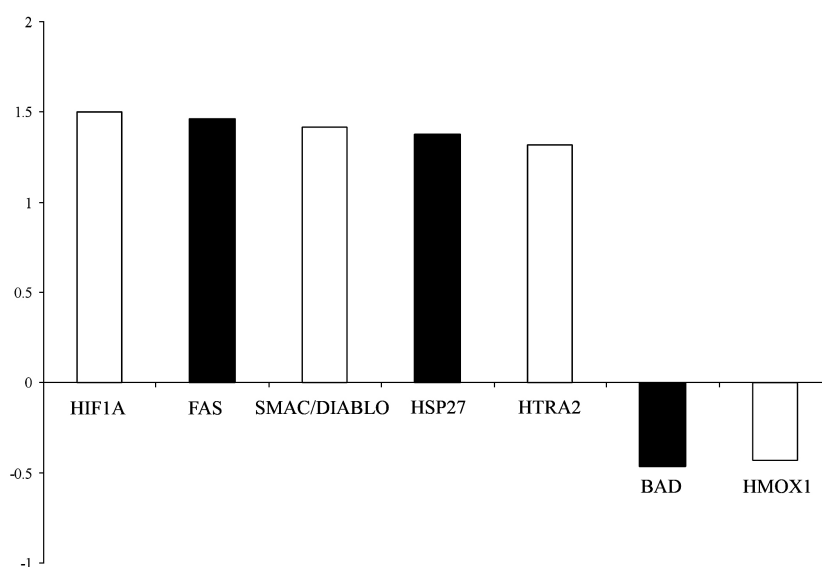


Figure 3.12: Quantitative summary of the protein profiler apoptosis array. A selection of up- or downregulated apoptosis-related proteins upon *miR-24* modulation in ECs is plotted.

To delineate mechanisms involved in *miR-24* mediated apoptosis we focused on downregulated proteins related to anti-apoptotic function or cardiovascular protection.

Therefore, two candidate proteins, BAD and HMOX1, were further investigated to validate the array result. BAD belongs to the BCL2 family and either stimulates apoptosis by heterodimerization at mitochondrial membran sites (Zha *et al.*, 1997) or protects towards cell death in phosphorylated state (Zha *et al.*, 1996). Cardioprotective heme-oxygenase 1 (HMOX1) has been characterised as an outstanding factor for heme metabolism thereby mediating anti-oxidant effects (Clark *et al.*, 2000). Endothelial cells were modulated either by precursor or antagonistic *miR-24* transfection. *MiR-24* dependent HMOX1 downregulation was confirmed by Western Blot in HUVECs (0.19 ± 0.09 vs. 1 ± 0.25 ; $p < 0.05$; figure 3.12). In line, antagonizing endogeneous *miR-24* increased HMOX1 expression compared to control level (1.42 ± 0.37 vs. 1 ± 0.25 ; $p = \text{n.s.}$; figure 3.13).

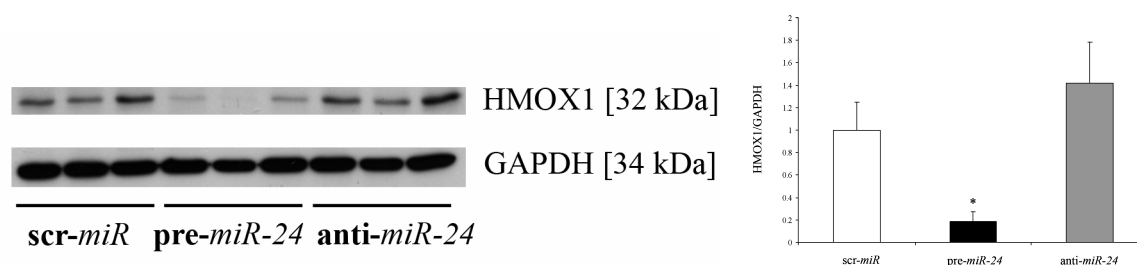


Figure 3.13: Western Blot analysis of HMOX1 protein in scr-*miR*, pre-*miR-24* or anti-*miR-24* modulated (100 nM each) HUVECs. Loading control is GAPDH. HMOX1 signal density was normalized to GAPDH, N = 3 experiments per group. * = $p < 0.05$

In contrast to direct quantification of HMOX1 by Western Blot, BAD expression level was investigated differently since its prominent anti-apoptotic characteristic depends on its phosphorylation status controlled by kinases (Datta *et al.*, 1997). Thus, post-translational modification might also contribute to decreased BAD expression in the protein apoptosis array. To dissect this issue, Western Blot in combination with phospho-Bad specific ELISA was performed. This approach showed that the level of unphosphorylated BAD was slightly decreased in *miR-24* overexpressing ECs (0.74 ± 0.11 vs. 1 ± 0.17 ; $p = \text{n.s.}$; figure 3.14). Repression of *miR-24* also decreased total BAD protein (0.57 ± 0.14 vs. 1 ± 0.17 ; $p = \text{n.s.}$; figure 3.14).

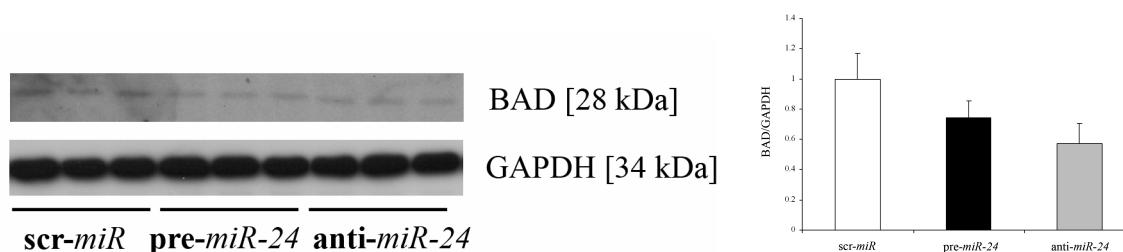


Figure 3.14: Representative Western Blot analysis of BAD protein in *scr-miR*, *pre-miR-24* or *anti-miR-24* modulated (100 nM each) HUVECs. Loading control is GAPDH. BAD signal density was normalized to GAPDH, N = 3 experiments per group.

Further normalizing the total BAD protein values to relevant BAD phosphorylation status at serine residue 112 revealed a massive downregulation by *miR-24* overexpression (0.31 ± 0.03 vs. 1 ± 0.16 ; $p < 0.05$, figure 3.15). This indicates loss of anti-apoptotic phospho-BAD (p-BAD) function induced by *miR-24*. In contrast, inhibiting *miR-24* increased phosphorylated BAD levels (1.76 ± 0.34 vs. 1 ± 0.16 ; $p = \text{n.s.}$).

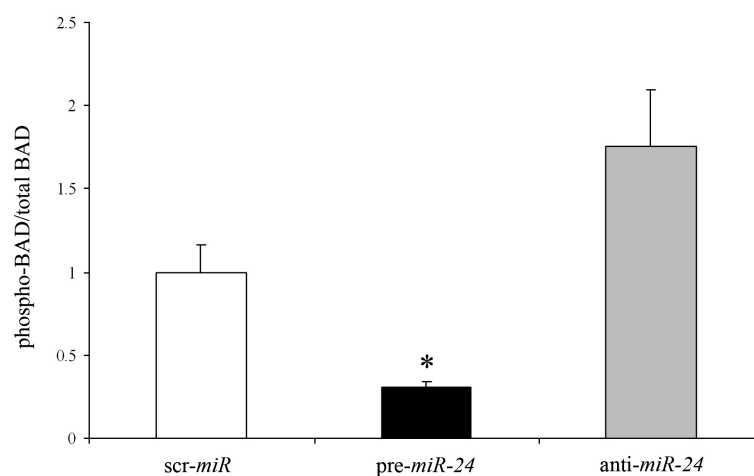


Figure 3.15: Summary of phospho-BAD ELISA data (p112) normalized to total BAD protein values. HUVECs were miRNA modulated (100 nM each), lysed and analyzed by phospho-BAD specific ELISA. N = 3 experiments per group. * = $p < 0.05$

The data indicate the involved factors to trigger apoptotic pathways by *miR-24* overexpression in ECs. Underlying molecular mechanisms are therefore potentially mediated by p-BAD and HMOX1 downregulation. However, these proteins are no predicted *miR-24* targets.

Thus, regulative impact should be mediated by other modulators that are direct *miR-24* targets (see section 3.3).

3.2.3 Elevated reactive oxygen species (ROS) upon *miR-24* overexpression in ECs

In ECs, *miR-24* overexpression induces apoptosis. The cellular consequences are cell shrinkage, chromatin condensation and the induction of proteolytic cascades. Apoptosis progression can be accompanied by certain side reactions, enhancing the apoptotic signalling (Johnson *et al.*, 1996). As validated before, *miR-24* overexpressing ECs have a deficit in antioxidant HMOX1. To answer the question, if increased reactive oxygen species (ROS) are present in *miR-24* overexpressing and apoptotic ECs, cells underwent dihydroethidium (DHE) staining and FACS analysis. Shown in figure 3.16, ROS levels were significantly increased in *miR-24* overexpressing ECs (1.86 ± 0.03 vs. 1 ± 0.01 ; $p < 0.001$). This finding implies that the generation of ROS may contribute to *miR-24* mediated apoptosis.

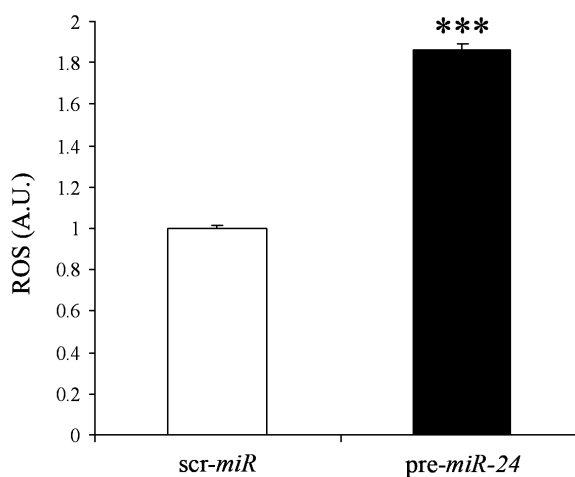


Figure 3.16: Measurement of reactive oxygen species (ROS) by dihydroethidium (DHE) staining in scr-*miR* and *miR-24* modulated (100 nM each) ECs. Cells were miRNA-transfected for 72 h, stained with 2.5 μ M DHE and analyzed on a FACS Calibur. N = 4 experiments per group. *** = $p < 0.001$

3.2.4 Capillary tube formation is impaired in *miR-24* overexpressing ECs

A major characteristic of ECs is the capability to form tube-like capillaries supporting angiogenic response *in vivo*. This feature can be investigated *in vitro* by monitoring tube-formation in matrigel-coated wells (Grant *et al.*, 1989). To answer the question if *miR-24* modulation influences angiogenic properties *in vitro*, a tube-formation assay was performed. To test this, cells are seeded onto matrigel-coated slides where tube formation is favoured. Again, HUVECs were *miR-24* modulated and then analyzed for tube-formation qualitatively. As can be seen in figure 3.17, control and anti-*miR-24* modulated ECs show comparable capillary formation. Nevertheless, angiogenic response is impaired in *miR-24* overexpressing ECs indicated by the lack of proper capillary density. In summary, this assay reveals a first functional defect for *miR-24* overexpressing ECs.

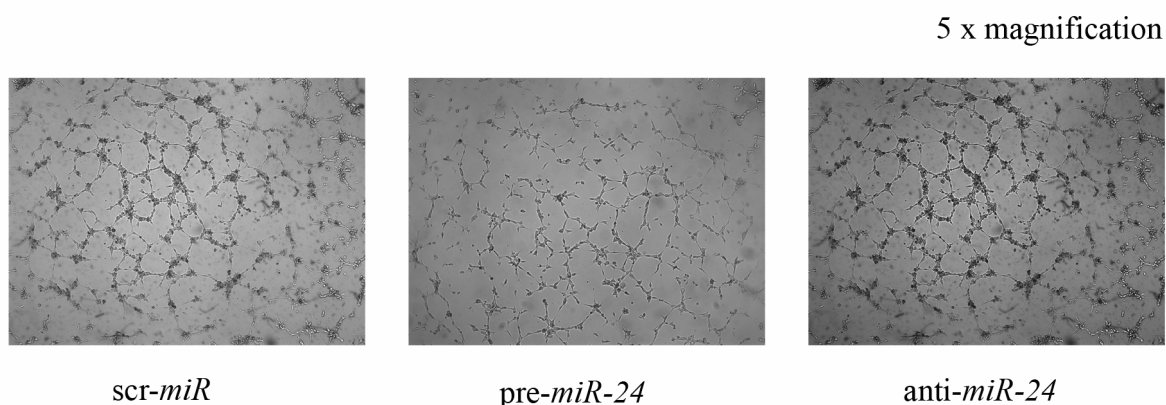


Figure 3.17: Tube formation assay on matrigel coated wells. HUVECs were miRNA-modulated (100 nM each) for 72 h. Then, 15000 cells were put on matrigel for up to 24 h. Qualitative pictures were taken at 8 h. N = 3 experiments per group.

3.3 *MiR-24* regulates endothelial GATA2, H2A.X, PAK4 and RASA1

The major hallmark of miRNA biology is the post-transcriptional regulation of miRNA-specific target genes. Thus, binding of miRNAs to the 3'-UTR of target mRNA can inhibit translation or induce degradation of the mRNA:miRNA heteroduplex.

Noteworthy, miRNA-guided protein regulation crucially depends on the abundant expression of miRNA and its target gene within the same cell. The aforementioned *miR-24* mediated defects in endothelial cell biology should be explained by exploring and validating direct *miR-24* targets in endothelial cells. More insight into the network of miRNA and its targets is provided by different miRNA target prediction tools available online. The miRNA prediction databases miRBase (www.mirbase.org), PicTar (www.pictar.mdc-berlin.de) and TargetScan (www.targetscan.org) were applied to screen for putative *miR-24* target genes potentially involved in fundamental EC biology processes, e.g. apoptosis or angiogenic response. In table 3.1, four putative *miR-24* targets are listed which are predicted by at least two databases. The genes *H2AFX*, *GATA2*, *PAK4* and *RASA1* are commonly expressed in endothelial cells.

Table 3.1: Selection of predicted *miR-24* targets provided by different databases.

Gene symbol	Gene name	Evolutionary conservation, no. of species (miRBase)	Predicted target (miRBase)	Predicted target (PicTar)	Seed match for <i>miR-24</i> (TargetScan)
<i>GATA2</i>	Endothelial transcription factor GATA-2 (GATA-binding protein 2)	4	yes	no	8mer (poorly conserved)
<i>H2AFX</i>	Histone 2A family member X (H2A.X)	5	yes	yes	7mer-m8 (two sites conserved)
<i>PAK4</i>	Serine/threonine-protein kinase PAK 4 (p21-activated kinase 4) (PAK-4)	5	no	yes	8mer (conserved)
<i>RASA1</i>	Ras GTPase-activating protein 1 (GTPase-activating protein) (GAP) (Ras p21 protein activator) (p120GAP) (RasGAP)	10/1	no	yes (2 transcript variants)	7mer-m8 (conserved)

To validate the prediction of *miR-24* targets, endothelial cells overexpressing *miR-24* were analyzed for target protein expression by Western Blot (figure 3.18). GATA2, an endothelial-specific transcription factor that also is known to control hematopoiesis (Tsai *et al.*, 1994), is decreased while *miR-24* expression is forced (0.57 ± 0.06 vs. 1 ± 0.09 ; $p < 0.05$). The histone 2 family member H2A.X is involved in DNA double strand repair and has recently been reported to have an essential role in postnatal angiogenesis (Lal *et al.*, 2009). In ECs, *miR-24* overexpression represses expression of nuclear H2A.X measured by Western Blot analysis (0.56 ± 0.13 vs. 1 ± 0.05 ; $p = 0.05$). In addition, the anti-apoptotic kinase PAK4 regulating Bad phosphorylation status (Gnesutta *et al.*, 2001) is decreased (0.31 ± 0.02 vs. 1 ± 0.10 ; $p < 0.01$). Finally, RASA1, a family member of the Ras GTPases essential for the formation of vasculature (Henkemeyer *et al.*, 1995), is downregulated upon *miR-24* overexpression (0.56 ± 0.04 vs. 1 ± 0.12 ; $p < 0.05$).

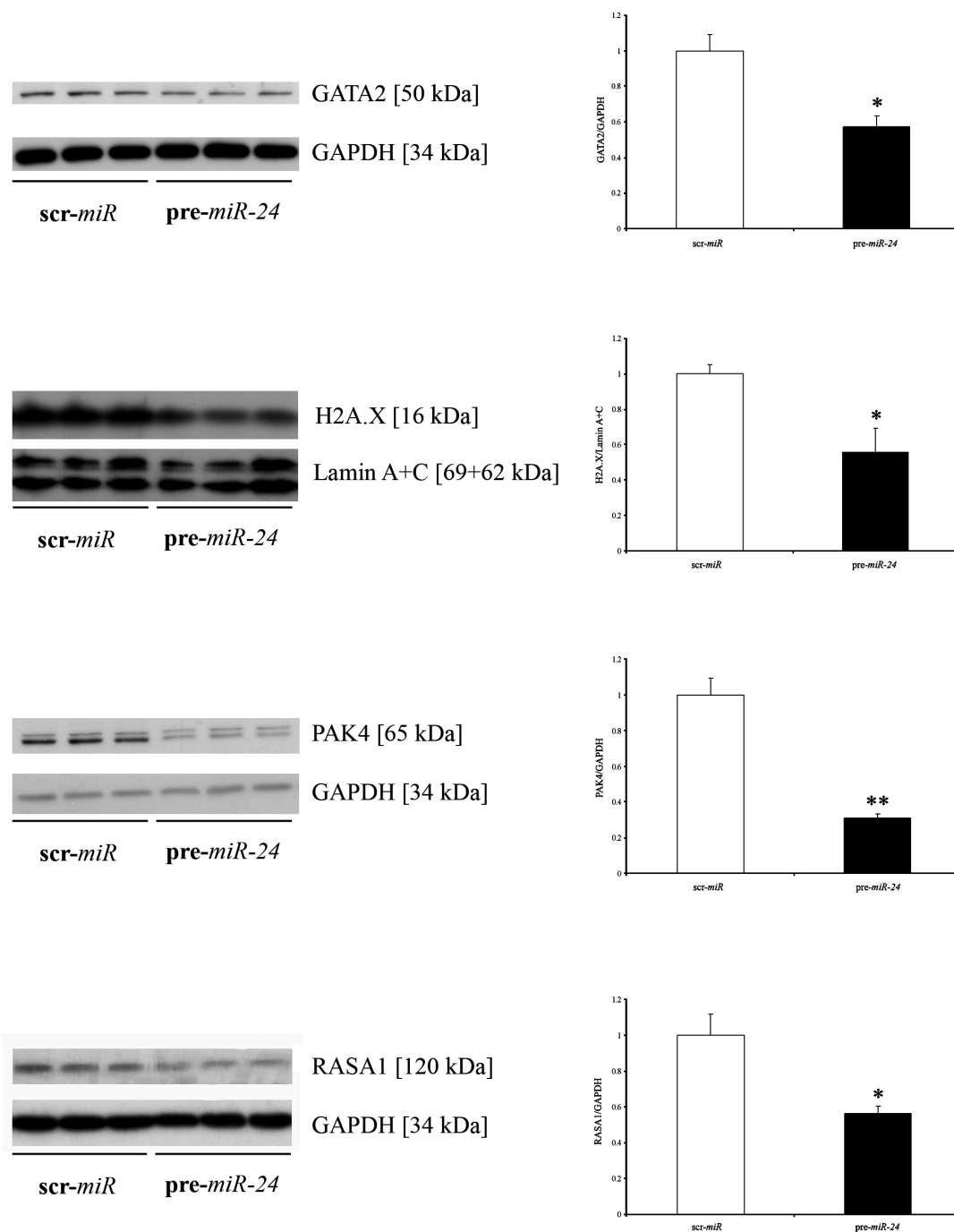


Figure 3.18: Western Blot analysis of putative *miR-24* targets in ECs. HUVECs were transfected with 100 nM scr control miRNA or pre-*miR-24* for 72 h, harvested and lysed. 10-50 μ g total protein, in case of H2A.X a nuclear fraction, was loaded onto 12% (v/v) SDS-Polyacrylamide gels and SDS-PAGE was performed. Gels were blotted onto PVDF-membranes, blocked with 5% (w/v) skim milk powder, incubated with appropriate primary antibodies, secondary antibodies linked to HRP and developed using chemiluminescent reaction. GAPDH was used as a loading control for GATA2, PAK4 and RASA1, whereas nuclear Lamin A+C was the normalizing factor for H2A.X. For each target, Western Blot results were normalized and validated statistically. N = 3 experiments each. * = $p < 0.05$; ** = $p < 0.01$

Cumulatively, *in vitro* overexpression of *miR-24* suggests H2A.X, GATA2, PAK4 and RASA1 to be potential *miR-24* targets. Investigated targets are expressed in endothelial cells and linked at least to cellular apoptosis or angiogenic signalling. To further proof these targets, reporter gene assays were performed to validate *bona fide* targets for *miR-24*.

3.3.1 Luciferase reporter gene assays confirm *miR-24* targets GATA2, H2A.X, PAK4 and RASA1

MiRNAs target mRNAs specifically at the 3'-untranslated region (3'-UTR) leading to transcript degradation or subsequent ribosome inhibition. As a direct consequence, target protein level decreases. A genetic tool to observe miRNA:mRNA interaction is a luciferase reporter gene assay. Therefore, 3'-UTR of interest is cloned adjacent to the luciferase gene in a reporter vector. *In vitro*, reporter vector, miRNAs of interest and a normalizing beta-Gal containing vector are co-transfected in HEK293 reporter cell line. Theoretically, interaction with an appropriate, specific miRNA should downregulate luciferase gene expression in respect to the aforementioned mechanism. For control reasons, different miRNAs with no binding prediction (non-related miRNAs) are also co-transfected. Thus, luciferase expression should be unaffected here.

In this work, human *GATA2*-, *H2A.X*-, *PAK4*- and *RASA1*-3'-UTR bearing *miR-24* binding site were cloned into a luciferase reporter vector and analyzed. Remarkably, *H2A.X*-3'-UTR contained two *miR-24* binding sites. As can be seen in figure 3.19, the investigated luciferase constructs were specifically downregulated in the presence of *miR-24* compared to control group (*H2A.X*: 0.63 ± 0.01 vs. 1 ± 0.03 ; $p < 0.001$; *GATA2*: 0.68 ± 0.02 vs. 1 ± 0.01 ; $p < 0.001$; *PAK4*: 0.68 ± 0.01 vs. 1 ± 0.07 ; $p = 0.005$; *RASA1*: 0.52 ± 0.04 vs. 1 ± 0.02 ; $p < 0.001$). However, luciferase activity for non-related miRNAs with no predicted binding site in 3'-UTR like *miR-1*, *miR-22* and *miR 210*, remained basically unchanged.

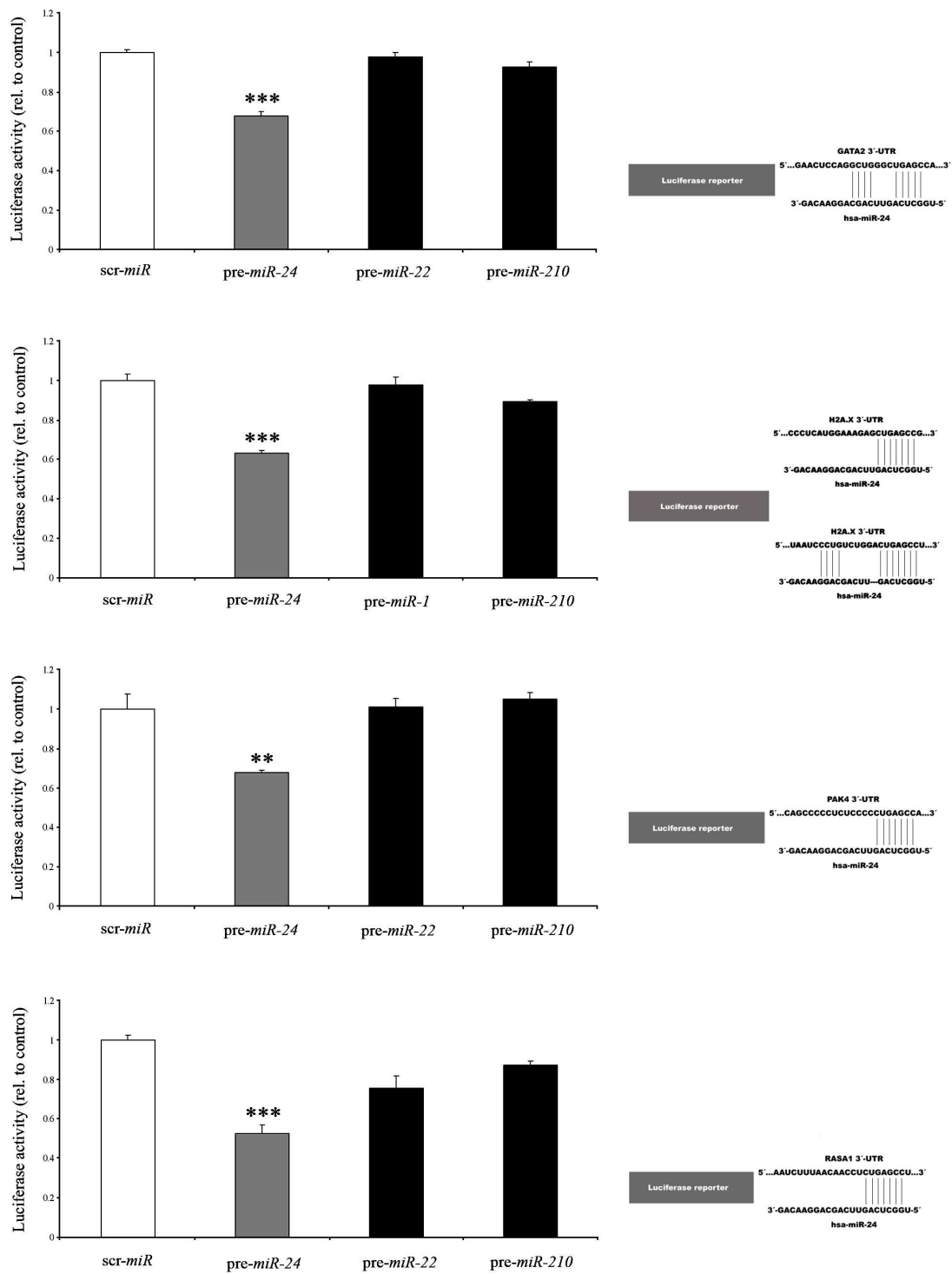


Figure 3.19: Luciferase assays to validate the potential *miR-24* targets GATA2, H2.AX., PAK4 and RASA1. HEK293 reporter cells were transfected for 24 h with cloned reporter vector bearing the predicted *miR-24* binding site, miRNA and for normalizing reasons, beta-galactosidase expression vector. Finally, cells were lysed and analyzed for luminescence and beta-galactosidase activity. N = 4 experiments per group. ** = $p < 0.05$; *** = $p < 0.001$

3.3.2 Transient knockdown of *miR-24* targets GATA2, PAK4 and RASA1 induces apoptosis in ECs

As mentioned before, GATA2, H2A.X, PAK4 and RASA1 were validated as direct *miR-24* targets through its recognition sites in 3'-UTR. In addition, overexpression of *miR-24* was pro-apoptotic implicating a role of its target genes in regulating apoptosis outcome. To test for an impact on apoptosis, validated targets were transiently downregulated and analyzed by Annexin-V-FITC/PI staining. Noteworthy, as can be seen in figure 3.20, all targets were efficiently repressed by their specific siRNA.

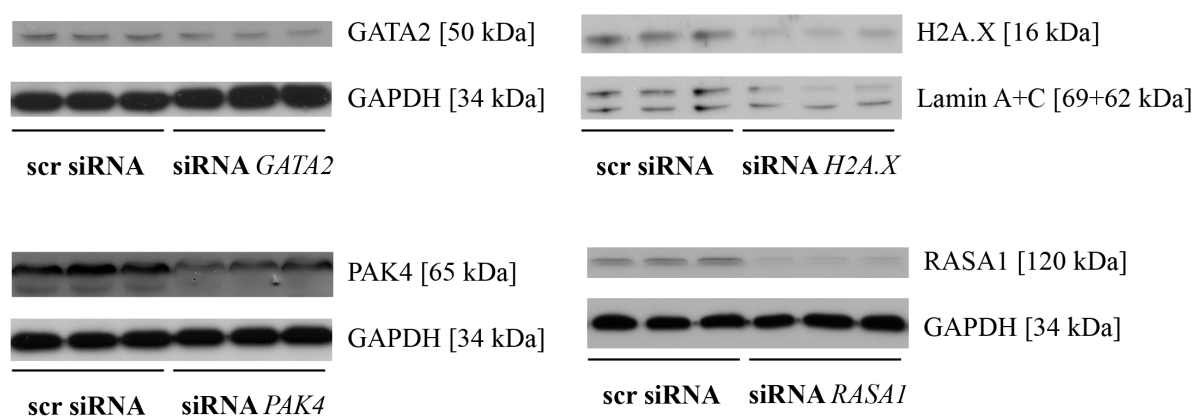


Figure 3.20: Western Blot analysis for transient knockdown of GATA2, H2A.X, PAK4 and RASA1 in ECs. HUVECs were transfected with 100 nM scr control siRNA or target specific siRNA, harvested and lysed. 10-50 μ g total protein, in case of H2A.X a nuclear fraction, was loaded onto 12% (v/v) SDS-Polyacrylamide gels and SDS-PAGE was performed. Gels were blotted onto PVDF-membranes, blocked with 5% (w/v) skim milk powder, incubated with appropriate primary antibodies, secondary antibodies linked to HRP and developed using chemiluminescent reaction. GAPDH was used as a loading control for GATA2, PAK4 and RASA1, whereas nuclear Lamin A+C was the normalizing factor for H2A.X. N = 3 experiments each.

Modulated endothelial cells were then analyzed for an apoptotic phenotype. In case of *GATA2*, *PAK4* and *RASA1*, knockdown increased apoptosis compared to scrambled control siRNA transfected ECs (*GATA2*: 2.40 ± 0.07 vs. 1 ± 0.03 ; $p < 0.001$; *PAK4*: 1.79 ± 0.03 vs. 1 ± 0.03 ; $p < 0.001$; *RASA1*: 1.41 ± 0.10 vs. 1 ± 0.04 ; $p < 0.05$; figure 3.21). In contrast, transient H2A.X silencing had no effect on apoptotic events (0.85 ± 0.07 vs. 1 ± 0.13 ; $p = \text{n.s.}$).

To sum up, three out of four identified direct *miR-24* targets, namely GATA2, PAK4 and RASA1 directly foster apoptosis in ECs.

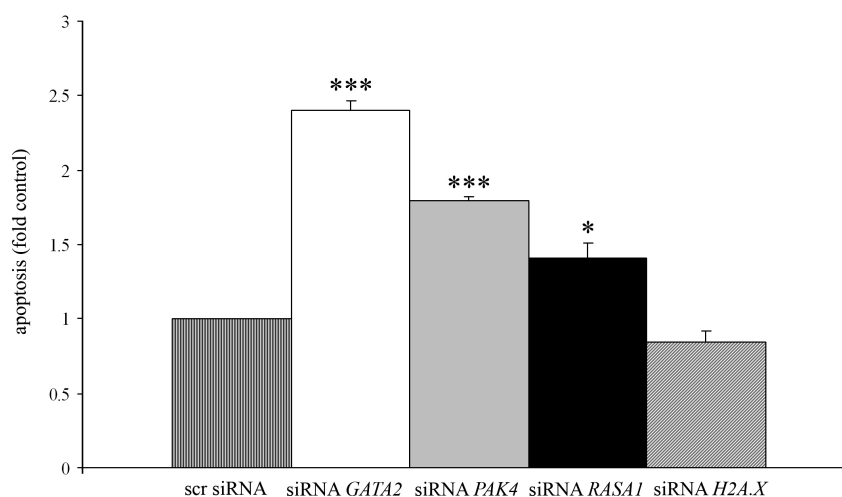


Figure 3.21: Apoptosis analysis in siRNA modulated ECs. ECs were transfected with gene specific siRNA (150 nM each) for 48 h. Afterwards samples underwent Annexin-V-FITC/PI staining and were analyzed by FACS. N = 4 experiments per group. * = $p < 0.05$; *** = $p < 0.001$

3.3.3 GATA2 is a key player for cell cycle progression in ECs

In ECs, silencing of the *bona fide miR-24* target GATA2, elevates apoptosis progression remarkably (figure 3.21). Apoptosis was described to be triggered by transcription factor-dependent control of cell cycle (Field *et al.*, 1996). To check for a direct relationship between repressed GATA2 protein level and proliferative status, GATA2 modulated ECs underwent cell cycle analysis by propidium iodide (PI) stain. In line with the aforementioned effect on apoptosis, cell cycle progression was disturbed in *GATA2*-deficient ECs compared to control group (figure 3.22). Resting cells in G0/G1 phase decreased (0.86 ± 0.008 vs. 1 ± 0.02 ; $p < 0.01$), as well as DNA-synthesizing in S-phase (0.65 ± 0.01 vs. 1 ± 0.03 ; $p < 0.001$) and finally mitotically active ones (0.60 ± 0.03 vs. 1 ± 0.04 $p < 0.001$). Taken together, the GATA2 transcription factor also seems to be a key effector for cell cycle progression in endothelial cells.

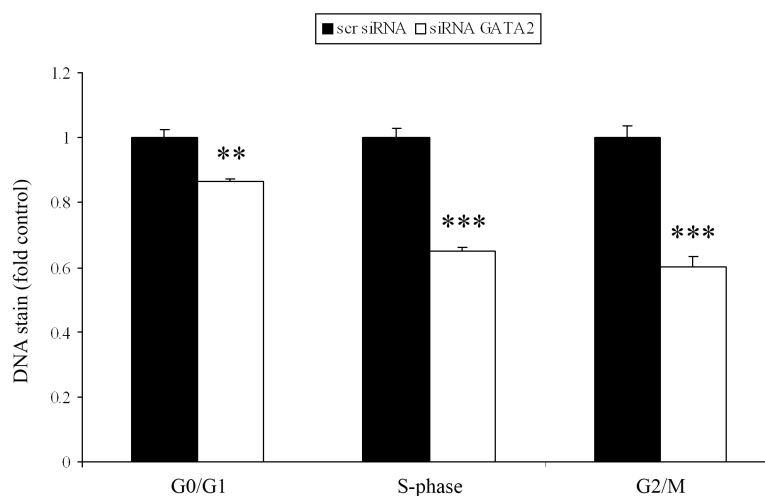


Figure 3.22: Cell cycle analysis in GATA2 silenced ECs. Endothelial cells were transfected with gene specific siRNA (150 nM each) for 48 h. Afterwards samples underwent PI staining and were analyzed by FACS. N = 4 experiments per group. ** = $p < 0.01$; *** = $p < 0.001$

3.3.4 Impairment in tube formation ability in ECs when silencing GATA2 or PAK4

Forced *miR-24* expression induces apoptosis, ROS formation and leads to a disturbance in angiogenic signalling measured by decreased *in vitro* tube formation (figure 3.16). The identification of the *miR-24* downstream effectors GATA2, H2A.X, PAK4 and RASA1 raised the question if single target knockdown also affects the formation of capillary-like structures on matrigel. Thus, siRNA experiments were performed and afterwards angiogenic response was investigated. The qualitative analysis reveals that again silencing *GATA2* has the strongest effects on endothelial tube formation (figure 3.23). *PAK4* knockdown also slightly impairs tube formation whereas inhibiting *H2A.X* or *RASA1* does not alter capillary tube formation.

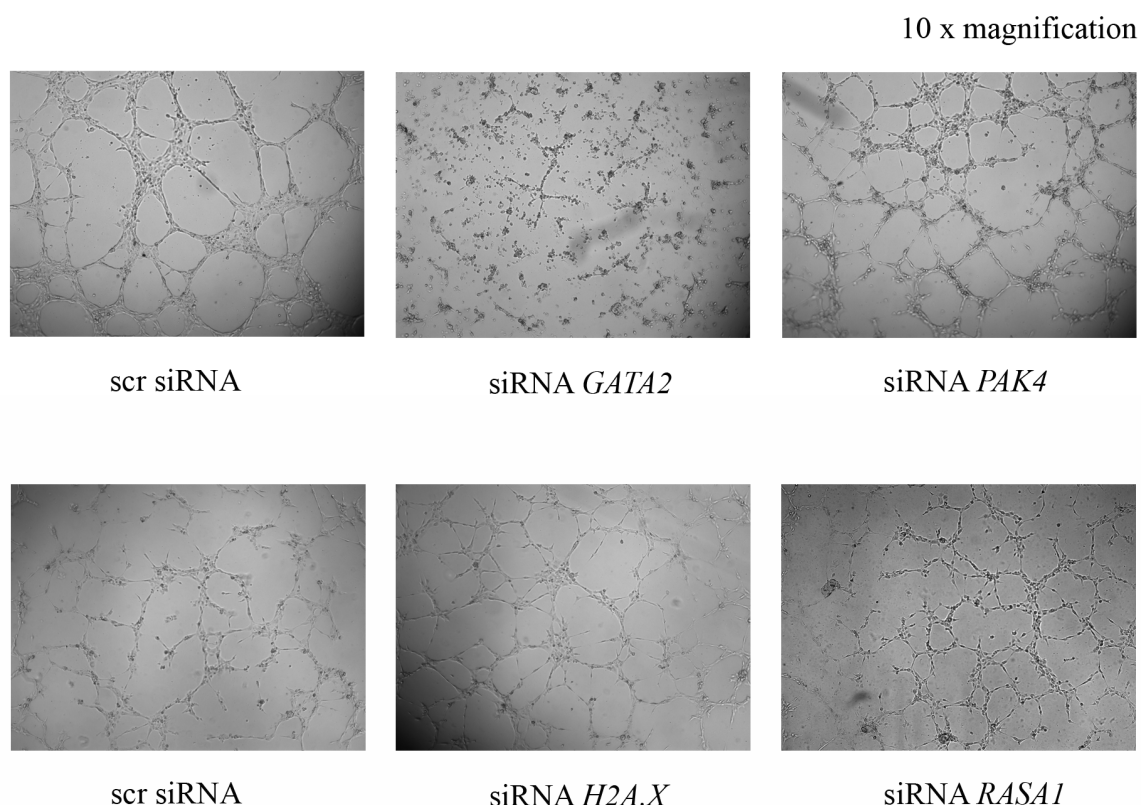


Figure 3.23: Tube formation assay on matrigel coated wells. HUVECs were siRNA-modulated (150 nM each) for 48 h. Then, 15000 cells were put on matrigel for up to 24 h. Qualitative pictures were taken at 4-8 h. N = 3 experiments per group.

3.3.5 PAK4 and RASA1 are downregulated under hypoxic conditions in ECs

This work describes *miR-24* induction by cardiac stress and through hypoxia. Certainly, hypoxia-driven transcriptome changes occur to counteract the changing environment. To test the hypothesis if the elevated *miR-24* expression levels correlate with a parallel decrease in target protein, endothelial cells were exposed to hypoxia for 24 h. Total protein was isolated and subsequently Western Blot analysis for *miR-24* targets GATA2, PAK4 and RASA1 was performed (figure 3.24). Indeed, *miR-24* targets were deregulated by oxygen depletion but regulatory effects were diverse. While GATA2 expression was induced (1.32 ± 0.03 vs. 1 ± 0.05 ; $p = 0.001$), PAK4 and RASA1 expression was repressed on protein level (PAK4: 0.52 ± 0.10 vs. 1 ± 0.13 ; $p < 0.05$; RASA1: 0.69 ± 0.09 vs. 1 ± 0.05 ; $p < 0.05$).

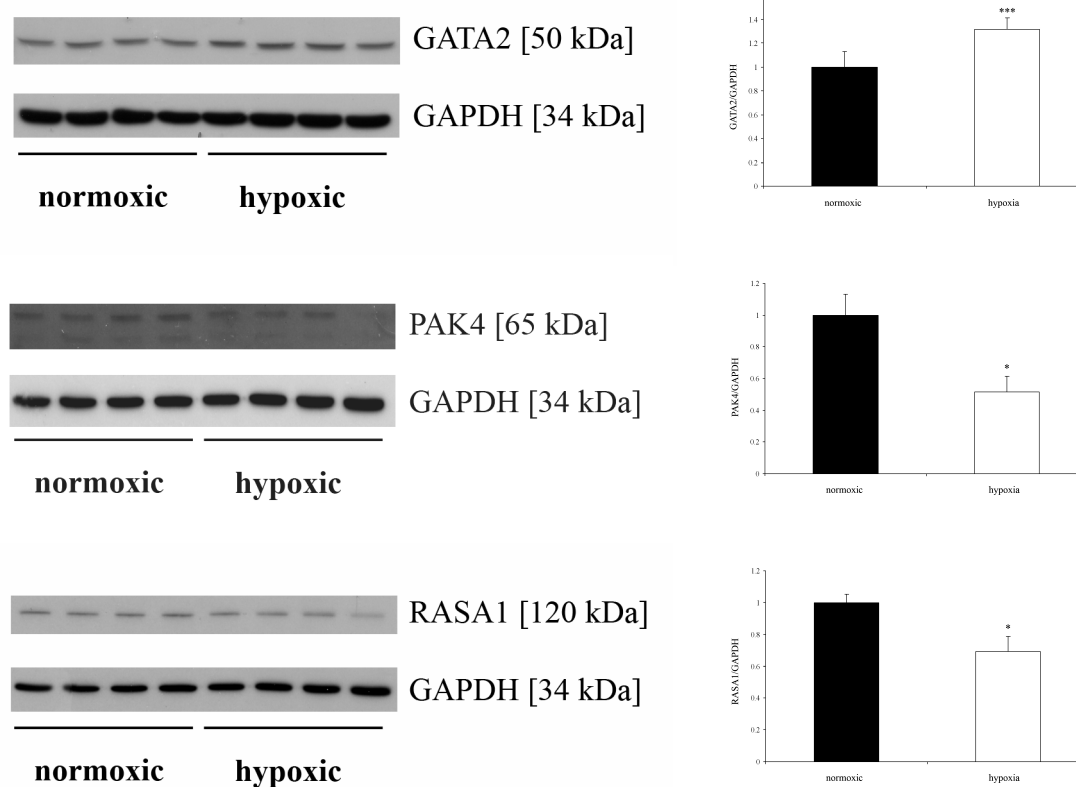


Figure 3.24: Hypoxia regulated expression of *miR-24* targets in ECs. HUVECs were exposed to normoxia or hypoxia (1%) for 24 h, harvested and lysed. 15-35 μ g total protein was loaded onto 12% (v/v) SDS-Polyacrylamide gels and SDS-PAGE was performed. Gels were blotted onto PVDF-membranes, blocked with 5% (w/v) skim milk powder, incubated with appropriate primary antibodies, secondary antibodies linked to HRP and developed using chemiluminescent reaction. GAPDH was used as a loading control. For each target, Western Blot results were normalized and validated statistically. N = 4 experiments each. * = $p < 0.05$; *** = $p < 0.001$

3.4. Affymetrix and ChIP data indicate GATA2-regulated genes related to angiogenic processes

The direct *miR-24* target GATA2 is a key mediator for endothelial biology. Different experiments showed the necessity for GATA2-dependent transcriptional regulation. GATA2 silencing resulted in apoptosis, cell cycle disturbance and decreased angiogenic response. Thus, transcriptional control in promoter regions of target genes should be responsible for these observations. Identification of possible GATA2 target genes is facilitated by whole genome transcriptome approaches using Affymetrix gene chip analysis.

By this method, global mRNA changes are monitored and can be compared in groups. Further *in vitro* assays such as chromatin immunoprecipitation (ChIP) may then validate GATA2-bound DNA regions.

3.4.1 Overexpression of murine Gata2 in ECs

In vitro loss- and gain-of function experiments are an appropriate tool to define the impact for a gene of interest. Therefore, GATA2 was specifically down- or upregulated in ECs. By now, transient silencing of GATA2 has been applied (figure 3.20). For GATA2 overexpression, N-terminal GFP-tagged murine GATA2 was cloned into adenoviral constructs (cooperation in biosafety level 2 with group Prof. Engelhardt, Rudolf-Virchow-Center, University of Würzburg). Then, ECs were infected with viral particles for 24 h. For control reasons, an YFP expressing control vector was also applied with the same multiplicity of infection (m.o.i.). Fluorescence microscopy revealed the subcellular localization of the GFP-GATA2 fusion protein solely in the nucleus (figure 3.25a). In contrast, control cells expressed YFP reporter protein ubiquitously.

Western Blot analysis further confirmed the overexpression of GFP-GATA2 in the nuclear fraction (figure 3.25b). The fusion protein could be detected at the estimated weight of 75 kDa. Taken together, successful GATA2 overexpression set the basis for comparison of transcriptome changes induced by repression or induction of transcription factor GATA2.

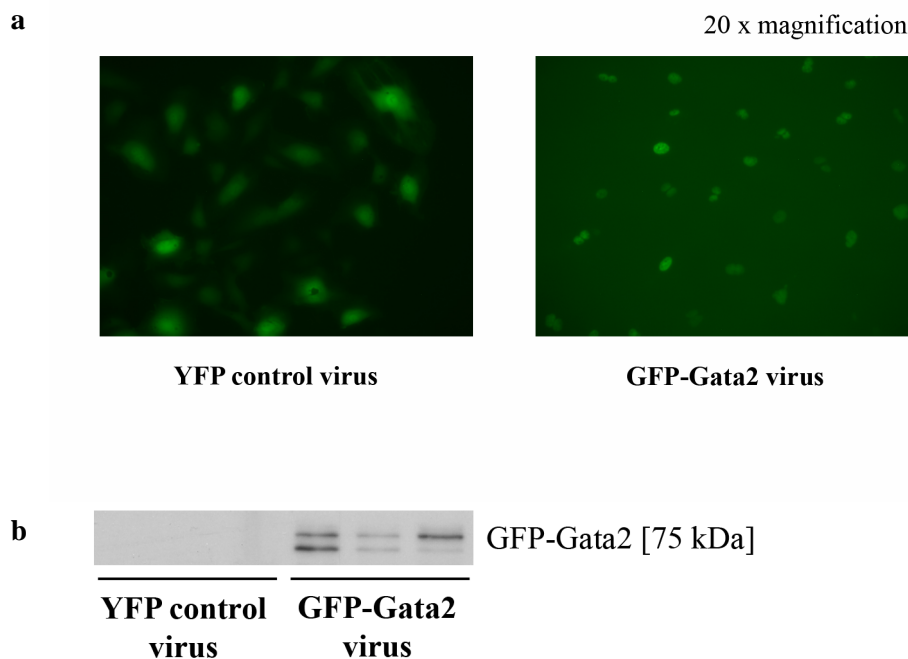


Figure 3.25: GATA2 overexpression in ECs. (a) ECs were infected with YFP control virus or GFP-GATA2 adenovirus with m.o.i. 40. 24 h post infection fluorescence microscopy was performed. (b) Western Blot analysis for overexpression of GFP-GATA2. ECs were infected with control or GFP-GATA2 virus for 24 h, harvested and lysed. An aliquot of nuclear fraction was loaded onto 12% (v/v) SDS-Polyacrylamide gels and SDS-PAGE was performed. Gels were blotted onto PVDF-membranes, these blocked with 5% (w/v) skim milk powder, incubated with appropriate primary antibody, secondary antibody linked to HRP and developed using chemiluminescent reaction. N = 3 experiments.

3.4.2 Transcriptome analysis upon GATA2 modulation by Affymetrix gene chip

Transcription factors are key proteins regulating the transcriptome. Naturally, these regulators are expressed dynamically. As a result, cells undergo permanent changes in their genome. Quite necessary, transcription factors are specific in their ability to recognize DNA binding sites. For GATA2, it is known that it binds to consensus [T/A(GATA)A/G] DNA sequences (Evans *et al.*, 1988). Nevertheless, target genes in ECs are elusive. Thus, manipulating GATA2 expression level in ECs by either knockdown or overexpression should reflect GATA2's impact on direct target gene regulation. Therefore, it is assumed that putative GATA2 target genes are reciprocally regulated when GATA2 is either repressed or induced.

In advance, ECs underwent silencing by liposomal siRNA transfection or adenoviral overexpression of GATA2. Then, total RNA was isolated and analyzed by Agilent capillary electrophoresis. RNA integrity number (RIN) can be investigated by this method. For subsequent Affymetrix gene chip analysis RINs should be comparable between groups and near to the maximum RIN of 10 which is indicated by distinct RNA peaks in the electropherogramme for 28 S and 18 S RNA. By way of example a gel electropherogramme is shown in figure 3.26 indicating a RIN of 9.9.

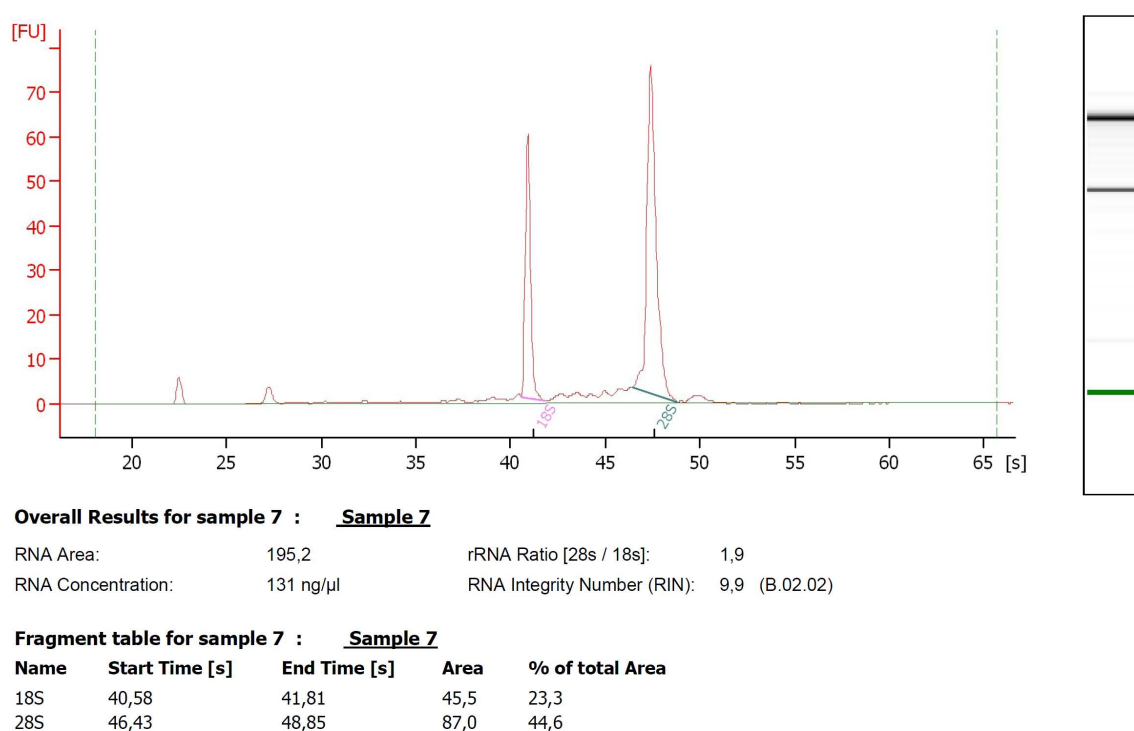


Figure 3.26: Total RNA analysis with Agilent capillary gelelectrophoresis. Isolated total RNA was placed onto an Agilent RNA nano chip, mixed with fluorescent dye and run with the use of Agilent bioanalyzer software. The resulting electropherogramme indicated the presence of 28 S and 18 S RNA in a ratio of 1.9 giving a RIN of 9.9.

For Affymetrix gene chip analysis following groups were compared: scr siRNA *versus*(vs) siRNA GATA2 and YFP control virus *vs* GFP-GATA2 virus. Isolated total RNAs had RINs between 9.5 and 10.0 (data not shown). Finally, 1 µg total RNA of each group was hybridized onto Affymetrix arrays in the department of Dr. Susanne Kneitz (IZKF Microarray Core Facility, University of Würzburg). Subsequently, data analysis was applied with the help of an R-programmed tool from Dr. Paolo Galuppo (Cardiology, University of Würzburg).

Firstly, data sets were screened for genes that were regulated $> +1.5$ -/ < -1.5 -fold. Then, data were further validated with the assumption, that GATA2 could regulate target mRNAs reciprocally if knocked down or induced by overexpression. With these restrictions, the putative GATA2 target genes *BAMBI*, *ESM1* and *NTN4* were identified (table 3.2).

Table 3.2: Overview on reciprocally regulated genes upon GATA2 modulation by siRNA or viral overexpression.

Gene assignment	Fold Change (siRNA <i>GATA2</i> vs scr siRNA)	Fold Change (viral <i>GATA2</i> overexpression vs control virus)
NM_012342 // BAMBI // BMP and activin membrane- bound inhibitor homolog	-1.52	1.60
NM_007036 // ESM1 // endothelial cell-specific molecule 1	1.54	-1.79
NM_021229 // NTN4 // netrin 4	1.51	-1.51

Noteworthy, *ESM1* and *NTN4* have been described to be essential for angiogenesis (Shin *et al.*, 2008; Lejmi *et al.*, 2008). Thus, GATA2 can be considered as a key mediator for angiogenic signalling. Taken together, global transcriptome analysis in GATA2 modulated ECs revealed certain reciprocally regulated mRNAs. This might imply that their host genes are putatively regulated by GATA2.

3.4.3 ChIP analysis for GATA2

Chromatin-immunoprecipitation (ChIP) is a method to validate transcription factor binding sites in DNA. Initially, transcription factor and DNA are crosslinked. DNA:transcription factor complex is then sheared to fragments of about 200-1000 bp in length. Afterwards, immunoprecipitation is performed. Then transcription factor-bound DNA can be isolated. Mostly, precipitated DNA belongs to promoter regions of a gene which can be analyzed by PCR for example. ChIP analysis for GATA2 should further support the initial clue for direct regulation of *BAMBI*, *ESM1* and *NTN4*.

ChIP analysis for GATA2 was performed in ECs resulting in precipitated GATA2-bound chromatin. Next, potential GATA2 binding sites in promoter regions of *BAMBI*, *ESM1* and *NTN4* were acquired *in silico*. Therefore, 2000 nucleotides upstream of exon 1 GATA2 binding analysis was performed with Alggen Promo (http://alggen.lsi.upc.es/cgi-bin/promo_v3/promo/promoinit.cgi?dirDB=TF_8.3, Messeguer *et al.*, 2002; Farre *et al.*, 2003). Potential GATA2 binding sites for *BAMBI*, *ESM1* and *NTN4* are listed in table 3.3. Appropriate primers were designed spanning these sites. GATA2 immunoprecipitated chromatin then underwent PCR analysis with these primers (figure 3.27). Resulting PCR products were enriched in samples generated with the GATA2 specific IP compared to samples incubated with mouse IgG. This indicates that GATA2 has regulative function towards endothelial *BAMBI*, *ESM1* and *NTN4*.

Table 3.3: Predicted GATA2 binding sites in promoter region of *BAMBI*, *ESM1* and *NTN4*. Transcription factor binding analysis was performed with Allgen Promo (<http://alggen.lsi.upc.es>).

Gene symbol	Predicted GATA2 binding site at upstream bp position
<i>BAMBI</i>	-1220, -1370
<i>ESM1</i>	-540, -880, -1430, -1530, -1790
<i>NTN4</i>	-110

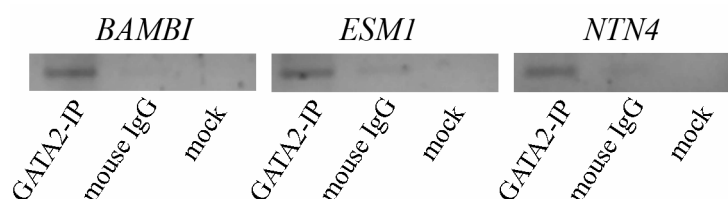


Figure 3.27: Chromatin immunoprecipitation (ChIP) for GATA2 and analyzing PCR products. ECs were subjected to ChIP in three groups: GATA2 immunoprecipitation (IP) with specific GATA2 antibody, mouse IgG control antibody and mock control (no antibody). Isolated chromatin was analyzed with primers detecting GATA2 binding sites in promoter regions of *BAMBI*, *ESM1* and *NTN4*. Amplified PCR products were separated on 1.8 % (w/v) agarose gel.

3.4.4 Pro-angiogenic HMOX1 and SIRT1 are regulated on protein level by the *miR-24* target GATA2

Our previous data show that the *miR-24* downstream effector GATA2 has an important role in regulating the endothelial transcriptome. Specifically, angiogenesis-related genes are either induced or repressed by GATA2 binding to respective promoter regions. Noteworthy, ECs overexpressing *miR-24* show reduced GATA2 and HMOX1 levels (figures 3.13/18). HMOX1 is, in addition to its important function for heme metabolism, a natural source of carbon monoxide thereby mediating pro-angiogenic properties (Dulak *et al.*, 2008). To address the question if HMOX1 expression is effected by GATA2 modulation, Western Blots were performed upon GATA2 overexpression or silencing (figure 3.28). GATA2 knockdown resulted in decreased HMOX1 expression (0.41 ± 0.05 vs. 1 ± 0.05 ; $p < 0.001$) whereas inducing GATA2 forced elevated HMOX1 levels (1.63 ± 0.08 vs. 1 ± 0.11 ; $p < 0.001$). The reciprocal regulation indicates that GATA2 seems to be a transcriptional enhancer of HMOX1.

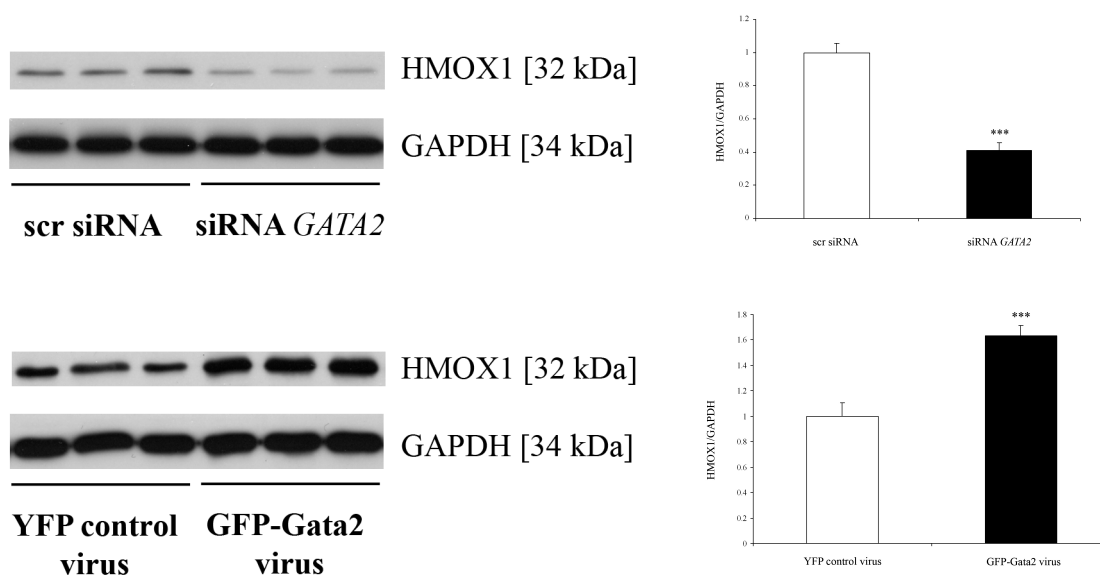


Figure 3.28: Representative Western Blots for HMOX1 in GATA2-modulated ECs. Control siRNA and siRNA *GATA2* (150 nM each) were transfected in ECs for 48 h. In addition, ECs were transduced with adenoviral control virus and GFP-GATA2 virus (m.o.i. = 40). Then cells were harvested and lysed. Total protein was loaded onto 12% (v/v) SDS-Polyacrylamide gels and SDS-PAGE was performed. Gels were blotted onto PVDF-membranes, these were blocked with 5% (w/v) skim milk powder, incubated with appropriate primary antibody, secondary antibody linked to HRP and developed using chemiluminescent reaction. HMOX1 expression was normalized to GAPDH and validated statistically. N = 4 experiments per group. *** = $p < 0.001$

This finding also implicates that GATA2 is the mediator for *miR-24* dependent HMOX1 regulation. Antagonizing *miR-24* in *GATA2* deficient ECs should therefore not rescue HMOX1 expression. To test this hypothesis ECs underwent *miR-24* and *GATA2* modulation in parallel. In figure 3.29 HMOX1 and GATA2 expression are plotted for different treatment groups: HMOX1 expression is elevated in *miR-24* deficient (anti-24) compared to *GATA2* silenced ECs (1 ± 0.04 vs. 0.68 ± 0.05 ; $p < 0.01$). Nevertheless, parallel antagonistic modulation of *miR-24* and transient silencing of *GATA2* could not rescue HMOX1 expression compared to control levels (0.71 ± 0.05 vs. 1 ± 0.04 ; $p < 0.01$). Taken together, HMOX1 dysregulation induced by *miR-24* is dependent on GATA2 function.

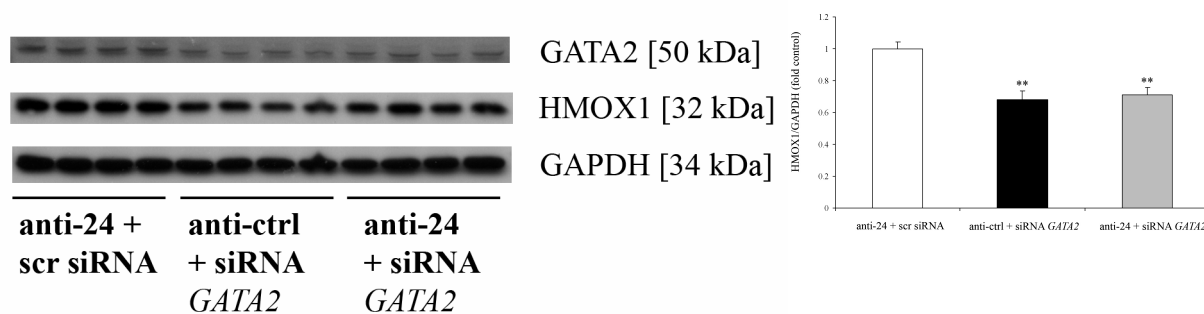


Figure 3.29: HMOX1 and GATA2 protein level in miRNA and siRNA modulated ECs analyzed by Western Blot. miRNAs (100 nM each) and siRNAs (150 nM each) were transfected in ECs for 72 h. Then cells were harvested and lysed. Total protein was loaded onto 12% (v/v) SDS-Polyacrylamide gels and SDS-PAGE was performed. Gels were blotted onto PVDF-membranes, these were blocked with 5% (w/v) skim milk powder, incubated with appropriate primary antibody, secondary antibody linked to HRP and developed using chemiluminescent reaction. HMOX1 expression was normalized to GAPDH and validated statistically. N = 4 experiments per group. ** = $p < 0.01$

Next to HMOX1, the histone deacetylase sirtuin1 (SIRT1) has been recently described as a potent regulator of angiogenesis (Potente *et al.*, 2007). Indeed, bioinformatic analysis reveals GATA2 binding sites in *SIRT1* promoter region. To validate GATA2-dependent regulation of SIRT1, GATA2-modulated ECs were analyzed for SIRT1 expression (figure 3.30). In line, SIRT1 expression was found to be downregulated in *GATA2*-deficient ECs (0.36 ± 0.08 vs. 1 ± 0.09 ; $p < 0.01$) whereas expression was increased in *GATA2*-overexpressing ECs (1.52 ± 0.19 vs. 1 ± 0.26 ; $p = \text{n.s.}$)

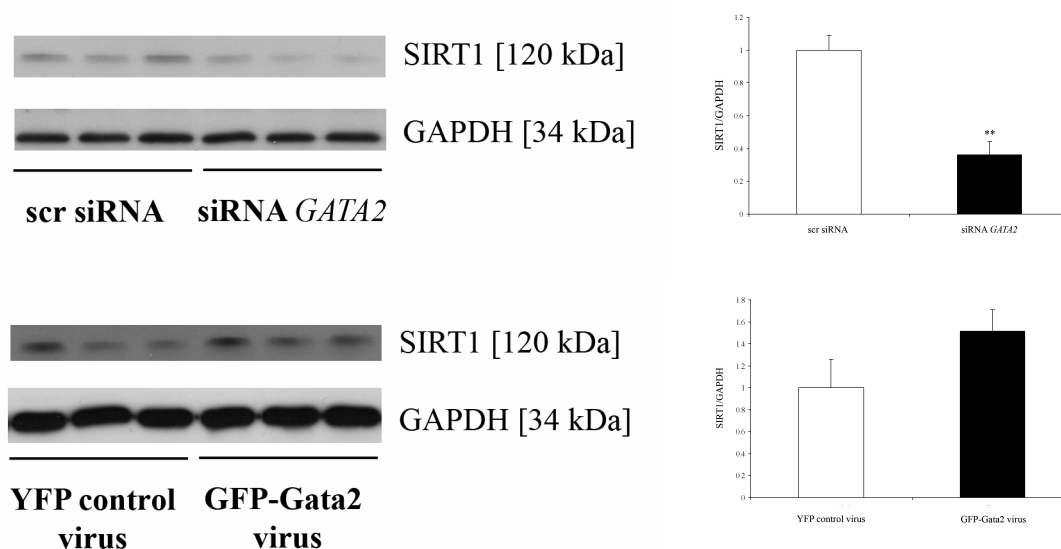


Figure 3.30: Representative Western Blots for SIRT1 in GATA2-modulated ECs. Control siRNA and siRNA *GATA2* (150 nM each) were transfected in ECs for 48 h. In addition, ECs were transduced with adenoviral control virus and GFP-GATA2 virus (m.o.i. = 40). Then cells were harvested and lysed. Total protein was loaded onto 12% (v/v) SDS-Polyacrylamide gels and SDS-PAGE was performed. Gels were blotted onto PVDF-membranes, these were blocked with 5% (w/v) skim milk powder, incubated with appropriate primary antibody, secondary antibody linked to HRP and developed using chemiluminescent reaction. SIRT1 expression was normalized to GAPDH and validated statistically. N = 4 experiments per group. ** = $p < 0.01$

In conclusion, pro-angiogenic factors HMOX1 and SIRT1 are regulated on transcriptional level by endothelial transcription factor GATA2. Downregulation of GATA2 inhibits expression of HMOX1 and SIRT1 thus contributing to negative effects in angiogenic signalling.

3.5 Bad phosphorylation status is regulated by the *miR-24* target PAK4

Identifying downstream effectors for *miR-24* is essential to highlight underlying signal transduction. Besides *miR-24* dependent regulation of HMOX1 anti-apoptotic phospho-Bad is dysregulated by increased *miR-24* levels (figure 3.15). Of particular interest, the validated *miR-24* target PAK4 has been reported to phosphorylate Bad at serine 112, which then functions anti-apoptotic (Gnesutta *et al.*, 2001). This finding might also be true in ECs where PAK4 kinase was found to trigger apoptosis protection (figure 3.21).

To test for Bad phosphorylation status dependent on PAK4 expression ECs were modulated with PAK4-specific siRNA. Afterwards, Western Blot for unphosphorylated Bad and ELISA measurement for phospho-Bad (Ser112) was performed. As it can be seen in figure 3.31 unphosphorylated Bad is not affected in PAK4-silenced ECs (1.09 ± 0.11 vs. 1 ± 0.22 ; $p = \text{n.s.}$).

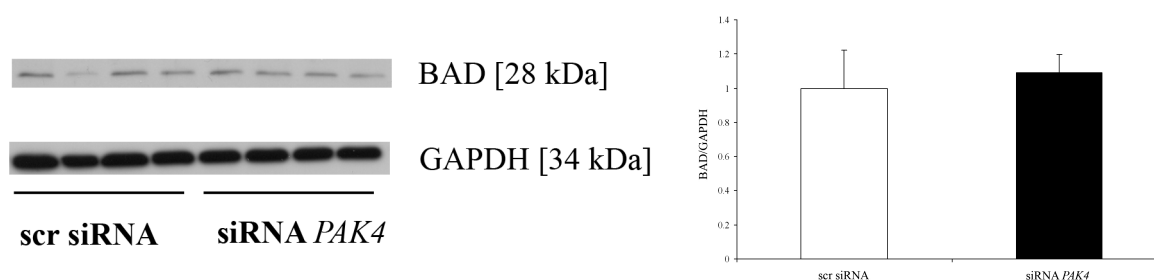


Figure 3.31: Bad protein level in siRNA modulated ECs analyzed by Western Blot. siRNAs (150 nM each) were transfected in ECs for 48 h. Then cells were harvested and lysed. Total protein was loaded onto 12% (v/v) SDS-Polyacrylamide gels and SDS-PAGE was performed. Gels were blotted onto PVDF-membranes, these were blocked with 5% (w/v) skim milk powder, incubated with appropriate primary antibody, secondary antibody linked to HRP and developed using chemiluminescent reaction. Bad expression was normalized to GAPDH and validated statistically. N = 4 experiments per group.

However, Bad phosphorylation decreases in *PAK4* knockdown ECs measured by phospho-Bad specific ELISA (0.45 ± 0.03 vs. 1 ± 0.21 ; $p < 0.05$; figure 3.32). Cumulatively, these experiments proof that PAK4 function is necessary to phosphorylate endothelial Bad protein. Mechanistically, *miR-24*-dependent PAK4 repression is responsible for reduced phospho-Bad levels observed in *miR-24* overexpressing ECs.

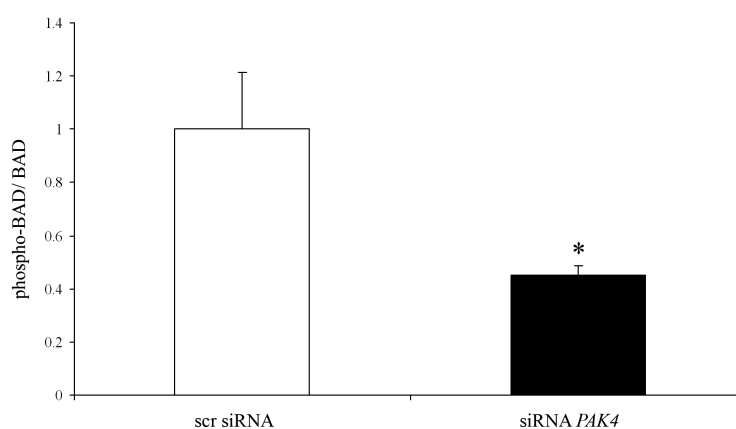


Figure 3.32: Summary of phospho-BAD ELISA data (p112) normalized to total BAD protein values. Scrambled and *PAK4* specific siRNA were transfected in ECs (150 nM each) for 48 h. Then cells were lysed and analyzed by phospho-BAD specific ELISA. N = 4 experiments per group. * = $p < 0.05$

3.6 *In vivo* treatment of myocardial infarction by a specific *miR-24* antagonist (antagomir)

In case of MI, pathological cardiac injury results in altered gene expression. Derailed signalling pathways accompany cardiac remodelling processes. The exploration of miRNA biology offers a new regulative tool to counteract genomic changes. Whole gene networks are regulated by conductor miRNAs dynamically expressed upon diverse stimuli. More recently, novel therapeutic strategies were developed to decrease miRNA expression *in vivo* by chemically-modified miRNA-specific antagonists (antagomirs). In this work, the finding that MI induced *miR-24* expression (figure 3.1) set the basis for *in vivo* treatment with antagomir-24. Furthermore, describing and explaining a pro-apoptotic characteristic for *miR-24* in ECs pointed out to investigate angiogenesis *in vivo*. To study the effects of *miR-24* on vascularization *in vivo*, an experimental design was built spanning 14 days (figure 3.32). Initially, MI or matrigel plug implantation was applied in wildtype mice. Immediately thereafter antagomir-24 treatment was performed and was repeated two days later. For control reasons, an antagomir bearing a scrambled sequence was also injected. Matrigels were isolated one week after implantation whereas on day 14 heart function tests were performed with subsequent tissue analysis.

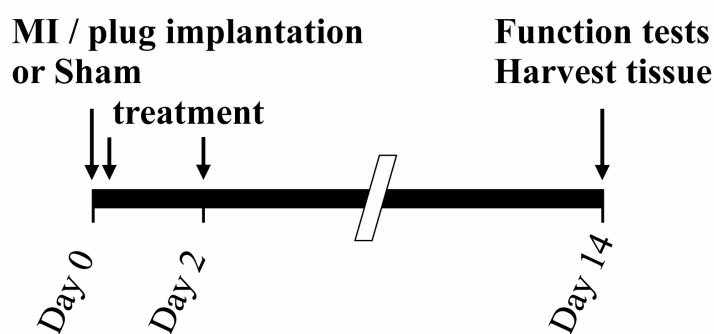


Figure 3.33: Experimental design and treatment scheme of the antagomir-24 study. On day 0, MI or Matrigel plug implantation along with sham controls was performed in mice. Antagomir injection immediately followed and was repeated on day 2. Matrigels were isolated and analyzed one week after implantation. For MI-studies, heart function tests and tissue analysis were applied on day 14.

Noteworthy, two experiments were performed in advance of this study. First, it was proven that antagomirs are delivered effectively to ECs *in vitro*. Therefore ECs were incubated with Cy3-labeled antagomir. Cellular uptake was highly efficient (figure 3.34).

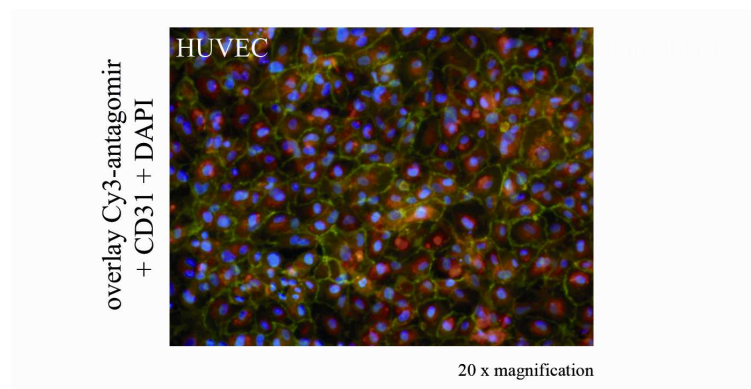


Figure 3.34: Cellular uptake of Cy3-Antagomir in HUVECs. Confluent cells were incubated with Cy3-labelled Antagomir for 1-2 h. Afterwards cells were fixed and stained for endothelial CD31 (green) and nuclei (DAPI, blue). Fluorescent pictures were taken with 20x magnification.

Next, titration experiments for antagomir concentration were applied since the aim was to target cardiovascular endothelial cells mainly. Low (5 mg/kg body weight) and high dose (80 mg/kg body weight) Cy3-antagomir were injected retroorbitally in mice. Immunohistochemical analysis of heart tissue revealed that low-dose injection resulted in cellular uptake in cardiac vessels and the surrounding tissue whereas injection of a high dose led to a strong homogeneous stain of all cardiac cells including cardiomyocytes (figure 3.35).

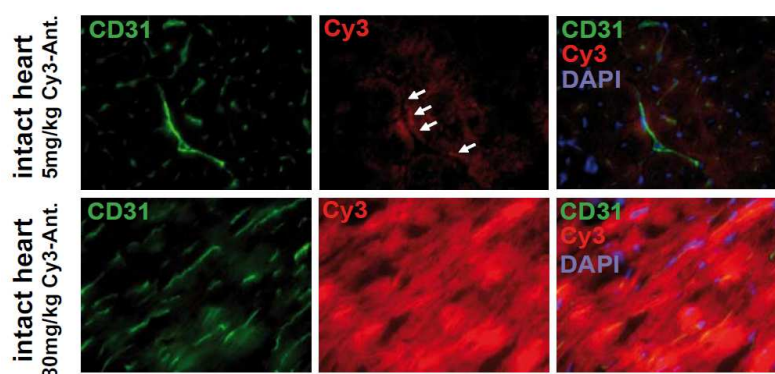


Figure 3.35: *In vivo* uptake of Cy3-antagomir in heart tissue. Two doses of Cy3-antagomir were injected retroorbitally in mice. Hearts were isolated, sliced and stained for CD31 (green) and nuclei (DAPI, blue).

3.6.1 Antagomir-24 efficiently lowers cardiac *miR-24* expression

The efficient delivery of antagomirs into the heart has been shown before thus being a prerequisite for therapeutic therapy in cardiac stress conditions (Thum *et al.*, 2008). Nevertheless, in this study, antagomir-24 treatment was investigated quantitatively 14 d after intervention to check for knockdown of cardiac *miR-24*. Therefore, heart tips were subjected to RNA analysis with subsequent miRNA RT-PCR. As shown in figure 3.36, antagomir-24 lowers *miR-24* expression in comparison to placebo control (10 ± 8.27 vs. 50000 ± 9290 ; $p < 0.001$).

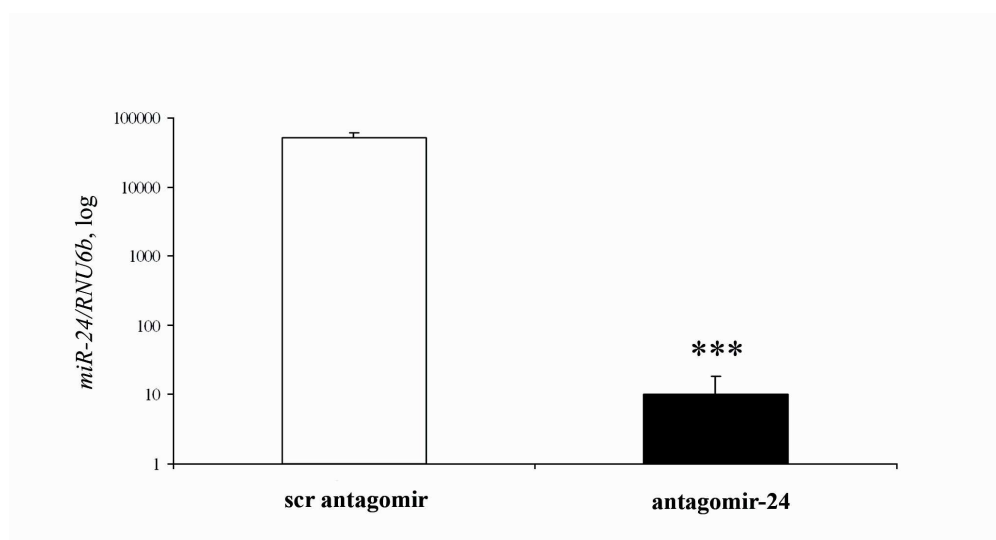


Figure 3.36: Ratio of *miR24/RNU6b* in scrambled antagomir or antagomir-24 treated murine hearts. Antagomir treatment followed twice after intervention. 14 d after coronary ligation, heart tips underwent total RNA isolation and miRNA detection. N = 7 animals per group. *** = $p < 0.001$

3.6.2 Heart function tests after MI

We first characterized basic cardiac parameters in the different study groups. For control reasons, an antagomir against a scrambled miRNA sequence (placebo/ctrl) was also injected. Analysis of cardiac function by echocardiography 14 days after initial intervention proved that MI led to an impairment of cardiac function measured by decreased fractional shortening in scrambled antagomir treated animals compared to sham ($12.63 \% \pm 0.75 \%$ vs. $36.12 \% \pm 2.79 \%$; $p < 0.001$, figure 3.37a). In addition, an increase in lung wet weight ($150.32 \text{ mg} \pm 4.61 \text{ mg}$ vs. $98.5 \text{ mg} \pm 5.17 \text{ mg}$; $p < 0.001$, figure 3.37b) and systolic ($0.48 \text{ cm} \pm 0.02 \text{ cm}$ vs. $0.22 \text{ cm} \pm 0.017 \text{ cm}$; $p < 0.001$, figure 3.37c) as well as diastolic left ventricular diameter ($0.55 \text{ cm} \pm 0.02 \text{ cm}$ vs. $0.34 \text{ cm} \pm 0.016 \text{ cm}$; $p < 0.001$, figure 3.37d) was observed.

These observations were consistent to normal cardiac disease progression after MI. Remarkably, injecting antagomir-24 as an immediate interventional treatment after MI at day 0 and 2, partly rescued cardiac function when comparing parameters to scrambled antagomir treated group. First of all, fractional shortening was improved by antagomir-24 treatment ($20.88 \% \pm 4.03 \%$ vs. $12.63 \% \pm 0.75 \%$; $p < 0.01$, figure 3.37a). Additionally, pulmonary congestion decreased slightly ($132.35 \text{ mg} \pm 7.16 \text{ mg}$ vs. $150.32 \text{ mg} \pm 4.61 \text{ mg}$; $p = \text{n.s.}$, figure 3.37b). The increase in left ventricular systolic ($0.36 \text{ cm} \pm 0.04 \text{ cm}$ vs. $0.48 \text{ cm} \pm 0.02 \text{ cm}$; $p < 0.05$, figure 3.37c) and diastolic dilatation ($0.45 \text{ cm} \pm 0.03 \text{ cm}$ vs. $0.55 \text{ cm} \pm 0.02$; $p < 0.05$, figure 3.37d) was also attenuated.

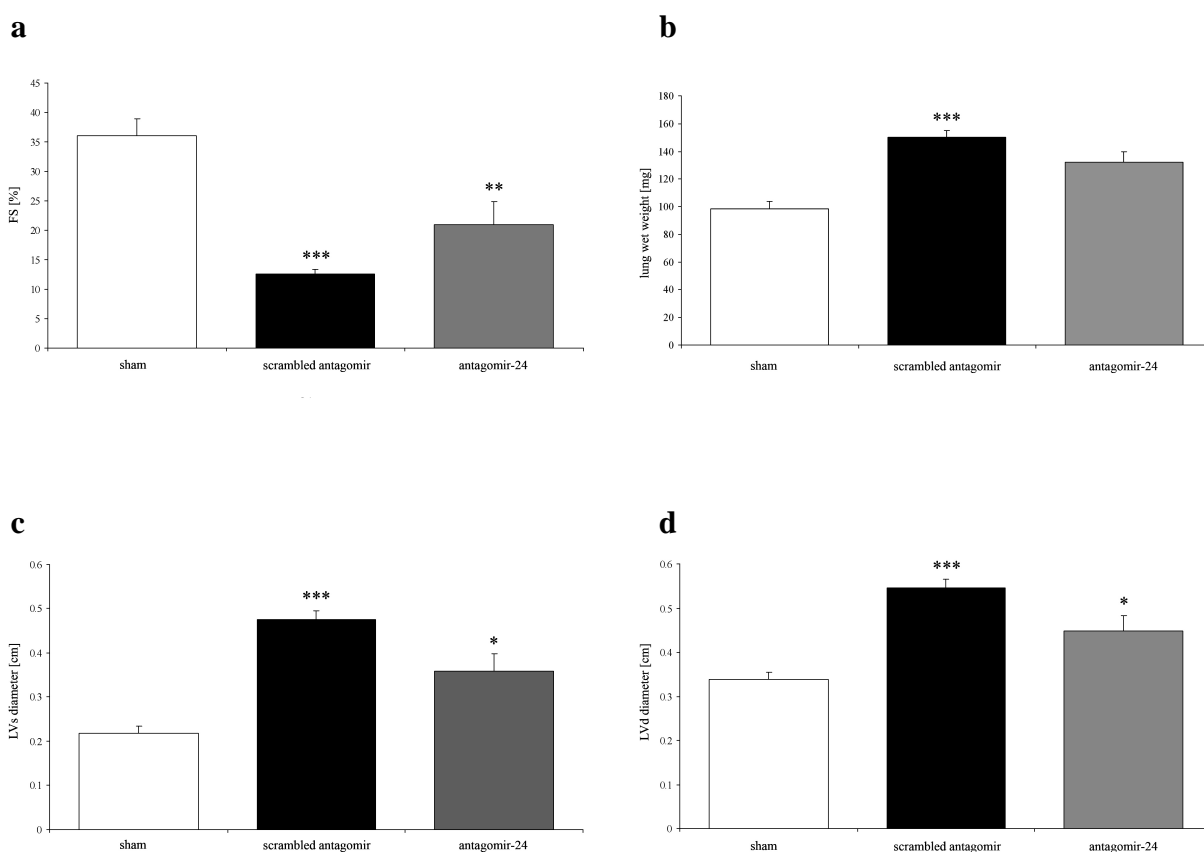


Figure 3.37: Basic heart parameters derived from mice subjected to antagomir-24 study 14 days after intervention. Three groups are indicated: sham, scrambled antagomir and antagomir-24. (a) Fractional shortening (FS) is lowered after MI. Antagomir-24 treatment increases FS compared to placebo. (b) Lung wet weight is increased after MI. Repression of *miR-24* indicates prevention of pulmonary congestion. (c+d) Systolic and diastolic left ventricular diameters (LVs/LVd) are elevated due to MI. Eliminating *miR-24* lowers the extension of LVs and LVd diameter. N = 4-7 animals per group. * = $p < 0.05$; ** = $p < 0.01$; *** = $p < 0.001$

In conclusion, therapeutic antagomir-24 treatment after MI indicates a global improvement in cardiac function. Necessarily, underlying cardiac molecular mechanisms and general structural alterations have to be determined.

3.6.3 Cardiac angiogenesis is improved upon antagomir-24 treatment

Myocardial infarction leads to a hypoxic insult and upregulation of miR-24 in EC. In this work, *in vitro* data suggest a role for *miR-24*-dependent negative regulation of angiogenic signalling in endothelial cells. Antagonizing *miR-24* expression might thus improve angiogenic response upon myocardial infarction *in vivo*. To test this hypothesis, mice underwent MI and were treated with antagomir-24. Finally, heart tissue from control scrambled antagomir or antagomir-24 treated animals was collected, sliced to appropriate sections and analyzed for CD31 expression, an endothelial cell marker indicating capillaries or vessels. In addition, sections were also stained for cardiomyocyte Troponin I (TnI) and nuclei (figure 3.38a). Remarkably, antagomir-24-receiving animals are characterized by an increased capillary density indicated by elevated CD31 staining (arbitrary units, a.u.) in border (12.13 ± 0.38 vs. 6.96 ± 0.25 ; $p < 0.001$, figure 3.38b) and infarct zone (10.50 ± 0.61 vs. 4.96 ± 0.39 ; $p < 0.001$, figure 3.38b) in comparison to scrambled antagomir treated animals. However, capillar density remains unchanged in remote myocardium (8.63 ± 0.14 vs. 8.17 ± 0.40 ; $p = \text{n.s.}$, figure 3.38b). Taken together, these data proof a pro-angiogenic effect of therapeutic antagomir-24 treatment in diseased hearts.

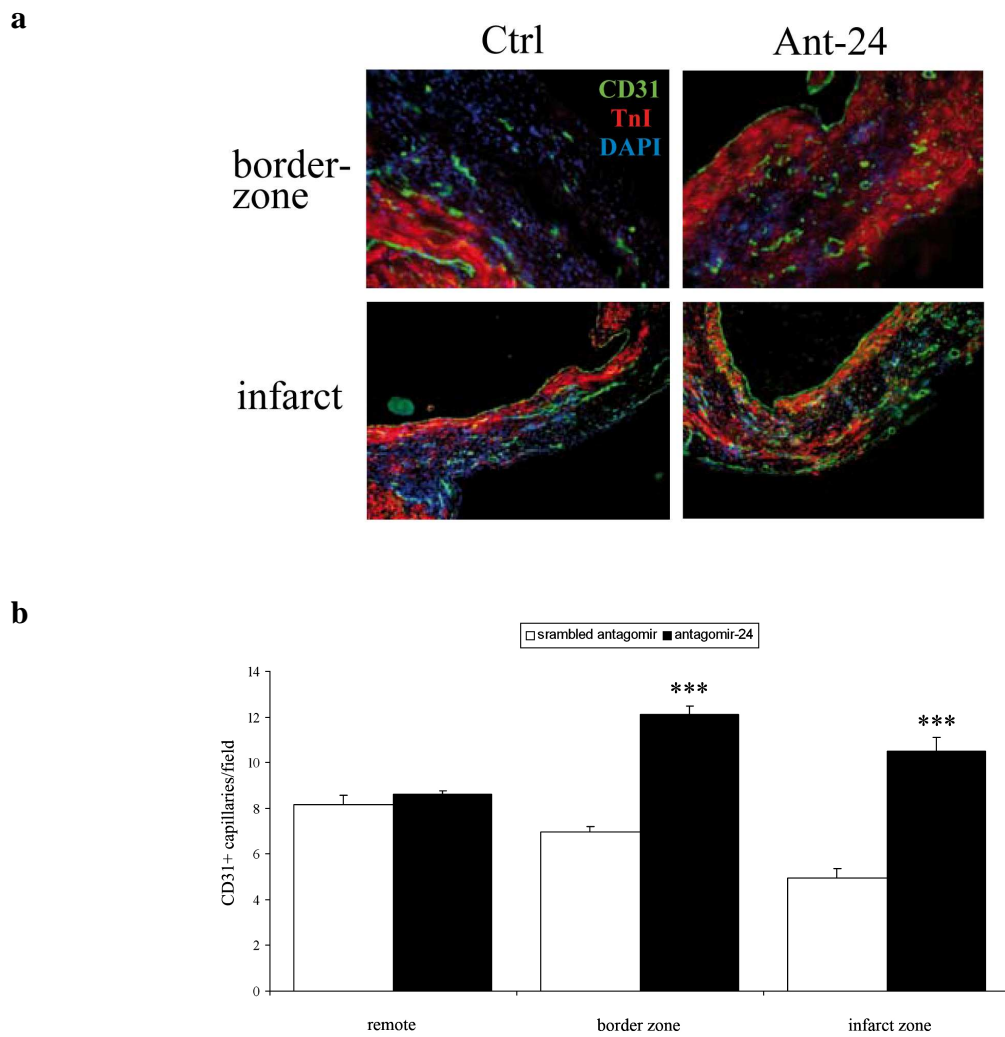


Figure 3.38: Immunohistochemical analysis of murine heart tissue derived from antagomir-24 study. (a) Hearts from scrambled antagomir (ctrl) and antagomir-24 (Ant-24) treated mice were collected, sliced to 10 μ m sections and stained for CD31 (green), Troponin I (TnI, red) and nuclei (DAPI, blue). (B) Statistical summary of CD31-positive capillaries present in remote, infarct and border zone. N = 4 animals per group. *** = $p < 0.001$

3.6.4 Implantation of matrigel plugs to characterize global neovascularization *in vivo*

Basically, antagomir technique delivers cholesterol-bound antisense miRNAs to every organ except the brain. As shown before, antagonizing *miR-24* in a murine disease model of myocardial infarction improves cardiac angiogenesis. The effect of antagomir-24 therapy on global neovascularization has not been monitored yet. To address this question a matrigel-based assay to detect angiogenesis *in vivo* was applied (Akhtar *et al.*, 2002).

Matrigel plus were injected subcutaneously in mice in advance to antagomir-24 treatment. After one week, matrigels were collected and analyzed. Whole matrigels were divided into two pieces. One half underwent hemoglobin detection, the other part was analyzed by immunohistochemistry. Hemoglobin-specific ELISA validated that plugs derived from antagomir-24 treated mice showed an increased hemoglobin content compared to scrambled antagomir treated group (265.07 $\mu\text{g}/\text{mg}$ \pm 51.34 $\mu\text{g}/\text{mg}$ vs. 88.65 $\mu\text{g}/\text{mg}$ \pm 34.89 $\mu\text{g}/\text{mg}$; $p < 0.05$; figure 3.39).

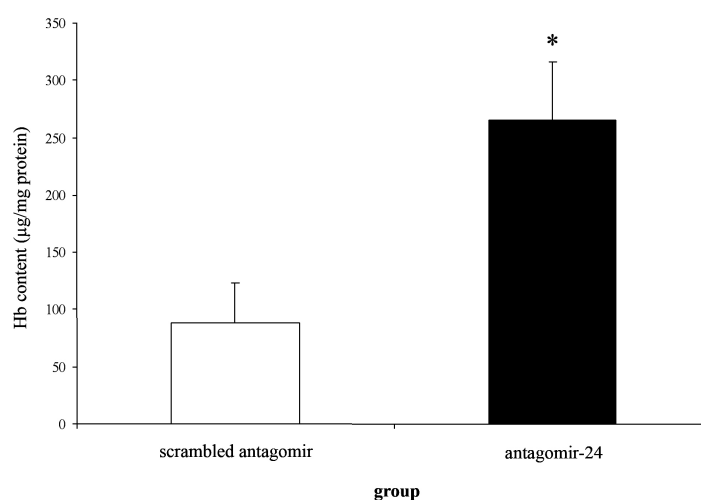


Figure 3.39: Hemoglobin (Hb) ELISA to quantify neovascularization in a matrigel plug assay. Matrigels were injected subcutaneously in mice. Control and antagomir-24 treatment followed and was repeated two days later. After one week matrigels were isolated and underwent hemoglobin-specific ELISA. Values were normalized to total protein content and validated statistically. N = 4 animals per group.

Immunohistochemical analysis of matrigel plugs further confirmed the pro-angiogenic property of antagomir-24 treatment. Sliced matrigel plugs were stained for endothelial CD31 surface marker and nuclei (figure 3.40). Qualitatively, antagomir-24 treatment increased capillar density in implanted matrigels.

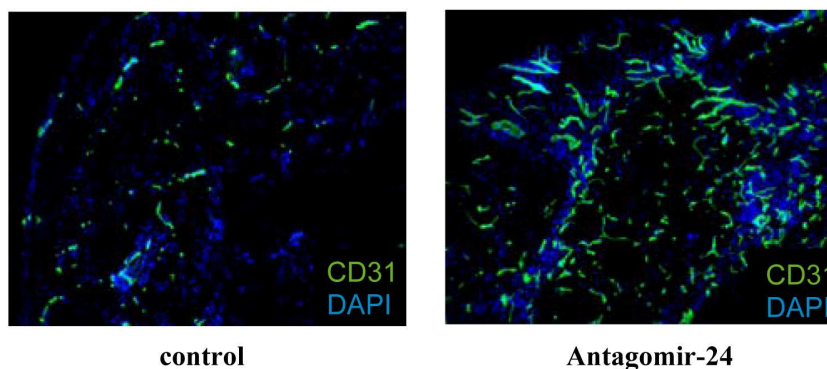


Figure 3.40: Representative cyroscetions of implanted matrigel plugs to characterize angiogenesis. 14 d after matrigel implantation and treatment with control (scrambled antagomir) or antagomir-24 plugs were isolated and sliced. Endothelial staining (CD31, green) and nuclei stain (DAPI, blue) followed.

In conclusion, antagomir-24 treatment promotes neovascularization *in vivo* and thus may be beneficial in treatment of ischemic cardiovascular disease.

4. Discussion

The work presented here suggests a *miR-24* based mechanism contributing to the regulation of capillary density in the infarcted heart (figure 4.1). Hypoxia or myocardial infarction increases endothelial *miR-24* expression triggering endothelial cell apoptosis and vascular defects. Mechanistically, GATA2, H2A.X, RASA1 and PAK4 were validated as direct *miR-24* targets in endothelium. Further downstream signalling pathways were identified for GATA2 and PAK4. GATA2-dependent transcriptional regulation was found for diverse target genes including HMOX1 and SIRT1. *MiR-24*-induced repression of PAK4 directly decreases the phosphorylation status of Bad thus contributing to apoptosis. In a mouse model of MI, blocking of *miR-24* by a specific antagonist (antagomir) enhances capillary density in the heart and preserves cardiac function. In conclusion, endothelial *miR-24* serves as a pro-apoptotic miRNA acting as a critical regulator of endothelial cell apoptosis and capillary density of the infarcted heart.

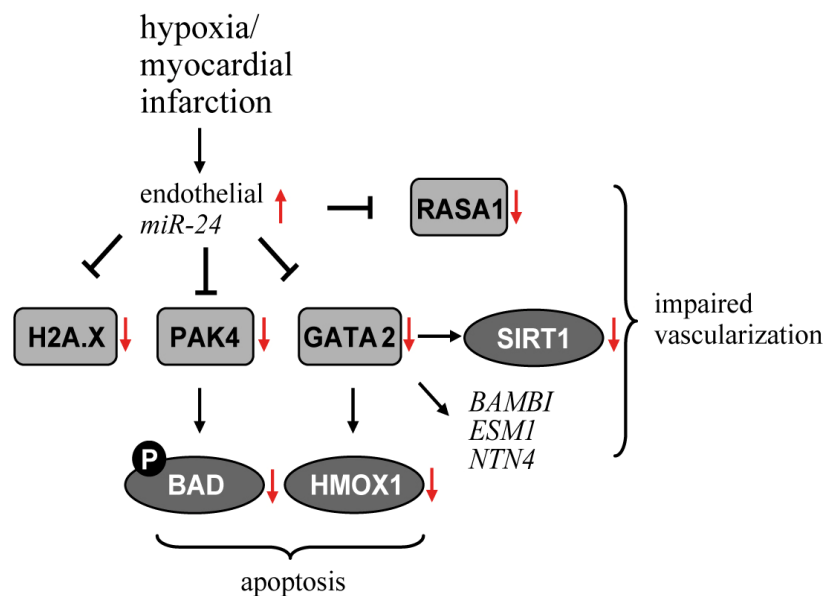


Figure 4.1: Scheme for the biological function of endothelial *miR-24*. Hypoxia or myocardial infarction induces expression of endothelial *miR-24*. As a consequence, *miR-24* targets GATA2, H2A.X, PAK4 and RASA1 are repressed. PAK4 kinase activity is impaired leading to decreased level of anti-apoptotic phospho-Bad. Repression of GATA2 downregulates anti-apoptotic HMOX1 and deregulates the transcription of further angiogenic genes. Cumulatively, induction of endothelial *miR-24* supports apoptosis and impairs capillary density.

4.1 *MiR-24* deregulation in cardiac disease

The endogenous expression of *miR-24* increases in murine hearts after myocardial infarction (figure 3.1). MicroRNAs regulated after myocardial infarction have also been investigated earlier (van Rooij *et al.*, 2008). However, in this previous publication, *miR-24* has not yet been characterized. There are two genomic loci for *miR-24* (mature miRs are identical, but *miR-24-1** and *miR-24-2** differ in sequence), which cluster together with *miR-23/27a/b*, and thus form a very complex miRNA family. Specifically, van Rooij *et al.* report a downregulation of *miR-24-2** in the border zone of infarcted myocardium. Thus, two important facts have to be taken into account when the two findings are compared: First, only the mature *miR-24* expression was investigated in the present work. Here, no data regarding the expression level of *miR-24-1** or *miR-24-2** were generated. No experiments to screen for changes in pre-miRNA expression were performed. However, further evidence for an upregulation in infarcted murine heart was gained by a collaboration with the RNA laboratory of Thomas Tuschl, Rockefeller University, New York. The Tuschl group performed miRNA *in situ* hybridization of cryosectioned hearts and found a strong *miR-24* expression in infarcted *versus* sham control hearts (unpublished). Enhanced *miR-24* signals indicate that a consistent upregulation is present in the infarct area 14 days after MI. A time course for *miR-24* expression during progression of cardiac disease has not been performed so far. However, we suggest that *miR-24* induction starts early after MI based on the heart cell fractionation experiments 2d after MI (figure 3.6).

The cellular source for *miR-24* upregulation signal remains unclear but there are some first findings in the literature; *miR-24* expression was attributed to microvascular cells derived from CD31⁺-sorting of different organs in mouse (Larsson *et al.*, 2009). Therefore, it can be assumed that cardiac endothelial cells contribute by large to enhanced *miR-24* signal upon MI. This hypothesis is also supported by different observations made in the current work. Fractionation of infarcted and control heart tissue into cardiomyocytes and endothelial cells revealed a selective *miR-24* upregulation in endothelial cells 2 d after infarction whereas the expression level in cardiomyocytes remained basically unchanged (figure 3.6).

In addition, hypoxic atmosphere serving as a model for reduced oxygen supply post MI induces *miR-24* expression specifically in endothelial cells *in vitro* (figure 3.3). However, no direct evidence was found for potential HIF1 α dependent transcriptional regulation as it has been suggested earlier in cancer cell lines (Kulshreshta *et al.*, 2007) or recently in lung and pulmonary arteries (Chan *et al.*, 2010). One could speculate that endothelial *miR-24* is regulated by different hypoxia-related transcription factors or other stress sensors because contribution of reactive oxygen species (ROS) towards *miR-24* expression was recently reported (Takagi *et al.*, 2010). Hepatocyte cells exposed to ROS inducing H₂O₂ were characterized by elevated *miR-24* expression. This in turn modulated the expression of metabolizing enzymes like HNF4 α and caused a defect in cell cycle progression indicating the need of tightly balanced *miR-24* expression. The exact mechanism of *miR-24* regulation in endothelial cells by hypoxia remains to be determined.

Enhanced *miR-24* expression levels post MI rise the question if the clustered *miR-23/27a/b* also are subject to transcriptional regulation in infarcted hearts. To address this issue, collaboration partners in the Tuschl laboratory also performed *in situ* hybridization for clustered miRNAs in cardiac tissue after MI. Indeed, they found a parallel upregulation of clustered miRNAs in the infarcted zone (unpublished). This in turn indicates that the *miR-23-27-24* cluster may act coordinatively in the infarcted heart, although different post-transcriptional regulation has been observed within this miRNA cluster (Sun F *et al.*, 2009; Buck *et al.*, 2010). Synergistic effects of this miRNA cluster have also been reported for the regulation of Smads during hepatocytic differentiation (Rogler *et al.*, 2009). The presented mechanism established a pivotal role of the *miR-23b* cluster for TGF-beta signalling with high expression levels shutting down the pathway. A previous functional study also suggests synergistic effects regarding apoptosis. Overexpression of clustered *miR-23a-27a-24-2* sensitized HEK293 cells to apoptosis either by the extrinsic or intrinsic apoptosis pathway (Chhabra *et al.*, 2009). Nevertheless, functional studies for the other members *miR-23a/b/27a/b* have not been addressed in this work. Therefore, putative effects of other members of this miRNA family on e.g. endothelial cell apoptosis or other endothelial functions cannot be ruled out. Analyzing the impact of modulated endothelial *miR-23a/b/27a/b* expression should be investigated in further studies. Nevertheless, cooperative function in a miRNA cluster is not obligatory.

Recently, it has been shown that the *miR-23a-27a-24-2* cluster is upregulated upon hypertrophic stimuli like aldosterone or isoproterenol in cardiomyocytes (Lin *et al.*, 2009). Noteworthy, silencing of *miR-23a* only prevents aldosterone or isoproterenol induced cardiomyocyte hypertrophy whereas antagonizing *miR-27a* or *miR-24* had no effects. In line with these observations, van Rooij *et al.* reported that adenoviral *miR-24* overexpression induces cardiomyocyte hypertrophy (van Rooij *et al.*, 2006). Additionally, enhanced *miR-24* expression was found in failing human hearts indicating that *miR-24* has a role in progression and manifestation of cardiac failure, although the cellular source of this regulation was not examined in this work. Taken together, these investigations emphasize that *miR-24* dysregulation may have potential impact in other cardiac cells than endothelial cells which has not been addressed in this work. Besides these adverse effects for *miR-24* on cardiac remodeling, interesting findings were made while exploring the miRNA expression panel upon ischemic preconditioning (IPC) (Yin *et al.*, 2009). During IPC, that might serve as a cardioprotective approach, *miR-1*, *miR-21* and *miR-24* expression is induced. Parallel injection of these miRNAs led to a reduced infarct area upon ischemia/reperfusion which demonstrates that upregulation of *miR-24* can also guide defense mechanisms *prior* to cardiac stress. However, the current work emphasizes that increased *miR-24* expression induced by MI exerts negative effects on cardiac endothelial cell biology contributing to adverse cardiac remodeling.

4.2 Induction of endothelial cell apoptosis by *miR-24*

Myocardial infarction or hypoxia induces endothelial *miR-24* expression (figure 3.1). Mimicking this situation *in vitro* modulates apoptosis outcome because *miR-24* overexpressing ECs suffer from more apoptotic events (figure 3.9). Therefore, endothelial *miR-24* can be viewed as a pro-apoptotic miRNA. In contrast, antagonizing *miR-24*, even under hypoxic conditions, counteracts endothelial apoptosis (figure 3.10). Additionally, ROS generation increases in parallel further amplifying cellular stress signalling (figure 3.16). By this, EC biology is crucially disturbed as defined by impaired capillary tube formation *in vitro*. The importance of miRNAs for angiogenesis has been described by Suarez *et al.*

Silencing of the miRNA processing enzyme Dicer in ECs abolished capillary tube formation due to unprocessed, not functional miRNAs (Suarez *et al.*, 2007). This clearly indicates that miRNAs are necessary for capillary formation. Interestingly, elevated *miR-24* levels affected apoptosis in ECs only (figure 3.9). Other cardiac cell types such as cardiomyocytes or cardiac fibroblasts were unaffected. A possible explanation for this observation is the variance of protein expression patterns and thus potential *miR-24* targets in these cell types. Cardiomyocytes, cardiac fibroblasts and endothelial cells have *per se* different functional relevance in the cardiac system. Thus, cellular transcriptome differs greatly with respect to functionality. In turn, this impacts on respective miRNA actions which is crucially dependent on its specific target availability within a given cell type. Taken together, endothelial cells seem to have a transcriptome “fitting” best for *miR-24* induced apoptosis formation in comparison to other cardiac cells. Of great importance, the pro-apoptotic character of *miR-24* in ECs is quite strong since overexpression triggers apoptosis even in the presence of serum. The presence of serum normally protects cells and its withdrawal sensitizes cells towards apoptosis which is also in part dependent on miRNA function (Asada *et al.*, 2008). The linkage of miRNAs towards the specific regulation of EC apoptosis has also recently been reported. The exposure of ECs to shear stress upregulated *miR-21* (Weber *et al.*, 2010). Increased *miR-21* expression inhibited endothelial apoptosis although data from our group also show impairment of oxidative stress defense mechanisms in circulating angiogenic cells (unpublished). In this work, repression of endogenous *miR-24* displayed anti-apoptotic character only. This emphasizes that derepression of direct *miR-24* targets is responsible for anti-apoptotic signalling.

Further investigations characterizing proliferation or migratory capacity in *miR-24* overexpressing ECs should be performed. Due to the proapoptotic effects of *miR-24* in endothelial cells, it is likely that also other important characteristics of EC biology are affected. In fibroblasts, *miR-24* inhibits proliferation and cell cycle via downregulation of E2F2 and Myc, whereas depleting *miR-24* expression forced proliferation (Lal *et al.*, 2009). Target recognition studies revealed interactions of *miR-24* with “seedless” nucleotide elements in the 3′-UTR suggesting an alternative miRNA *modus operandi*.

Such different target regulation mechanisms were also found in cancer cells where *miR-24* displayed target recognition elements in the coding sequence of FAF1 thus abolishing apoptosis (Qin *et al.*, 2010).

The proapoptotic and antiangiogenic effects of *miR-24* in mature endothelium raise the question if developmental processes in endothelial cells are also affected when *miR-24* expression is modulated. To dissect miRNA-dependent developmental processes, the zebrafish model is often used. MiRNAs are injected as either precursors or antagonists (morpholinos) into the developing zebrafish embryo. In a period of two or three days after injection the developing embryo is monitored. Thus, to gain insights into the role of *miR-24* for vascular development, zebrafish experiments have been performed in cooperation (AG Prof. Brand, Cell and Developmental Biology, University Würzburg; laboratory moved over to Imperial College London recently). Transgenic zebrafishes bearing a *flk*-driven GFP reporter (*flk:GFP*), thus marking the vasculature, were modulated by injection of miRNA precursors. Indeed, enhanced *miR-24* expression disturbed the formation of the vascular network indicated by lack of vessel branching and hemorrhage compared to control miRNA injected embryos (figure 4.1 and personal communication). The impairment of vascular development demonstrates that *miR-24* can already influence EC biology during early stages *in vivo*. It is assumable that endothelial apoptosis, as described in this work, is triggered by enhanced *miR-24* expression in the developing zebrafish and thus impairs vascularization processes.

In parallel, amplifying the disturbances in vascular formation, erythropoiesis could be disturbed which was described for *miR-24* in erythroleukemic K562 cells by interfering with ALK4 receptor mediating erythroid differentiation (Wang *et al.*, 2008). In contrast, *miR-24* seems to negatively regulate apoptosis in the neural retina (Walker and Harland, 2009). In the developing *Xenopus laevis*, antagonizing *miR-24* caused marked apoptosis in the eye by derepressing pro-apoptotic factors like Caspase-9. Thus, besides effecting vascular development demonstrated in zebrafish, also loss of *miR-24* may exert specific target derepression in other organs regulating critical cellular events.

Taken together, endothelial *miR-24* influences cellular outcome in a pro-apoptotic manner and impairs the formation of new capillaries. The underlying molecular mechanisms are linked to the downregulation of target genes which should be considered as key players for EC biology.

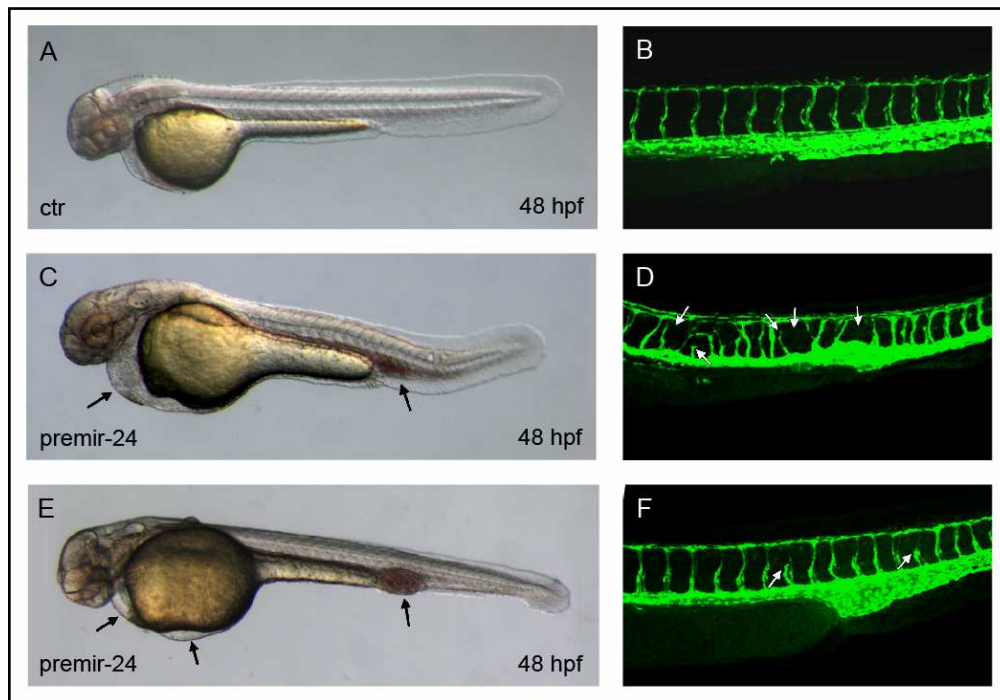


Figure 4.2: Effect of *miR-24* overexpression in *flk1:GFP* transgenic zebrafish. Control (ctr) or precursor-miRNA-24 (*premir-24*) were injected into developing zebrafish embryos. 48 h post fertilization, vascular structures were monitored. Arrows indicate sites of vascular defects observed in *miR-24* mutant embryos (figure provided by AG Prof. Brand, Bettina Kirchmaier, Cell and Developmental Biology, University Würzburg).

4.3 Target-specific regulation for *miR-24* in ECs

The use of *in silico* target prediction tools has accelerated the exploration of direct endothelial *miR-24* targets. Target databases like targetscan (www.targetscan.org) were screened for endothelial expressed downstream effectors of *miR-24*. Recently, a comprehensive database comparing miRNA expression *versus* mRNA expression in different tissues has been introduced further assisting in miRNA target finding (Ritchie *et al.*, 2010). Combining miRNA modulation with proteomics would be an interesting alternative to screen for global protein changes reflecting potential miRNA targets.

This work describes that endothelial *miR-24* represses the protein level of GATA2, H2A.X, PAK4 and RASA1 (figure 3.18). Targets are abundantly expressed in cultured ECs as well as in cardiac tissue monitored by immunohistochemistry (data not shown). Mechanistically, downstream signalling was deciphered by different assays. Downregulation of GATA2, PAK4 and RASA1 mediates *miR-24* apoptosis progression analyzed by transient silencing of these factors in ECs (figure 3.21). Capillary formation *in vitro* is disturbed by silencing of GATA2 and PAK4 only (figure 3.23). This highlights a general concept of combined miRNA target effects. Single target repression does not obligatory reflect miRNA-induced effects. The sum of global proteome changes is crucial since one single miRNA orchestrates often complete gene networks. Repressive miRNA effects are mostly modest with reduction rates of 20-30% in protein. In turn, this fine-tuning balances different cellular events. Probably, *miR-24* has other endothelial targets that do not support apoptosis or angiogenesis defects. By way of example, p27/Kip1 expression was found to be repressed upon *miR-24* overexpression in ECs (data not shown). The p27/Kip1 protein functions as a cell-cycle inhibitor potent of forcing cellular proliferation in cancer cells when depleted (Roy *et al.*, 2008), which did not match to the aforementioned apoptotic phenotype. However the net effect of altered targets drive the phenotypic alterations.

One of the most important endothelial *miR-24* targets based on the results in this work, is the zinc-finger transcription factor GATA2. Downregulation of GATA2 impairs EC function measured by increased apoptosis rate, disturbance in cell cycle progression and finally decreased capillary formation (figures 3.21/22/23). Linkage of GATA2 to these processes has been reported in different settings. In line with the current work, reduced GATA2 expression coincidences with decreased cell survival in embryonic stem cells *in vitro* (Tsai and Orkin, 1997). Moreover, GATA2 reduction in haploinsufficient animals was attributed to lower amounts of hematopoietic progenitors and in parallel to increased apoptotic events by reduction of anti-apoptotic Bcl-x (Rodrigues *et al.*, 2005). Noteworthy, increased levels of GATA2 also support apoptotic signalling in a B-cell line by inducing pro-apoptotic alpha globin (Brecht *et al.*, 2005). This indicates that GATA2 deregulation may impact on apoptosis in both ways. As aforementioned for *miR-24* action, transcriptional activity of GATA2 is also dependent on target gene accessibility thus explaining cell-type specific effects. Furthermore, transcriptive (upstream) regulation sets another level for GATA2-guided signal pathways.

Although miRNA-mediated post-transcriptional control reported in this work is possible and also seen for *miR-451* in zebrafish erythroid maturation (Pase *et al.*, 2009), potential other regulative motifs in the enhancer/promotor region of GATA2 contribute to direct transcriptional regulation. For instance, GATA2 occupies sites in its own promoter thereby establishing a positive feedback loop (Martowicz *et al.*, 2006; Wozniak *et al.*, 2007). Remarkably, endothelial GATA2 is upregulated under hypoxic conditions (figure 3.24) which coincides with hypoxia-induced VEGF expression regulating global angiogenesis (Marti and Risau, 1998). In addition, enhanced GATA2 expression has recently been shown to transduce angiogenic signalling by crosstalk with another transcription factor further emphasizing the pivotal angiogenic role of GATA2 (Mammoto *et al.*, 2009). Besides its anti-apoptotic, pro-angiogenic function, GATA2 also controls endothelial cell cycle progression since GATA2 knockdown induces G₀/G₁-arrest measured by DNA staining in this work (figure 3.22). Indeed, GATA2 expression has been linked to cell cycle control previously. Hematopoietic progenitor cells expressed GATA2 in an oscillating manner during cell cycle with highest expression in S-phase (Koga *et al.*, 2007). Regarding the short half-life of a transcription factor oscillation is feasible but fast expression or dose changes have certainly profound effects on GATA2 target genes that are either transcriptionally induced or repressed.

As shown in this work, GATA2 modulation experiments led to the identification of further downstream targets in ECs. Affymetrix gene chip analysis identified reciprocally regulated GATA2 target genes which then were further validated by ChIP analysis. Notably, *BAMBI*, *ESM1* and *NTN4* have not been reported before as directly regulated by transcription factor GATA2. Nevertheless, *ESM1* and *NTN4* are deeply attributed to endothelial biology. During angiogenesis, endothel-specific molecule 1 (ESM1) is highly induced by angiogenic mediators VEGF-A and VEGF-C (Aitkenhead *et al.*, 2002; Shin *et al.*, 2008). Secreted netrin-4 (NTN4) has also been proven as an active inductor of angiogenesis, even after ischemia *in vivo* and in the zebrafish model (Wilson *et al.*, 2006). Controversially, endothelial NTN4 knockdown increases tube formation ability on matrigel (Lejmi *et al.*, 2008). This suggests pro-angiogenic property of NTN4 which is further reflected by the recent finding that GATA2 silencing reduces NTN4 and then contributes to impaired tube formation in GATA2-deficient ECs. Next to the regulation of angiogenesis-related genes, GATA2 regulates heme oxygenase-1 (HMOX1) at the protein level (figure 3.28).

Loss-of function experiments in GATA2- and *miR-24*-deficient ECs demonstrated that *miR-24* target GATA2 is the critical regulator for HMOX1 repression in *miR-24* overexpressing ECs (figure 3.29). HMOX1 has been described as a cytoprotective enzyme towards ischemic disease when administrated into the myocardium (Melo *et al.*, 2002). Furthermore, carbon dioxide production by HMOX1 protects against EC apoptosis (Wang *et al.*, 2007). Additionally, elevated HMOX1 expression reduced ROS levels in vascular ECs (Asija *et al.*, 2007). In contrast, HMOX1 downregulation induced by endothelial overexpression of *miR-24* expression induced maladaptive ROS as it has been shown in this work. Noteworthy, ROS generation is attributed to support cell apoptosis by facilitating cytochrome C release from mitochondrial intermembrane space (Petrosillo *et al.*, 2003). Likewise, this scenario may also be present for *miR-24* induced endothelial apoptosis. Besides HMOX1, histone deacetylase sirtuin1 (SIRT1) expression has been identified to be GATA2-dependent because SIRT1 expression was markedly decreased in GATA2 deficient ECs (figure 3.30). Remarkably, SIRT1 has a central role in EC biology regulating angiogenic response *in vitro* and *in vivo* by post-translational modification of anti-angiogenic transcription factor Foxo1 (Potente *et al.*, 2007). Cumulatively, newly identified GATA2-regulated genes as well as effector proteins HMOX1 and SIRT1 emphasize a master function of endothelial transcription factor GATA2 for endothelial homeostasis.

Another important signal pathway identified in this work is the *miR-24*-induced repression of the anti-apoptotic kinase PAK4. Mechanistically, downregulation of endothelial PAK4 is responsible for decreased phospho-Bad expression observed in *miR-24* overexpressing ECs (figures 3.15/32). This supports endothelial cell apoptosis which is accompanied by impaired tube formation in PAK4 silenced ECs. Indeed, previous reports have shown that PAK4 drives downstream phosphorylation of Bad thereby preventing its mitochondrial membrane binding which in turn is a prerequisite for apoptosis by cytochrome C release from the mitochondrial intermembrane space (Gnesutta *et al.*, 2001; Hekman *et al.*, 2006). In line, a defective vascular phenotype has also been observed for endothelial PAK4 knockdown before (Koh *et al.*, 2008). Lessons from PAK4 knockout animals dying in the embryonic phase further revealed an essential role for developmental vessel formation which fits to the phenotype of aforementioned mutant zebrafish (Tian *et al.*, 2009). It is likely that endothelial PAK4 not solely controls apoptotic decision by Bad phosphorylation.

Speculations on additional cellular tasks, like reported PKC-activated function for migration processes (Paliouras et al., 2009), links PAK4 kinase to further general cellular aspects which have not been addressed in the current work.

Besides GATA2 and PAK4, endothelial *miR-24* also targets RASA1 and H2A.X. Downstream analysis has not been performed for these factors but both proteins participate in *miR-24* signalling. Notably, RASA1 knockouts also suffer from defective vasculogenesis and of clinical importance, as RASA1 mutations are regarded to guide capillary malformation-arteriovenous malformation (Lapinski et al., 2007; Eerola et al., 2003). In a mechanistic view, RASA1 is negatively controlling mitogenic RAS activity by hydrolyzing GTP thus functioning as a tumor suppressor (Bos et al., 2007). However, endothelial RASA1 shows weak pro-apoptotic function and no effects on capillary tube formation were found (figures 3.21/23). Endothelial modulation of *miR-24* target H2A.X also revealed no severe functional changes measured by apoptosis analysis or capillary tube formation (figures 3.21/23). Interestingly, H2A.X mediates DNA strand repair by a *miR-24* dependent mechanism in differentiated blood cells (Lal et al., 2009). Putatively, endothelial H2A.X executes similar functions. Therefore, repression would sensitize ECs to cellular stress mechanisms like apoptosis or ROS seen in this work.

Altogether, endothelial cell characteristics are critically regulated by identified *miR-24* targets. Nevertheless, there are certainly more target proteins and signal mediators awaiting exploration. Despite the lack of comprehensive target overview, it should be emphasized that *miR-24* signalling is maladaptive due to direct target repression and that antagonistic approaches may be favorable.

4.4 Antagonizing *miR-24* as a therapeutic option in treatment of cardiovascular disease

The current working model suggests that blocking of elevated endothelial *miR-24* expression counteracts endothelial deterioration *in vitro*. Theoretically, downstream target repression is abrogated and effects on apoptosis and vascularization are diminished.

Indeed, under basal and hypoxic conditions, anti-miRNA-24 transfection increases viable endothelial cell number (figure 3.9/10). Furthermore, repression of endogenous *miR-24* sustains and even slightly improves EC ability to form capillary tubes on matrigel (3.17). However, it is a great challenge to translate these findings into a therapeutic cardiovascular setting although translational miRNA research has been applied in different cardiac disease settings before. Usage of chemically modified antagonistic miRNA sequences, so-called "antagomirs", markedly repressed endogenous miRNA expression *in vivo* and modulated disease recovery. By way of example, our group pioneered the first miRNA-based therapeutic approach in a cardiac hypertrophy model (Thum *et al.*, 2008). Furthermore, antagonism of *miR-92a* improved vascularization in ischemic disease (Bonauer *et al.*, 2009). In contrast, silencing of endogenous endothelial-specific *miR-126* inhibited angiogenesis after ischemic insult (van Solingen *et al.*, 2009). These findings indicate that miRNA downregulation can especially modulate angiogenic response. While Bonauer *et al.* applied a low dose for several times, van Solingen *et al.* applied a single high dose injection antagomir. In our study, titration experiments in comparing low (5 mg/kg) *versus* high (80 mg/kg) antagomir retroorbital application revealed that a low dose is sufficient to mainly target cardiac endothelial cells (figure 3.35). Therefore, antagomir was injected twice with 5 mg/kg after experimental MI to minimize antagomir off-side effects and effects on other cells such as cardiomyocytes. Analysis of *miR-24* expression in placebo and antagomir-treated hearts validated an efficient repressive function of antagomir-24 in the cardiac system (figure 3.36). Certainly, other highly vascularized organs may also be affected but have not been in the scope of this study. To further exclude therapeutic side effects, other organs have to be intensively characterized to weigh positive *versus* negative effects of an antagomir-24 treatment.

Characterization of functional heart parameters after antagomir-24 treatment highlighted a general improvement in cardiac function (figure 3.37). Measurements for fractional shortening, left ventricular diameter and pulmonary congestion emphasized that cardiac function is preserved after MI-treatment with antagomir-24. Noteworthy, antagomir-24-induced changes in cardiac function parameters point to a possible involvement of cardiomyocytes in the therapeutic response.

Induction of cardiomyocyte hypertrophy by *miR-24* overexpression has been shown before (van Rooij *et al.*, 2006). Nevertheless, application of low dose antagomir-24 should have precluded strong impact on none-endothelial cells. Taken together, a contribution of *miR-24* antagonism towards cardiomyocyte hypertrophy cannot be ruled out.

The main idea for performing the antagomir-24 study resulted from the fact that *miR-24* was upregulated after MI and triggered endothelial apoptosis. Taking into account that *miR-24* downregulation would positively influence on endothelial survival, it was assumed that *miR-24* repression is beneficial under ischemic disease conditions. In line, cardiac CD31 staining in placebo and antagomir-24 treated animals depicted a markedly enhanced capillary density in border and infarcted zone (figure 3.38). Enhanced angiogenesis after myocardial infarction is generally described by the release of growth factors like VEGF and induction in endothelial Flk-1 expression (Li *et al.*, 1996). Therefore, blocking *miR-24* expression is capable to support such vascular processes. In addition and also reflecting the proposed model, endothelial apoptosis might be blocked in antagomir treated hearts compared to placebo ones. Overall, increased cardiac capillary density contributes to improved cardiac function *post* antagomir-24 treatment. Further matrigel implantation experiments revealed a general improvement in vascularization by repression of *miR-24* under basal conditions (3.39/40). This indicates that modulation of endogenous *miR-24* expression may lead to side-effects related to cancer progression (for cancers that rely on angiogenesis). Indeed, *miR-24* has been described as a tumor suppressor miRNA before (Mishra *et al.*, 2009). Direct targeting of dihydrofolate reductase (DHFR) induced cell cycle arrest and blocked proliferation. Moreover and of importance, cancer tumor miRNA profiling revealed decreased *miR-24* expression levels. Furthermore, DHFR single nucleotide polymorphisms in 3'-UTR comprising the *miR-24* binding site were attributed to chemodrug resistance (Mishra *et al.*, 2007). These findings emphasize that *miR-24* modulation guides angiogenic pathways in cancer disease. Therefore, *in vivo* application of antagomir-24 must be carefully considered. To overcome such diametral effects, meaning positive effects for capillary density in the heart but risk for cancer progression, antagomirs' chemical characteristics need to be modified to develop cardiac specific approaches. Unspecific and systemic delivery should be substituted to a highly specific and efficient cell-type or organ delivery.

4.5 Concluding remarks

The current work identified an endothelial *miR-24* –related mechanism that may be translated into a potential cardiovascular therapeutic application.

Hypoxia and myocardial infarction enhance *miR-24* expression selectively in endothelial cells. Thereby, apoptosis in endothelial cells is induced and formation of capillary structures is abolished. Functional consequences are explained by the downregulation of important endothelial mediators GATA2, H2A.X, PAK4 and RASA1. *MiR-24* antagonism prevented endothelial apoptosis and was applied in an *in vivo* model of myocardial infarction. Therapeutic intervention by injection of *miR-24* antagonists preserved cardiac function and improved capillary density in the infarcted heart.

Currently miRNA research covers many diseases and new therapeutic approaches may have great clinical relevance. Fundamental observations with respect to miRNA origin and mechanism are deciphered but many unsolved issues remain. For instance, upstream and downstream signalling differs for nearly every miRNA and needs to be deciphered in many cell types. Furthermore, translation into clinical scenarios is a future aim but careful consideration is needed since current antagomir approaches are systemic and not cell-type or organ specific and thus may have side-effects. Noteworthy, great efforts are underway to translate promising findings for the treatment of Hepatitis C infection in primates by repression of *miR-122* to the clinic (Lanford *et al.*, 2010) and indeed the first clinical study has recently started (Santaris, Denmark, personal communication). Thus, miRNA-dependent therapeutics will be in focus of future extensive characterization and clinical drug development.

References

1. Aitkenhead M, Wang SJ, Nakatsu MN, Mestas J, Heard C, Hughes CC. Identification of endothelial cell genes expressed in an in vitro model of angiogenesis: induction of ESM-1, (beta)ig-h3, and NrCAM. *Microvasc Res.* 2002;63(2):159-171.
2. Akhtar N, Dickerson EB, Auerbach R. The sponge/Matrigel angiogenesis assay. *Angiogenesis.* 2002;5(1-2):75-80.
3. Altuvia Y, Landgraf P, Lithwick G, Elefant N, Pfeffer S, Aravin A, Brownstein MJ, Tuschl T, Margalit H. Clustering and conservation patterns of human microRNAs. *Nucleic Acids Res.* 2005;33(8):2697-2706.
4. Asada S, Takahashi T, Isodono K, Adachi A, Imoto H, Ogata T, Ueyama T, Matsubara H, Oh H. Downregulation of Dicer expression by serum withdrawal sensitizes human endothelial cells to apoptosis. *Am J Physiol Heart Circ Physiol.* 2008;295(6):H2512-2521.
5. Asahara T, Masuda H, Takahashi T, Kalka C, Pastore C, Silver M, Kearne M, Magner M, Isner JM. Bone marrow origin of endothelial progenitor cells responsible for postnatal vasculogenesis in physiological and pathological neovascularization. *Circ Res.* 1999;85(3):221-228.
6. Ashkenazi A, Dixit VM. Apoptosis control by death and decoy receptors. *Curr Opin Cell Biol.* 1999;11(2):255-260.
7. Asija A, Peterson SJ, Stec DE, Abraham NG. Targeting endothelial cells with heme oxygenase-1 gene using VE-cadherin promoter attenuates hyperglycemia-mediated cell injury and apoptosis. *Antioxid Redox Signal.* 2007;9(12):2065-2074.
8. Bass BL. RNA editing by adenosine deaminases that act on RNA. *Annu Rev Biochem.* 2002;71:817-846.
9. Bonauer A, Carmona G, Iwasaki M, Mione M, Koyanagi M, Fischer A, Burchfield J, Fox H, Doebele C, Ohtani K, Chavakis E, Potente M, Tjwa M, Urbich C, Zeiher AM, Dimmeler S. MicroRNA-92a controls angiogenesis and functional recovery of ischemic tissues in mice. *Science.* 2009;324(5935):1710-1713.
10. Bos JL, Rehmann H, Wittinghofer A. GEFs and GAPs: critical elements in the control of small G proteins. *Cell.* 2007;129(5):865-877.
11. Brecht K, Simonen M, Kamke M, Heim J. Hematopoietic transcription factor GATA-2 promotes upregulation of alpha globin and cell death in FL5.12 cells. *Apoptosis.* 2005;10(5):1063-1078.
12. Brennecke J, Hipfner DR, Stark A, Russell RB, Cohen SM. bantam encodes a developmentally regulated microRNA that controls cell proliferation and regulates the proapoptotic gene hid in Drosophila. *Cell.* 2003;113(1):25-36.
13. Buck AH, Perot J, Chisholm MA, Kumar DS, Tuddenham L, Cognat V, Marcinowski L, Dolken L, Pfeffer S. Post-transcriptional regulation of miR-27 in murine cytomegalovirus infection. *Rna.* 2010;16(2):307-315.
14. Callis TE, Pandya K, Seok HY, Tang RH, Tatsuguchi M, Huang ZP, Chen JF, Deng Z, Gunn B, Shumate J, Willis MS, Selzman CH, Wang DZ. MicroRNA-208a is a regulator of cardiac hypertrophy and conduction in mice. *J Clin Invest.* 2009;119(9):2772-2786.

15. Cao R, Eriksson A, Kubo H, Alitalo K, Cao Y, Thyberg J. Comparative evaluation of FGF-2-, VEGF-A-, and VEGF-C-induced angiogenesis, lymphangiogenesis, vascular fenestrations, and permeability. *Circ Res.* 2004;94(5):664-670.
16. Care A, Catalucci D, Felicetti F, Bonci D, Addario A, Gallo P, Bang ML, Segnalini P, Gu Y, Dalton ND, Elia L, Latronico MV, Hoydal M, Autore C, Russo MA, Dorn GW, 2nd, Ellingsen O, Ruiz-Lozano P, Peterson KL, Croce CM, Peschle C, Condorelli G. MicroRNA-133 controls cardiac hypertrophy. *Nat Med.* 2007;13(5):613-618.
17. Carmeliet P, Ferreira V, Breier G, Pollefeyt S, Kieckens L, Gertsenshtein M, Fahrig M, Vandenhoeck A, Harpal K, Eberhardt C, Declercq C, Pawling J, Moons L, Collen D, Risau W, Nagy A. Abnormal blood vessel development and lethality in embryos lacking a single VEGF allele. *Nature.* 1996;380(6573):435-439.
18. Chan MC, Hilyard AC, Wu C, Davis BN, Hill NS, Lal A, Lieberman J, Lagna G, Hata A. Molecular basis for antagonism between PDGF and the TGFbeta family of signalling pathways by control of miR-24 expression. *Embo J.* 2010;29(3):559-573.
19. Chen L, Willis SN, Wei A, Smith BJ, Fletcher JI, Hinds MG, Colman PM, Day CL, Adams JM, Huang DC. Differential targeting of prosurvival Bcl-2 proteins by their BH3-only ligands allows complementary apoptotic function. *Mol Cell.* 2005;17(3):393-403.
20. Chendrimada TP, Gregory RI, Kumaraswamy E, Norman J, Cooch N, Nishikura K, Shiekhattar R. TRBP recruits the Dicer complex to Ago2 for microRNA processing and gene silencing. *Nature.* 2005;436(7051):740-744.
21. Chhabra R, Adlakha YK, Hariharan M, Scaria V, Saini N. Upregulation of miR-23a-27a-24-2 cluster induces caspase-dependent and -independent apoptosis in human embryonic kidney cells. *PLoS One.* 2009;4(6):e5848.
22. Clark JE, Foresti R, Sarathchandra P, Kaur H, Green CJ, Motterlini R. Heme oxygenase-1-derived bilirubin ameliorates postischemic myocardial dysfunction. *Am J Physiol Heart Circ Physiol.* 2000;278(2):H643-651.
23. Cleutjens JP, Kandala JC, Guarda E, Guntaka RV, Weber KT. Regulation of collagen degradation in the rat myocardium after infarction. *J Mol Cell Cardiol.* 1995;27(6):1281-1292.
24. Cleutjens JP, Verluyten MJ, Smiths JF, Daemen MJ. Collagen remodeling after myocardial infarction in the rat heart. *Am J Pathol.* 1995;147(2):325-338.
25. Cross MJ, Claesson-Welsh L. FGF and VEGF function in angiogenesis: signalling pathways, biological responses and therapeutic inhibition. *Trends Pharmacol Sci.* 2001;22(4):201-207.
26. da Costa Martins PA, Bourajjaj M, Gladka M, Kortland M, van Oort RJ, Pinto YM, Molkenin JD, De Windt LJ. Conditional dicer gene deletion in the postnatal myocardium provokes spontaneous cardiac remodeling. *Circulation.* 2008;118(15):1567-1576.
27. Datta SR, Dudek H, Tao X, Masters S, Fu H, Gotoh Y, Greenberg ME. Akt phosphorylation of BAD couples survival signals to the cell-intrinsic death machinery. *Cell.* 1997;91(2):231-241.
28. Desmouliere A, Geinoz A, Gabbiani F, Gabbiani G. Transforming growth factor-beta 1 induces alpha-smooth muscle actin expression in granulation tissue myofibroblasts and in quiescent and growing cultured fibroblasts. *J Cell Biol.* 1993;122(1):103-111.

29. Dews M, Homayouni A, Yu D, Murphy D, Seignani C, Wentzel E, Furth EE, Lee WM, Enders GH, Mendell JT, Thomas-Tikhonenko A. Augmentation of tumor angiogenesis by a Myc-activated microRNA cluster. *Nat Genet.* 2006;38(9):1060-1065.
30. Dill T, Schachinger V, Rolf A, Mollmann S, Thiele H, Tillmanns H, Assmus B, Dimmeler S, Zeiher AM, Hamm C. Intracoronary administration of bone marrow-derived progenitor cells improves left ventricular function in patients at risk for adverse remodeling after acute ST-segment elevation myocardial infarction: results of the Reinfusion of Enriched Progenitor cells And Infarct Remodeling in Acute Myocardial Infarction study (REPAIR-AMI) cardiac magnetic resonance imaging substudy. *Am Heart J.* 2009;157(3):541-547.
31. Dimmeler S, Fleming I, Fisslthaler B, Hermann C, Busse R, Zeiher AM. Activation of nitric oxide synthase in endothelial cells by Akt-dependent phosphorylation. *Nature.* 1999;399(6736):601-605.
32. Dimmeler S, Haendeler J, Galle J, Zeiher AM. Oxidized low-density lipoprotein induces apoptosis of human endothelial cells by activation of CPP32-like proteases. A mechanistic clue to the 'response to injury' hypothesis. *Circulation.* 1997;95(7):1760-1763.
33. Dimmeler S, Hermann C, Galle J, Zeiher AM. Upregulation of superoxide dismutase and nitric oxide synthase mediates the apoptosis-suppressive effects of shear stress on endothelial cells. *Arterioscler Thromb Vasc Biol.* 1999;19(3):656-664.
34. Dimmeler S, Zeiher AM. Endothelial cell apoptosis in angiogenesis and vessel regression. *Circ Res.* 2000;87(6):434-439.
35. Du C, Fang M, Li Y, Li L, Wang X. Smac, a mitochondrial protein that promotes cytochrome c-dependent caspase activation by eliminating IAP inhibition. *Cell.* 2000;102(1):33-42.
36. Duisters RF, Tijssen AJ, Schroen B, Leenders JJ, Lentink V, van der Made I, Herias V, van Leeuwen RE, Schellings MW, Barenbrug P, Maessen JG, Heymans S, Pinto YM, Creemers EE. miR-133 and miR-30 regulate connective tissue growth factor: implications for a role of microRNAs in myocardial matrix remodeling. *Circ Res.* 2009;104(2):170-178, 176p following 178.
37. Dulak J, Deshane J, Jozkowicz A, Agarwal A. Heme oxygenase-1 and carbon monoxide in vascular pathobiology: focus on angiogenesis. *Circulation.* 2008;117(2):231-241.
38. Economopoulou M, Langer HF, Celeste A, Orlova VV, Choi EY, Ma M, Vassilopoulos A, Callen E, Deng C, Bassing CH, Boehm M, Nussenzweig A, Chavakis T. Histone H2AX is integral to hypoxia-driven neovascularization. *Nat Med.* 2009;15(5):553-558.
39. Eerola I, Boon LM, Mulliken JB, Burrows PE, Domp Martin A, Watanabe S, Vanwijck R, Vikkula M. Capillary malformation-arteriovenous malformation, a new clinical and genetic disorder caused by RASA1 mutations. *Am J Hum Genet.* 2003;73(6):1240-1249.
40. Erlebacher JA, Weiss JL, Weisfeldt ML, Bulkley BH. Early dilation of the infarcted segment in acute transmural myocardial infarction: role of infarct expansion in acute left ventricular enlargement. *J Am Coll Cardiol.* 1984;4(2):201-208.
41. Esquela-Kerscher A, Slack FJ. Oncomirs - microRNAs with a role in cancer. *Nat Rev Cancer.* 2006;6(4):259-269.

42. Evans T, Reitman M, Felsenfeld G. An erythrocyte-specific DNA-binding factor recognizes a regulatory sequence common to all chicken globin genes. *Proc Natl Acad Sci U S A*. 1988;85(16):5976-5980.
43. Farre D, Roset R, Huerta M, Adsuara JE, Rosello L, Alba MM, Messeguer X. Identification of patterns in biological sequences at the ALGGEN server: PROMO and MALGEN. *Nucleic Acids Res*. 2003;31(13):3651-3653.
44. Ferrara N, Carver-Moore K, Chen H, Dowd M, Lu L, O'Shea KS, Powell-Braxton L, Hillan KJ, Moore MW. Heterozygous embryonic lethality induced by targeted inactivation of the VEGF gene. *Nature*. 1996;380(6573):439-442.
45. Field SJ, Tsai FY, Kuo F, Zubiaga AM, Kaelin WG, Jr., Livingston DM, Orkin SH, Greenberg ME. E2F-1 functions in mice to promote apoptosis and suppress proliferation. *Cell*. 1996;85(4):549-561.
46. Fish JE, Santoro MM, Morton SU, Yu S, Yeh RF, Wythe JD, Ivey KN, Bruneau BG, Stainier DY, Srivastava D. miR-126 regulates angiogenic signaling and vascular integrity. *Dev Cell*. 2008;15(2):272-284.
47. Forsythe JA, Jiang BH, Iyer NV, Agani F, Leung SW, Koos RD, Semenza GL. Activation of vascular endothelial growth factor gene transcription by hypoxia-inducible factor 1. *Mol Cell Biol*. 1996;16(9):4604-4613.
48. Francis GS, Goldsmith SR, Levine TB, Olivari MT, Cohn JN. The neurohumoral axis in congestive heart failure. *Ann Intern Med*. 1984;101(3):370-377.
49. Friedman RC, Farh KK, Burge CB, Bartel DP. Most mammalian mRNAs are conserved targets of microRNAs. *Genome Res*. 2009;19(1):92-105.
50. Fulton D, Gratton JP, McCabe TJ, Fontana J, Fujio Y, Walsh K, Franke TF, Papapetropoulos A, Sessa WC. Regulation of endothelium-derived nitric oxide production by the protein kinase Akt. *Nature*. 1999;399(6736):597-601.
51. Gerber HP, McMurtrey A, Kowalski J, Yan M, Keyt BA, Dixit V, Ferrara N. Vascular endothelial growth factor regulates endothelial cell survival through the phosphatidylinositol 3'-kinase/Akt signal transduction pathway. Requirement for Flk-1/KDR activation. *J Biol Chem*. 1998;273(46):30336-30343.
52. Gnesutta N, Qu J, Minden A. The serine/threonine kinase PAK4 prevents caspase activation and protects cells from apoptosis. *J Biol Chem*. 2001;276(17):14414-14419.
53. Grant DS, Tashiro K, Segui-Real B, Yamada Y, Martin GR, Kleinman HK. Two different laminin domains mediate the differentiation of human endothelial cells into capillary-like structures in vitro. *Cell*. 1989;58(5):933-943.
54. Gregory RI, Chendrimada TP, Cooch N, Shiekhattar R. Human RISC couples microRNA biogenesis and posttranscriptional gene silencing. *Cell*. 2005;123(4):631-640.
55. Gregory RI, Yan KP, Amuthan G, Chendrimada T, Doratotaj B, Cooch N, Shiekhattar R. The Microprocessor complex mediates the genesis of microRNAs. *Nature*. 2004;432(7014):235-240.
56. Griffiths-Jones S. The microRNA Registry. *Nucleic Acids Res*. 2004;32(Database issue):D109-111.
57. Griffiths-Jones S. miRBase: the microRNA sequence database. *Methods Mol Biol*. 2006;342:129-138.
58. Griffiths-Jones S, Saini HK, van Dongen S, Enright AJ. miRBase: tools for microRNA genomics. *Nucleic Acids Res*. 2008;36(Database issue):D154-158.

59. Grimson A, Farh KK, Johnston WK, Garrett-Engele P, Lim LP, Bartel DP. MicroRNA targeting specificity in mammals: determinants beyond seed pairing. *Mol Cell*. 2007;27(1):91-105.
60. Hakem R, Hakem A, Duncan GS, Henderson JT, Woo M, Soengas MS, Elia A, de la Pompa JL, Kagi D, Khoo W, Potter J, Yoshida R, Kaufman SA, Lowe SW, Penninger JM, Mak TW. Differential requirement for caspase 9 in apoptotic pathways in vivo. *Cell*. 1998;94(3):339-352.
61. Hanahan D, Christofori G, Naik P, Arbeit J. Transgenic mouse models of tumour angiogenesis: the angiogenic switch, its molecular controls, and prospects for preclinical therapeutic models. *Eur J Cancer*. 1996;32A(14):2386-2393.
62. Hekman M, Albert S, Galmiche A, Rennefahrt UE, Fueller J, Fischer A, Puehringer D, Wiese S, Rapp UR. Reversible membrane interaction of BAD requires two C-terminal lipid binding domains in conjunction with 14-3-3 protein binding. *J Biol Chem*. 2006;281(25):17321-17336.
63. Henkemeyer M, Rossi DJ, Holmyard DP, Puri MC, Mbamalu G, Harpal K, Shih TS, Jacks T, Pawson T. Vascular system defects and neuronal apoptosis in mice lacking ras GTPase-activating protein. *Nature*. 1995;377(6551):695-701.
64. Hermann C, Assmus B, Urbich C, Zeiher AM, Dimmeler S. Insulin-mediated stimulation of protein kinase Akt: A potent survival signaling cascade for endothelial cells. *Arterioscler Thromb Vasc Biol*. 2000;20(2):402-409.
65. Hermann C, Zeiher AM, Dimmeler S. Shear stress inhibits H₂O₂-induced apoptosis of human endothelial cells by modulation of the glutathione redox cycle and nitric oxide synthase. *Arterioscler Thromb Vasc Biol*. 1997;17(12):3588-3592.
66. Heymans S, Lutun A, Nuyens D, Theilmeyer G, Creemers E, Moons L, Dyspersin GD, Cleutjens JP, Shipley M, Angellilo A, Levi M, Nube O, Baker A, Keshet E, Lupu F, Herbert JM, Smits JF, Shapiro SD, Baes M, Borgers M, Collen D, Daemen MJ, Carmeliet P. Inhibition of plasminogen activators or matrix metalloproteinases prevents cardiac rupture but impairs therapeutic angiogenesis and causes cardiac failure. *Nat Med*. 1999;5(10):1135-1142.
67. Hill JA, Olson EN. Cardiac plasticity. *N Engl J Med*. 2008;358(13):1370-1380.
68. Huang LE, Arany Z, Livingston DM, Bunn HF. Activation of hypoxia-inducible transcription factor depends primarily upon redox-sensitive stabilization of its alpha subunit. *J Biol Chem*. 1996;271(50):32253-32259.
69. Hutvagner G, McLachlan J, Pasquinelli AE, Balint E, Tuschl T, Zamore PD. A cellular function for the RNA-interference enzyme Dicer in the maturation of the let-7 small temporal RNA. *Science*. 2001;293(5531):834-838.
70. Izumo S, Nadal-Ginard B, Mahdavi V. Protooncogene induction and reprogramming of cardiac gene expression produced by pressure overload. *Proc Natl Acad Sci U S A*. 1988;85(2):339-343.
71. Jessup M, Brozena S. Heart failure. *N Engl J Med*. 2003;348(20):2007-2018.
72. Jimenez B, Volpert OV, Crawford SE, Febbraio M, Silverstein RL, Bouck N. Signals leading to apoptosis-dependent inhibition of neovascularization by thrombospondin-1. *Nat Med*. 2000;6(1):41-48.
73. Johnson TM, Yu ZX, Ferrans VJ, Lowenstein RA, Finkel T. Reactive oxygen species are downstream mediators of p53-dependent apoptosis. *Proc Natl Acad Sci U S A*. 1996;93(21):11848-11852.

74. Kerr JF, Wyllie AH, Currie AR. Apoptosis: a basic biological phenomenon with wide-ranging implications in tissue kinetics. *Br J Cancer*. 1972;26(4):239-257.
75. Khan R, Sheppard R. Fibrosis in heart disease: understanding the role of transforming growth factor-beta in cardiomyopathy, valvular disease and arrhythmia. *Immunology*. 2006;118(1):10-24.
76. Khvorova A, Reynolds A, Jayasena SD. Functional siRNAs and miRNAs exhibit strand bias. *Cell*. 2003;115(2):209-216.
77. Khwaja A. Akt is more than just a Bad kinase. *Nature*. 1999;401(6748):33-34.
78. Kim I, Kim HG, So JN, Kim JH, Kwak HJ, Koh GY. Angiopoietin-1 regulates endothelial cell survival through the phosphatidylinositol 3'-Kinase/Akt signal transduction pathway. *Circ Res*. 2000;86(1):24-29.
79. Kim I, Moon SO, Koh KN, Kim H, Uhm CS, Kwak HJ, Kim NG, Koh GY. Molecular cloning, expression, and characterization of angiopoietin-related protein. angiopoietin-related protein induces endothelial cell sprouting. *J Biol Chem*. 1999;274(37):26523-26528.
80. Kim VN, Han J, Siomi MC. Biogenesis of small RNAs in animals. *Nat Rev Mol Cell Biol*. 2009;10(2):126-139.
81. Kiriakidou M, Tan GS, Lamprinaki S, De Planell-Saguer M, Nelson PT, Mourelatos Z. An mRNA m7G cap binding-like motif within human Ago2 represses translation. *Cell*. 2007;129(6):1141-1151.
82. Knowlton AA, Connelly CM, Romo GM, Mamuya W, Apstein CS, Brecher P. Rapid expression of fibronectin in the rabbit heart after myocardial infarction with and without reperfusion. *J Clin Invest*. 1992;89(4):1060-1068.
83. Koga S, Yamaguchi N, Abe T, Minegishi M, Tsuchiya S, Yamamoto M, Minegishi N. Cell-cycle-dependent oscillation of GATA2 expression in hematopoietic cells. *Blood*. 2007;109(10):4200-4208.
84. Koh W, Mahan RD, Davis GE. Cdc42- and Rac1-mediated endothelial lumen formation requires Pak2, Pak4 and Par3, and PKC-dependent signaling. *J Cell Sci*. 2008;121(Pt 7):989-1001.
85. Koopman G, Reutelingsperger CP, Kuijten GA, Keehnen RM, Pals ST, van Oers MH. Annexin V for flow cytometric detection of phosphatidylserine expression on B cells undergoing apoptosis. *Blood*. 1994;84(5):1415-1420.
86. Krek A, Grun D, Poy MN, Wolf R, Rosenberg L, Epstein EJ, MacMenamin P, da Piedade I, Gunsalus KC, Stoffel M, Rajewsky N. Combinatorial microRNA target predictions. *Nat Genet*. 2005;37(5):495-500.
87. Krutzfeldt J, Kuwajima S, Braich R, Rajeev KG, Pena J, Tuschl T, Manoharan M, Stoffel M. Specificity, duplex degradation and subcellular localization of antagomirs. *Nucleic Acids Res*. 2007;35(9):2885-2892.
88. Krutzfeldt J, Poy MN, Stoffel M. Strategies to determine the biological function of microRNAs. *Nat Genet*. 2006;38 Suppl:S14-19.
89. Krutzfeldt J, Rajewsky N, Braich R, Rajeev KG, Tuschl T, Manoharan M, Stoffel M. Silencing of microRNAs in vivo with 'antagomirs'. *Nature*. 2005;438(7068):685-689.
90. Krutzfeldt J, Stoffel M. MicroRNAs: a new class of regulatory genes affecting metabolism. *Cell Metab*. 2006;4(1):9-12.
91. Kuehbacher A, Urbich C, Zeiher AM, Dimmeler S. Role of Dicer and Drosha for endothelial microRNA expression and angiogenesis. *Circ Res*. 2007;101(1):59-68.

92. Kuhnert F, Mancuso MR, Hampton J, Stankunas K, Asano T, Chen CZ, Kuo CJ. Attribution of vascular phenotypes of the murine *Egfl7* locus to the microRNA miR-126. *Development*. 2008;135(24):3989-3993.
93. Kulshreshtha R, Ferracin M, Wojcik SE, Garzon R, Alder H, Agosto-Perez FJ, Davuluri R, Liu CG, Croce CM, Negrini M, Calin GA, Ivan M. A microRNA signature of hypoxia. *Mol Cell Biol*. 2007;27(5):1859-1867.
94. Kvietikova I, Wenger RH, Marti HH, Gassmann M. The transcription factors ATF-1 and CREB-1 bind constitutively to the hypoxia-inducible factor-1 (HIF-1) DNA recognition site. *Nucleic Acids Res*. 1995;23(22):4542-4550.
95. Lal A, Kim HH, Abdelmohsen K, Kuwano Y, Pullmann R, Jr., Srikantan S, Subrahmanyam R, Martindale JL, Yang X, Ahmed F, Navarro F, Dykxhoorn D, Lieberman J, Gorospe M. p16(INK4a) translation suppressed by miR-24. *PLoS One*. 2008;3(3):e1864.
96. Lal A, Navarro F, Maher CA, Maliszewski LE, Yan N, O'Day E, Chowdhury D, Dykxhoorn DM, Tsai P, Hofmann O, Becker KG, Gorospe M, Hide W, Lieberman J. miR-24 Inhibits cell proliferation by targeting E2F2, MYC, and other cell-cycle genes via binding to "seedless" 3'UTR microRNA recognition elements. *Mol Cell*. 2009;35(5):610-625.
97. Lal A, Pan Y, Navarro F, Dykxhoorn DM, Moreau L, Meire E, Bentwich Z, Lieberman J, Chowdhury D. miR-24-mediated downregulation of H2AX suppresses DNA repair in terminally differentiated blood cells. *Nat Struct Mol Biol*. 2009;16(5):492-498.
98. Lanford RE, Hildebrandt-Eriksen ES, Petri A, Persson R, Lindow M, Munk ME, Kauppinen S, Orum H. Therapeutic silencing of microRNA-122 in primates with chronic hepatitis C virus infection. *Science*. 2010;327(5962):198-201.
99. Lapinski PE, Bauler TJ, Brown EJ, Hughes ED, Saunders TL, King PD. Generation of mice with a conditional allele of the p120 Ras GTPase-activating protein. *Genesis*. 2007;45(12):762-767.
100. Larsson E, Fredlund Fuchs P, Heldin J, Barkefors I, Bondjers C, Genove G, Arrondel C, Gerwins P, Kurschat C, Schermer B, Benzing T, Harvey SJ, Kreuger J, Lindahl P. Discovery of microvascular miRNAs using public gene expression data: miR-145 is expressed in pericytes and is a regulator of Fli1. *Genome Med*. 2009;1(11):108.
101. Lee RC, Feinbaum RL, Ambros V. The *C. elegans* heterochronic gene *lin-4* encodes small RNAs with antisense complementarity to *lin-14*. *Cell*. 1993;75(5):843-854.
102. Lee Y, Kim M, Han J, Yeom KH, Lee S, Baek SH, Kim VN. MicroRNA genes are transcribed by RNA polymerase II. *Embo J*. 2004;23(20):4051-4060.
103. Lejmi E, Leconte L, Pedron-Mazoyer S, Ropert S, Raoul W, Lavalette S, Bouras I, Feron JG, Maitre-Boube M, Assayag F, Feumi C, Alemany M, Jie TX, Merkulova T, Poupon MF, Ruchoux MM, Tobelem G, Sennlaub F, Plouet J. Netrin-4 inhibits angiogenesis via binding to neogenin and recruitment of Unc5B. *Proc Natl Acad Sci U S A*. 2008;105(34):12491-12496.
104. Lew WY, Ban-Hayashi E. Mechanisms of improving regional and global ventricular function by preload alterations during acute ischemia in the canine left ventricle. *Circulation*. 1985;72(5):1125-1134.
105. Lew WY, Chen ZY, Guth B, Covell JW. Mechanisms of augmented segment shortening in nonischemic areas during acute ischemia of the canine left ventricle. *Circ Res*. 1985;56(3):351-358.

106. Lewis BP, Burge CB, Bartel DP. Conserved seed pairing, often flanked by adenosines, indicates that thousands of human genes are microRNA targets. *Cell*. 2005;120(1):15-20.
107. Li J, Brown LF, Hibberd MG, Grossman JD, Morgan JP, Simons M. VEGF, flk-1, and flt-1 expression in a rat myocardial infarction model of angiogenesis. *Am J Physiol*. 1996;270(5 Pt 2):H1803-1811.
108. Lin Z, Murtaza I, Wang K, Jiao J, Gao J, Li PF. miR-23a functions downstream of NFATc3 to regulate cardiac hypertrophy. *Proc Natl Acad Sci U S A*. 2009;106(29):12103-12108.
109. Liu J. Control of protein synthesis and mRNA degradation by microRNAs. *Curr Opin Cell Biol*. 2008;20(2):214-221.
110. Liu J, Carmell MA, Rivas FV, Marsden CG, Thomson JM, Song JJ, Hammond SM, Joshua-Tor L, Hannon GJ. Argonaute2 is the catalytic engine of mammalian RNAi. *Science*. 2004;305(5689):1437-1441.
111. Lowes BD, Minobe W, Abraham WT, Rizeq MN, Bohlmeyer TJ, Quaipe RA, Roden RL, Dutcher DL, Robertson AD, Voelkel NF, Badesch DB, Groves BM, Gilbert EM, Bristow MR. Changes in gene expression in the intact human heart. Downregulation of alpha-myosin heavy chain in hypertrophied, failing ventricular myocardium. *J Clin Invest*. 1997;100(9):2315-2324.
112. Luciano DJ, Mirsky H, Vendetti NJ, Maas S. RNA editing of a miRNA precursor. *Rna*. 2004;10(8):1174-1177.
113. Lund E, Guttinger S, Calado A, Dahlberg JE, Kutay U. Nuclear export of microRNA precursors. *Science*. 2004;303(5654):95-98.
114. Mammoto A, Connor KM, Mammoto T, Yung CW, Huh D, Aderman CM, Mostoslavsky G, Smith LE, Ingber DE. A mechanosensitive transcriptional mechanism that controls angiogenesis. *Nature*. 2009;457(7233):1103-1108.
115. Mann DL. Mechanisms and models in heart failure: A combinatorial approach. *Circulation*. 1999;100(9):999-1008.
116. Marti HH, Risau W. Systemic hypoxia changes the organ-specific distribution of vascular endothelial growth factor and its receptors. *Proc Natl Acad Sci U S A*. 1998;95(26):15809-15814.
117. Martinou JC, Youle RJ. Which came first, the cytochrome c release or the mitochondrial fission? *Cell Death Differ*. 2006;13(8):1291-1295.
118. Martowicz ML, Grass JA, Bresnick EH. GATA-1-mediated transcriptional repression yields persistent transcription factor IIB-chromatin complexes. *J Biol Chem*. 2006;281(49):37345-37352.
119. McFadden DG, Barbosa AC, Richardson JA, Schneider MD, Srivastava D, Olson EN. The Hand1 and Hand2 transcription factors regulate expansion of the embryonic cardiac ventricles in a gene dosage-dependent manner. *Development*. 2005;132(1):189-201.
120. McKay RG, Pfeffer MA, Pasternak RC, Markis JE, Come PC, Nakao S, Alderman JD, Ferguson JJ, Safian RD, Grossman W. Left ventricular remodeling after myocardial infarction: a corollary to infarct expansion. *Circulation*. 1986;74(4):693-702.
121. McMurray J, Pfeffer MA. New therapeutic options in congestive heart failure: Part II. *Circulation*. 2002;105(18):2223-2228.

122. Melo LG, Agrawal R, Zhang L, Rezvani M, Mangi AA, Ehsan A, Griese DP, Dell'Acqua G, Mann MJ, Oyama J, Yet SF, Layne MD, Perrella MA, Dzau VJ. Gene therapy strategy for long-term myocardial protection using adeno-associated virus-mediated delivery of heme oxygenase gene. *Circulation*. 2002;105(5):602-607.
123. Merkle S, Frantz S, Schon MP, Bauersachs J, Buitrago M, Frost RJ, Schmitteckert EM, Lohse MJ, Engelhardt S. A role for caspase-1 in heart failure. *Circ Res*. 2007;100(5):645-653.
124. Messeguer X, Escudero R, Farre D, Nunez O, Martinez J, Alba MM. PROMO: detection of known transcription regulatory elements using species-tailored searches. *Bioinformatics*. 2002;18(2):333-334.
125. Mikhailov V, Mikhailova M, Degenhardt K, Venkatachalam MA, White E, Saikumar P. Association of Bax and Bak homo-oligomers in mitochondria. Bax requirement for Bak reorganization and cytochrome c release. *J Biol Chem*. 2003;278(7):5367-5376.
126. Mishra PJ, Humeniuk R, Mishra PJ, Longo-Sorbello GS, Banerjee D, Bertino JR. A miR-24 microRNA binding-site polymorphism in dihydrofolate reductase gene leads to methotrexate resistance. *Proc Natl Acad Sci U S A*. 2007;104(33):13513-13518.
127. Mishra PJ, Song B, Mishra PJ, Wang Y, Humeniuk R, Banerjee D, Merlino G, Ju J, Bertino JR. MiR-24 tumor suppressor activity is regulated independent of p53 and through a target site polymorphism. *PLoS One*. 2009;4(12):e8445.
128. Nakao K, Minobe W, Roden R, Bristow MR, Leinwand LA. Myosin heavy chain gene expression in human heart failure. *J Clin Invest*. 1997;100(9):2362-2370.
129. Newmeyer DD, Ferguson-Miller S. Mitochondria: releasing power for life and unleashing the machineries of death. *Cell*. 2003;112(4):481-490.
130. Niu Z, Li A, Zhang SX, Schwartz RJ. Serum response factor micromanaging cardiogenesis. *Curr Opin Cell Biol*. 2007;19(6):618-627.
131. Okamura K, Phillips MD, Tyler DM, Duan H, Chou YT, Lai EC. The regulatory activity of microRNA* species has substantial influence on microRNA and 3' UTR evolution. *Nat Struct Mol Biol*. 2008;15(4):354-363.
132. Paliouras GN, Naujokas MA, Park M. Pak4, a novel Gab1 binding partner, modulates cell migration and invasion by the Met receptor. *Mol Cell Biol*. 2009;29(11):3018-3032.
133. Pase L, Layton JE, Kloosterman WP, Carradice D, Waterhouse PM, Lieschke GJ. miR-451 regulates zebrafish erythroid maturation in vivo via its target gata2. *Blood*. 2009;113(8):1794-1804.
134. Petrosillo G, Ruggiero FM, Paradies G. Role of reactive oxygen species and cardiolipin in the release of cytochrome c from mitochondria. *Faseb J*. 2003;17(15):2202-2208.
135. Pillai RS, Bhattacharyya SN, Filipowicz W. Repression of protein synthesis by miRNAs: how many mechanisms? *Trends Cell Biol*. 2007;17(3):118-126.
136. Poliseno L, Tuccoli A, Mariani L, Evangelista M, Citti L, Woods K, Mercatanti A, Hammond S, Rainaldi G. MicroRNAs modulate the angiogenic properties of HUVECs. *Blood*. 2006;108(9):3068-3071.
137. Potente M, Ghaeni L, Baldessari D, Mostoslavsky R, Rossig L, Dequiedt F, Haendeler J, Mione M, Dejana E, Alt FW, Zeiher AM, Dimmeler S. SIRT1 controls endothelial angiogenic functions during vascular growth. *Genes Dev*. 2007;21(20):2644-2658.

138. Potts MB, Vaughn AE, McDonough H, Patterson C, Deshmukh M. Reduced Apaf-1 levels in cardiomyocytes engage strict regulation of apoptosis by endogenous XIAP. *J Cell Biol.* 2005;171(6):925-930.
139. Presta M, Dell'Era P, Mitola S, Moroni E, Ronca R, Rusnati M. Fibroblast growth factor/fibroblast growth factor receptor system in angiogenesis. *Cytokine Growth Factor Rev.* 2005;16(2):159-178.
140. Qin W, Shi Y, Zhao B, Yao C, Jin L, Ma J, Jin Y. miR-24 regulates apoptosis by targeting the open reading frame (ORF) region of FAF1 in cancer cells. *PLoS One.* 2010;5(2):e9429.
141. Rao PK, Toyama Y, Chiang HR, Gupta S, Bauer M, Medvid R, Reinhardt F, Liao R, Krieger M, Jaenisch R, Lodish HF, Blleloch R. Loss of cardiac microRNA-mediated regulation leads to dilated cardiomyopathy and heart failure. *Circ Res.* 2009;105(6):585-594.
142. Ritchie W, Flamant S, Rasko JE. mimiRNA: a microRNA expression profiler and classification resource designed to identify functional correlations between microRNAs and their targets. *Bioinformatics.* 2010;26(2):223-227.
143. Robaye B, Mosselmans R, Fiers W, Dumont JE, Galand P. Tumor necrosis factor induces apoptosis (programmed cell death) in normal endothelial cells in vitro. *Am J Pathol.* 1991;138(2):447-453.
144. Rodrigues NP, Janzen V, Forkert R, Dombkowski DM, Boyd AS, Orkin SH, Enver T, Vyas P, Scadden DT. Haploinsufficiency of GATA-2 perturbs adult hematopoietic stem-cell homeostasis. *Blood.* 2005;106(2):477-484.
145. Rogler CE, Levoci L, Ader T, Massimi A, Tchaikovskaya T, Norel R, Rogler LE. MicroRNA-23b cluster microRNAs regulate transforming growth factor-beta/bone morphogenetic protein signaling and liver stem cell differentiation by targeting Smads. *Hepatology.* 2009;50(2):575-584.
146. Rossig L, Haendeler J, Mallat Z, Hugel B, Freyssinet JM, Tedgui A, Dimmeler S, Zeiher AM. Congestive heart failure induces endothelial cell apoptosis: protective role of carvedilol. *J Am Coll Cardiol.* 2000;36(7):2081-2089.
147. Roy S, Singh RP, Agarwal C, Siriwardana S, Sclafani R, Agarwal R. Downregulation of both p21/Cip1 and p27/Kip1 produces a more aggressive prostate cancer phenotype. *Cell Cycle.* 2008;7(12):1828-1835.
148. Ruby JG, Jan CH, Bartel DP. Intronic microRNA precursors that bypass Drosha processing. *Nature.* 2007;448(7149):83-86.
149. Sadoshima J, Jahn L, Takahashi T, Kulik TJ, Izumo S. Molecular characterization of the stretch-induced adaptation of cultured cardiac cells. An in vitro model of load-induced cardiac hypertrophy. *J Biol Chem.* 1992;267(15):10551-10560.
150. Sadoshima J, Xu Y, Slayter HS, Izumo S. Autocrine release of angiotensin II mediates stretch-induced hypertrophy of cardiac myocytes in vitro. *Cell.* 1993;75(5):977-984.
151. Scaffidi C, Fulda S, Srinivasan A, Friesen C, Li F, Tomaselli KJ, Debatin KM, Krammer PH, Peter ME. Two CD95 (APO-1/Fas) signaling pathways. *Embo J.* 1998;17(6):1675-1687.

152. Schachinger V, Erbs S, Elsasser A, Haberbosch W, Hambrecht R, Holschermann H, Yu J, Corti R, Mathey DG, Hamm CW, Suselbeck T, Werner N, Haase J, Neuzner J, Germing A, Mark B, Assmus B, Tonn T, Dimmeler S, Zeiher AM. Improved clinical outcome after intracoronary administration of bone-marrow-derived progenitor cells in acute myocardial infarction: final 1-year results of the REPAIR-AMI trial. *Eur Heart J*. 2006;27(23):2775-2783.
153. Schmidt M, Paes K, De Maziere A, Smyczek T, Yang S, Gray A, French D, Kasman I, Klumperman J, Rice DS, Ye W. EGFL7 regulates the collective migration of endothelial cells by restricting their spatial distribution. *Development*. 2007;134(16):2913-2923.
154. Schwarz DS, Hutvagner G, Du T, Xu Z, Aronin N, Zamore PD. Asymmetry in the assembly of the RNAi enzyme complex. *Cell*. 2003;115(2):199-208.
155. Seghezzi G, Patel S, Ren CJ, Gualandris A, Pintucci G, Robbins ES, Shapiro RL, Galloway AC, Rifkin DB, Mignatti P. Fibroblast growth factor-2 (FGF-2) induces vascular endothelial growth factor (VEGF) expression in the endothelial cells of forming capillaries: an autocrine mechanism contributing to angiogenesis. *J Cell Biol*. 1998;141(7):1659-1673.
156. Shi Y. Mechanical aspects of apoptosome assembly. *Curr Opin Cell Biol*. 2006;18(6):677-684.
157. Shin JW, Huggenberger R, Detmar M. Transcriptional profiling of VEGF-A and VEGF-C target genes in lymphatic endothelium reveals endothelial-specific molecule-1 as a novel mediator of lymphangiogenesis. *Blood*. 2008;112(6):2318-2326.
158. Suarez Y, Fernandez-Hernando C, Pober JS, Sessa WC. Dicer dependent microRNAs regulate gene expression and functions in human endothelial cells. *Circ Res*. 2007;100(8):1164-1173.
159. Suarez Y, Fernandez-Hernando C, Yu J, Gerber SA, Harrison KD, Pober JS, Iruela-Arispe ML, Merckenschlager M, Sessa WC. Dicer-dependent endothelial microRNAs are necessary for postnatal angiogenesis. *Proc Natl Acad Sci U S A*. 2008;105(37):14082-14087.
160. Sun F, Wang J, Pan Q, Yu Y, Zhang Y, Wan Y, Wang J, Li X, Hong A. Characterization of function and regulation of miR-24-1 and miR-31. *Biochem Biophys Res Commun*. 2009;380(3):660-665.
161. Sun Q, Zhang Y, Yang G, Chen X, Zhang Y, Cao G, Wang J, Sun Y, Zhang P, Fan M, Shao N, Yang X. Transforming growth factor-beta-regulated miR-24 promotes skeletal muscle differentiation. *Nucleic Acids Res*. 2008;36(8):2690-2699.
162. Sutton MG, Sharpe N. Left ventricular remodeling after myocardial infarction: pathophysiology and therapy. *Circulation*. 2000;101(25):2981-2988.
163. Takagi S, Nakajima M, Kida K, Yamaura Y, Fukami T, Yokoi T. MicroRNAs regulate human hepatocyte nuclear factor 4alpha, modulating the expression of metabolic enzymes and cell cycle. *J Biol Chem*. 2010;285(7):4415-4422.
164. Thum T. Cardiac dissonance without conductors: how dicer depletion provokes chaos in the heart. *Circulation*. 2008;118(15):1524-1527.
165. Thum T, Galuppo P, Wolf C, Fiedler J, Kneitz S, van Laake LW, Doevendans PA, Mummery CL, Borlak J, Haverich A, Gross C, Engelhardt S, Ertl G, Bauersachs J. MicroRNAs in the human heart: a clue to fetal gene reprogramming in heart failure. *Circulation*. 2007;116(3):258-267.

166. Thum T, Gross C, Fiedler J, Fischer T, Kissler S, Bussen M, Galuppo P, Just S, Rottbauer W, Frantz S, Castoldi M, Soutschek J, Koteliansky V, Rosenwald A, Basson MA, Licht JD, Pena JT, Rouhanifard SH, Muckenthaler MU, Tuschl T, Martin GR, Bauersachs J, Engelhardt S. MicroRNA-21 contributes to myocardial disease by stimulating MAP kinase signalling in fibroblasts. *Nature*. 2008;456(7224):980-984.
167. Tian Y, Lei L, Cammarano M, Nekrasova T, Minden A. Essential role for the Pak4 protein kinase in extraembryonic tissue development and vessel formation. *Mech Dev*. 2009;126(8-9):710-720.
168. Tsai FY, Keller G, Kuo FC, Weiss M, Chen J, Rosenblatt M, Alt FW, Orkin SH. An early haematopoietic defect in mice lacking the transcription factor GATA-2. *Nature*. 1994;371(6494):221-226.
169. Tsai FY, Orkin SH. Transcription factor GATA-2 is required for proliferation/survival of early hematopoietic cells and mast cell formation, but not for erythroid and myeloid terminal differentiation. *Blood*. 1997;89(10):3636-3643.
170. van Rooij E, Olson EN. MicroRNAs: powerful new regulators of heart disease and provocative therapeutic targets. *J Clin Invest*. 2007;117(9):2369-2376.
171. van Rooij E, Sutherland LB, Liu N, Williams AH, McAnally J, Gerard RD, Richardson JA, Olson EN. A signature pattern of stress-responsive microRNAs that can evoke cardiac hypertrophy and heart failure. *Proc Natl Acad Sci U S A*. 2006;103(48):18255-18260.
172. van Rooij E, Sutherland LB, Thatcher JE, DiMaio JM, Naseem RH, Marshall WS, Hill JA, Olson EN. Dysregulation of microRNAs after myocardial infarction reveals a role of miR-29 in cardiac fibrosis. *Proc Natl Acad Sci U S A*. 2008;105(35):13027-13032.
173. van Solingen C, Seghers L, Bijkerk R, Duijs JM, Roeten MK, van Oeveren-Rietdijk AM, Baelde HJ, Monge M, Vos JB, de Boer HC, Quax PH, Rabelink TJ, van Zonneveld AJ. Antagomir-mediated silencing of endothelial cell specific microRNA-126 impairs ischemia-induced angiogenesis. *J Cell Mol Med*. 2009;13(8A):1577-1585.
174. Walker JC, Harland RM. microRNA-24a is required to repress apoptosis in the developing neural retina. *Genes Dev*. 2009;23(9):1046-1051.
175. Wang GL, Semenza GL. Desferrioxamine induces erythropoietin gene expression and hypoxia-inducible factor 1 DNA-binding activity: implications for models of hypoxia signal transduction. *Blood*. 1993;82(12):3610-3615.
176. Wang Q, Huang Z, Xue H, Jin C, Ju XL, Han JD, Chen YG. MicroRNA miR-24 inhibits erythropoiesis by targeting activin type I receptor ALK4. *Blood*. 2008;111(2):588-595.
177. Wang S, Aurora AB, Johnson BA, Qi X, McAnally J, Hill JA, Richardson JA, Bassel-Duby R, Olson EN. The endothelial-specific microRNA miR-126 governs vascular integrity and angiogenesis. *Dev Cell*. 2008;15(2):261-271.
178. Wang S, Olson EN. Angiomirs--key regulators of angiogenesis. *Curr Opin Genet Dev*. 2009;19(3):205-211.
179. Wang X, Wang Y, Kim HP, Nakahira K, Ryter SW, Choi AM. Carbon monoxide protects against hyperoxia-induced endothelial cell apoptosis by inhibiting reactive oxygen species formation. *J Biol Chem*. 2007;282(3):1718-1726.
180. Warren SE, Royal HD, Markis JE, Grossman W, McKay RG. Time course of left ventricular dilation after myocardial infarction: influence of infarct-related artery and success of coronary thrombolysis. *J Am Coll Cardiol*. 1988;11(1):12-19.

181. Weber KT. Extracellular matrix remodeling in heart failure: a role for de novo angiotensin II generation. *Circulation*. 1997;96(11):4065-4082.
182. Weber M, Baker MB, Moore JP, Searles CD. MiR-21 is induced in endothelial cells by shear stress and modulates apoptosis and eNOS activity. *Biochem Biophys Res Commun*. 2010;393(4):643-648.
183. Wightman B, Ha I, Ruvkun G. Posttranscriptional regulation of the heterochronic gene *lin-14* by *lin-4* mediates temporal pattern formation in *C. elegans*. *Cell*. 1993;75(5):855-862.
184. Wilson BD, Ii M, Park KW, Suli A, Sorensen LK, Larrieu-Lahargue F, Urness LD, Suh W, Asai J, Kock GA, Thorne T, Silver M, Thomas KR, Chien CB, Losordo DW, Li DY. Netrins promote developmental and therapeutic angiogenesis. *Science*. 2006;313(5787):640-644.
185. Wozniak RJ, Boyer ME, Grass JA, Lee Y, Bresnick EH. Context-dependent GATA factor function: combinatorial requirements for transcriptional control in hematopoietic and endothelial cells. *J Biol Chem*. 2007;282(19):14665-14674.
186. Yang WJ, Yang DD, Na S, Sandusky GE, Zhang Q, Zhao G. Dicer is required for embryonic angiogenesis during mouse development. *J Biol Chem*. 2005;280(10):9330-9335.
187. Yang Z, Mo X, Gong Q, Pan Q, Yang X, Cai W, Li C, Ma JX, He Y, Gao G. Critical effect of VEGF in the process of endothelial cell apoptosis induced by high glucose. *Apoptosis*. 2008;13(11):1331-1343.
188. Yin C, Salloum FN, Kukreja RC. A novel role of microRNA in late preconditioning: upregulation of endothelial nitric oxide synthase and heat shock protein 70. *Circ Res*. 2009;104(5):572-575.
189. Yin XM, Wang K, Gross A, Zhao Y, Zinkel S, Klocke B, Roth KA, Korsmeyer SJ. Bid-deficient mice are resistant to Fas-induced hepatocellular apoptosis. *Nature*. 1999;400(6747):886-891.
190. Zha J, Harada H, Osipov K, Jockel J, Waksman G, Korsmeyer SJ. BH3 domain of BAD is required for heterodimerization with BCL-XL and pro-apoptotic activity. *J Biol Chem*. 1997;272(39):24101-24104.
191. Zha J, Harada H, Yang E, Jockel J, Korsmeyer SJ. Serine phosphorylation of death agonist BAD in response to survival factor results in binding to 14-3-3 not BCL-X(L). *Cell*. 1996;87(4):619-628.
192. Zhao Y, Ransom JF, Li A, Vedantham V, von Drehle M, Muth AN, Tsuchihashi T, McManus MT, Schwartz RJ, Srivastava D. Dysregulation of cardiogenesis, cardiac conduction, and cell cycle in mice lacking miRNA-1-2. *Cell*. 2007;129(2):303-317.
193. Zhao Y, Samal E, Srivastava D. Serum response factor regulates a muscle-specific microRNA that targets *Hand2* during cardiogenesis. *Nature*. 2005;436(7048):214-220.

Abbreviations

Ang I:	Angiotensin I	FS:	Fractional shortening
Ang II:	Angiotensin II	GAPDH:	Glyceraldehyde-phosphate-dehydrogenase
ANP:	Atrial natriuretic peptide	GATA2:	GATA-binding protein 2
Anti- <i>miR</i> :	Antagonistic <i>miRNA</i>	GFP:	Green fluorescent protein
bFGF:	Basic fibroblast growth factor	H2A.X:	Histone 2A family member X
BNP:	Brain natriuretic peptide	HEK293:	Human embryonic kidney 293
APS:	Ammoniumpersulfate	HEPES:	4-(2-hydroxyethyl)-1-piperazineethane-sulfonic acid
BAMBI:	BMP and activin membrane-bound inhibitor homolog	HIF-1 α :	Hypoxia-inducible factor 1 α
BSA:	Bovine serum albumine	HMOX1:	Heme oxygenase 1
CAD:	Coronary artery disease	HRP:	Horseshoe peroxidase
Caspases:	Cysteine aspartate proteases	HUVEC:	Human umbilical vein endothelial cell
CD31:	Cluster of differentiation 31	LB:	Lysogeny broth
Cy3:	Carbocyanine 3	LDL:	Low-density lipoprotein
DAPI:	4',6-diamidino-2-phenylindol	LV:	Left ventricle
DFA:	Desferrioxamine	α -MHC:	α -myosin heavy chain
DISC:	Death induced silencing complex	β -MHC:	β -myosin heavy chain
DMEM:	Dulbecco's modified eagle medium	MACS:	Magnetic affinity based cell sorting
DMSO:	Dimethylsulfoxide	MEM:	Minimum essential medium
DNA:	Desoxyribonucleic acid	MI:	Myocardial infarction
EDTA:	Ethylen diamine tetra-acetate	NTN4:	Netrin-4
ELISA:	Enzyme-linked immunosorbent assay	miRNA:	microRNA
EC:	Endothelial cell	nm:	nanometer
ECG:	Electrocardiography	nM:	nanomolar
ESM1:	Endothelial cell-specific molecule 1	NP40:	Nonyl-phenoxypolyethoxyethanol
FACS:	Fluorescence-activated cell sorting	NO:	Nitric oxide
FCS:	Fetal calf serum	PAK4:	p21-activated kinase 4
FITC:	Fluorescein isothiocyanate		

PAGE:	Polyacrylamide gelelectrophoresis	TnI:	Troponin I
PBS:	Phosphate buffered saline	TRIS:	Tris(hydroxymethyl)-aminomethane
Pen/Strep:	Penicilline/streptomycine	VEGF:	Vascular endothelial growth factor
PCR:	Polymerase chain reaction	YFP:	Yellow fluorescent protein
PI:	Propidium iodide	v/v:	volume per volume
PI3K:	Phosphatidylinositol 3 kinase	w/v:	weight per volume
PKB:	Protein kinase B	°C:	Degrees celsius
PKC:	Protein kinase C	μl:	microliter
PVDF:	Polyvinylidifluoride	μM:	micromolar
PIPES:	1,4-(piperazinebis-ethane-sulfonic acid)	x g:	multiple of gravity
Pre- <i>miR</i> :	Precursor <i>miRNA</i>		
PVDF:	Polyvinylidene fluoride		
RASA1:	Ras p21 protein activator		
RISC:	RNA-induced silencing complex		
RNA:	Ribonucleic acid		
RNase A:	Ribonuclease A		
ROS:	Reactive oxygen species		
RT:	Room temperature		
RTK:	Receptor tyrosine kinase		
RT-PCR:	Real-time polymerase chain reaction		
Scr- <i>miR</i> :	Scrambled <i>miRNA</i>		
SDS:	Sodiumdodecylsulfate		
siRNA:	silencer RNA		
SIRT1:	Sirtuin 1		
SOC:	Super optimal broth with catabolite repression		
TAC:	Transverse aortic constriction		
TBP:	TATA box binding protein		
TBST:	Tris buffered saline with triton		
TEMED:	Tetramethylendiamine		
TGF-β1:	Transforming growth factor β1		
TNFα:	Tumor necrosis factor α		

Publications

List of publications

1. Thum T, Galuppo P, Wolf C, **Fiedler J**, Kneitz S, van Laake LW, Doevendans PA, Mummery CL, Borlak J, Haverich A, Gross C, Engelhardt S, Ertl G, Bauersachs J. MicroRNAs in the human heart: a clue to fetal gene reprogramming in heart failure. *Circulation*. 2007;116(3):258-267.
2. Thum T, Gross C, **Fiedler J**, Fischer T, Kissler S, Bussen M, Galuppo P, Just S, Rottbauer W, Frantz S, Castoldi M, Soutschek J, Koteliansky V, Rosenwald A, Basson MA, Licht JD, Pena JT, Rouhanifard SH, Muckenthaler MU, Tuschl T, Martin GR, Bauersachs J, Engelhardt S. MicroRNA-21 contributes to myocardial disease by stimulating MAP kinase signalling in fibroblasts. *Nature*. 2008;456(7224):980-984.
3. **Fiedler J**, Jazbutyte V, Kirchmaier B, Galuppo P, Kneitz S, Pena JT, Sohn-Lee C, Soutschek J, Brand T, Tuschl T, Ertl G, Engelhardt S, Bauersachs J, Thum T. MicroRNA-24 regulates angiogenesis in the infarcted heart. *Submitted and in revision*.

List of talks

1. 4th Mini-Symposium “Interaktionen von Endothelzellen und Leukozyten im SFB688”, Würzburg, Oct 10, 2006: **Dysfunction of endothelial progenitor cells in cardiovascular disease: Modulation of transcription factors as a therapeutic approach**
2. 74th Meeting German Society of Cardiology, Mannheim, Mar 28, 2008: **Dysfunction of endothelial progenitor cells in cardiovascular disease: Modulation of GATA transcription factors as a therapeutic approach**
3. Congress Hormones and Heart Failure, Naples, Apr 18, 2008: **The GH/IGF1 axis in cardiovascular regenerative medicine**
4. American Heart Association, Scientific Sessions 2008, New Orleans, Nov 10, 2008: **GATA transcription factors contribute to endothelial progenitor cell dysfunction in patients with coronary artery disease**
5. 76th Meeting German Society of Cardiology, Mannheim, Apr 09, 2010: **MicroRNA-24 regulates angiogenesis in the infarcted heart**

List of poster presentations

1. Winter Congress Internal Medicine University Hospital Würzburg, Bad Brückenau, Mar 16, 2007: **MicroRNAs in the human heart: A clue to fetal gene reprogramming in heart failure**
2. Meeting German Society of Internal Medicine, Wiesbaden, Mar 31, 2008: **Dysfunction of endothelial progenitor cells in cardiovascular disease: Modulation of GATA transcription factors as a therapeutic approach**
3. American Heart Association, Scientific Sessions 2008, New Orleans, Nov 11, 2008: **MicroRNA-21 derepresses MAPKinase signaling and its antagonism prevents cardiac failure**

Filed patent

1. European Patent Office, Jul 16, 2009: **Use of microRNA-24 and/or its targets for the treatment and prevention of ischemia and induction of angiogenesis**

Curriculum Vitae

Personal Data

Name	Jan Fiedler
Nationality	German
Date of Birth	31.05.1981
Place of Birth	Husum
Private Address	Glashüttenstraße 2, 30165 Hannover, Germany
E-Mail	Fiedler.Jan@mh-hannover.de

Education

Since 11/2009	Research assistant at the Institute for Molecular and Translational Therapeutic Strategies, Prof. Dr. Dr. T. Thum, Hannover Medical School, Germany
06/2006 - 10/2009	PhD thesis “Endothelial <i>microRNA-24</i> contributes to capillary density in the infarcted heart” at the University Hospital Würzburg, Germany, IZKF Junior Research Group “Cardiac Wounding and Healing”, Prof. Dr. Dr. T. Thum, Supervisors Prof. Dr. J. Bauersachs and Prof. Dr. T. Dandekar
05/2006	Diploma in Biochemistry (Dipl.-Biochem. Univ.)
10/2001 - 05/2006	Studies of Biochemistry at the University of Bayreuth, Germany Diploma thesis “Role of Mdm36 for mitochondrial morphogenesis in yeast” at the Chair of Cell Biology, University of Bayreuth, Germany, Supervisor Prof. Dr. B. Westermann
08/2000 - 06/2001	Civilian service: Mother and child Sanatorium Norderheide, Bordelum, Germany
06/2000	Final secondary-school examinations at the Hermann-Tast Schule, Husum, Germany
08/1991 - 06/2000	Secondary school: Hermann-Tast-Schule, Husum, Germany
08/1987 - 06/1991	Primary school: Grundschule Bredstedt, Germany

Acknowledgement

The current work was done at the University Hospital in Würzburg and partly at the Medical School in Hannover. At both places many nice people supported and encouraged me in completing my PhD thesis. Therefore, I would like to express my deep gratitude! But still, there are some special thanks left.

I am very grateful to my **supervisors**:

Prof. Thomas Thum – he gave me the opportunity to join his group “Cardiac Wounding and Healing” in Würzburg, placing me into a motivating and enthusiastic environment. He supported me at every time during my PhD and also brought me back to Northern Germany!

Prof. Johann Bauersachs – deputy of cardiology at the University Hospital Würzburg also supporting and encouraging me constantly for my studies.

Finally Prof. Thomas Dandekar who spontaneously agreed to supervise my work – thank you very much!

I am very grateful to my **colleagues** in Würzburg and Hannover:

Annette, Michaela, Sabrina, Kerstin, Virginija, Marten, René, Michal, Felix, Volker, Bernd, Julia, Anna from Würzburg; Annette, Angelika, Yvonne, Regina, Janet, Kumar and Shashi from Hannover for always keeping a friendly atmosphere in the Thum lab!

I am very grateful to our **collaboration** partners contributing to this work:

Prof. Engelhardt with Carina, Andrea and Petra supplying me with adenoviral constructs and methodically support. Next, Prof. Brand with Bettina linking my work to developmental biology in the zebrafish model. And last but not least Dr. Paolo Galuppo who helped me with microarray analysis and also became an important soccer discussion partner for me!

I am very grateful to my **PhD colleagues** from the labs nearby:

Julia and Felicitas for encouraging talks and some fun in spare-times when not thinking on PhD!

I am very grateful to my **friends** running along with me during past times:

Since I do not want to miss anyone, I would like to mention all the nice activities we have done together and balanced my “work – life”: Barbecues, watching soccer, cycling and walking tours, bowling, Hochberg table soccer tournaments, exploring Hochberg at night, beach times at the Stadtstrand, wine and games evenings, inside soccer matches with the junior... and many more!

An outstanding reviewer for my thesis has been my friend David – thank’s a lot!

Lastly, I would like to thank my and Uli’s family for overwhelming support!

My Uli has earned the last words here: The current work could have only been completed with your fantastic cakes and food, patience, excellent layouting skills and most importantly, deep love!

Affidavit

(Eidesstattliche Erklärung)

I hereby declare that the thesis entitled
“Endothelial *microRNA-24* contributes to capillary density in the infarcted heart”
is the result of my work.

I did not receive any help or support from commercial consultants.
All sources and /or materials are listed and specified in this thesis.

Furthermore, I verify that this thesis has not yet been submitted as part of another examination process neither in identical or similar form.

Hannover, 25.05.2010

Jan Fiedler